MONITORING, MULTI-RATE MODELING, AND ECONOMIC MODEL PREDICTIVE CONTROL OF CHEMICAL PROCESSES

MONITORING, MULTI-RATE MODELING, AND ECONOMIC MODEL PREDICTIVE CONTROL OF CHEMICAL PROCESSES

by

MUDASSIR M. RASHID, B.ENG.

A Thesis Submitted to the School of Graduate Studies in Partial Fulfilment of the Requirements for the Degree of Doctor of Philosophy

DOCTOR OF PHILOSOPHY (2016) McMaster Univeristy
(Chemical Engineering) Hamilton, Ontario, Canada

title: Monitoring, Multi-rate Modeling, and Economic Model Predictive Control of Chemical Processes

author: Mudassir M. Rashid, B.Eng. (Chemical Engineering)
McMaster University, Hamilton, Ontario, Canada

supervisor(s): Drs. Prashant Mhaskar and Christopher L.E. Swartz

number of pages: xxi, 144

In the name of Allah, the Most Beneficent, the Most Merciful.

ABSTRACT

In this thesis we develop methods and strategies for the design of advanced data-driven monitoring, control, and optimization algorithms for addressing the problems of handling severe faults and economically operating chemical processes while accounting for the complex process dynamics and intricate variable interactions, including issues such as lack of output measurements, process constraints and system uncertainty.

In the initial phase of this research, in an effort to better detect and identify process faults, we propose a novel pattern matching based process monitoring approach. Traditional multivariate statistical processes monitoring (MSPM) techniques like principal component analysis (PCA) and partial least squares (PLS) are not well-suited in monitoring non-Gaussian processes because the derivation of T^2 and SPE indices requires the approximate multivariate Gaussian distribution of the process data. In this work, a novel pattern analysis driven dissimilarity approach is developed by integrating multidimensional mutual information (MMI) with independent component analysis (ICA) in order to quantitatively evaluate the statistical dependency between the independent component subspaces of the normal benchmark and monitored data sets. The new MMI based ICA dissimilarity index is derived from the higher-order statistics so that the non-Gaussian process features can be extracted efficiently. Moreover, the moving-window strategy is used to deal with process dynamics. The multidimensional mutual information based ICA dissimilarity method is applied to the Tennessee Eastman Chemical process. The process monitoring results of the proposed

method are demonstrated to be superior to those of the regular PCA, PCA dissimilarity, regular ICA and angle based ICA dissimilarity approaches.

Next, we address the problem of the unavailability of reliable and computationally manageable first-principles-based models by developing a data-based multi-rate modeling and control approach. To this end, we consider the problem of multi-rate modeling and economic model predictive control (EMPC) of electric arc furnaces (EAF), which are widely used in the steel industry to produce molten steel from scrap metal. The two main challenges that we address are the multi-rate nature of the measurement availability, and the requirement to achieve final product of a desired characteristic, while minimizing the operation cost. To this end, multi-rate models are identified that include predictions for both the infrequently and frequently measured process variables. The models comprise local linear models and an appropriate weighting scheme to capture the nonlinear nature of the EAF. The resulting model is integrated into a two-tiered predictive controller that enables the target end-point to be achieved while minimizing the associated cost. The EMPC is implemented on the EAF process and the closed-loop simulation results subject to the limited availability of process measurements and noise illustrate the improvement in economic performance over existing trajectory-tracking approaches.

Finally, we consider the problem of variable duration economic model predictive control (EMPC) of batch processes subject to multi-rate and missing data. To this end, we first generalize a recently developed subspace-based model identification approach for batch processes to handle multi-rate and missing data by utilizing the incremental singular value decomposition technique. Exploiting the fact that the proposed identification approach is capable of handling inconsistent batch lengths, the resulting dynamic model is integrated into a tiered EMPC formulation that optimizes process economics (including batch duration). Simulation case studies involving application to the energy intensive electric arc furnace

process demonstrate the efficacy of the proposed approach compared to a traditional trajectory tracking approach subject to the limited availability of process measurements, missing data, measurement noise and constraints.

ACKNOWLEDGMENTS

All the praises and thanks are due to Allah, the Lord of the Worlds.

I am extremely grateful to my advisors, Dr. Prashant Mhaskar and Dr. Christopher L. E. Swartz, and thank them for all their patience and guidance. It has been a great honor to work with them, and I am greatly appreciative of their leadership, support and encouragement. They have instilled in me an appreciation for meaningful research, and I am continuously amazed by their technical knowledge and relentless enthusiasm. I would also like to thank the members of my committee, Dr. James P. Reilly and Mr. Kevin G. Dunn, for their insights, advice and time.

I would like to thank Dr. Heather Sheardown, Dr. Shiping Zhu and Dr. Carlos Filipe for enriching my graduate studies experience. I would also like to express my gratitude and appreciation to all the faculty and staff in the Department of Chemical Engineering at McMaster University for their support. I would like to especially thank Linda Ellis, Michelle Whalen and Kristina Trollip for putting up with me. I also thank Lynn Falkiner, Kathy Goodram, Cathie Roberts, Melissa Vasil and Nanci Cole.

There are also many friends who deserve my appreciation and thanks, both in Hamilton and beyond. To all of my colleagues at the McMaster Advanced Control Consortium – Jake, Matt, Chinedu, Masoud, Giancarlo, Pedro, Chris, Jaffer, Philip, Brandon, and Kushlani – thank you for supporting me, caffeinating me, keeping me (relatively) sane, and eating

my cookies. I really appreciate the numerous valuable and insightful conversations about research, sports, and life, not to mention our many lunches and experiences together. Thanks also goes to Amrit and Shahed for visiting me and staying in contact. I also express my sincerest gratitude for all my dear friends at Makki Masjid who continuously inspired me, encouraged this work, and sent inspirational messages to keep my spirits up.

I thank my brothers, Mobushir, Muzamil and Mustafa, for being there for me in the most difficult times and for making this journey enjoyable. I could not have asked for more inspiring, positive, hopeful, and encouraging brothers. Finally, this work would never have been possible without the unconditional love and support of my mother, Asfa Bibi, and my father, Mohammad Rashid. This dissertation is dedicated to my parents, for all their prayers, sacrifices, love, and support.

Mudassir M. Rashid

Hamilton, Ontario

September, 2016

TABLE OF CONTENTS

LIST OF FIGURES

LIST OF TABLES

CHAPTER 1

INTRODUCTION

1.1 Background and Motivation

A diverse assortment of industrial and commercial consumer products, that are vital for fulfilling the requirements of modern society and routinely encountered by individuals on a daily basis, are manufactured by the chemical process industries. These industries, faced with the exorbitant demands of improved resource management, low energy consumption, rigorous safety regulations, and minimal environmental impact, have transformed industrial plants into a complex networked arrangement of processing units that are highly integrated through material, energy and information flows. The more stringent operating conditions accompanying this transformation have placed new constraints on the operating flexibility of the process, and made the performance requirements for process plants increasingly difficult to satisfy. The increased levels of integration and automation, however, have also rendered process systems exceedingly susceptible to equipment malfunctions or sensor failures, which if not appropriately handled can lead to dire consequences ranging from deficient product quality specifications to complete plant shutdowns, incurring substantial economic losses, and even catastrophic safety hazards to manufacturing facilities and plant personnel, as well as environmental degradation. Therefore, monitoring, control, and optimization of industrial

processes is critically important for maintaining product quality, optimizing profit, ensuring plant safety, and improving energy efficiency and environmental sustainability.

The monitoring, control, and optimization of chemical processes involves employing models that enable the algorithms to learn and derive critical operational decisions from the process data being collected on-line. These models can be classified into two categories: (1) mechanistic/first-principles models that have a structure based on fundamental or first-principles knowledge of the system with parameters estimated from plant data; or (2) data-driven/empirical models that incorporate a structure and parameters, both of which are entirely identified exclusively from plant data. The important consideration is not the type and nature of the model used, rather whether or not that employed process model, in terms of its structure and assumptions, is appropriate or valid for the application. For example, mechanistic or first-principles models impose a structure that embodies many engineering assumptions about the underlying process system, whereas empirical models can readily capture the dominant sources of variation and causality, provided that a sufficient amount of data is available to adequately capture the complex relationships among process variables and not hinder the identifiability of the model. Nevertheless, the limitations imposed by the available data would also have a significant effect on the ability to accurately estimate the mechanistic model parameters. Furthermore, mechanistic models may not be readily available for many commercial processes and modeling of an integrated industrial process with complex physical and chemical phenomena can be a challenging and time-consuming endeavor, possibly resulting in a large-scale model that may be too computationally expensive and intractable for real-time applications.

The above considerations provide a strong motivation for the development of data-driven algorithms, derived from empirical models that are built using plant data, for the purposes of monitoring, control, and optimization of chemical processes. To this end, in this thesis

we develop methods and strategies for the design of advanced data-driven monitoring and control systems that can account for the complex process dynamics and intricate variable interactions, including issues such as process constraints and system uncertainty. This sandwich thesis discusses the findings of research work that synergize tools from control and systems theory, chemical engineering and computational sciences, to address important process monitoring and control problems including: (1) building models for monitoring and diagnosing dynamic processes using data mining and machine learning based computational intelligence techniques; (2) developing a multi-rate subspace-based system identification method to identify a dynamic linear time-invariant model from a finite number of noisy data samples disrupted with unmeasured process variables and asynchronous data; and (3) designing an economic model predictive controller for batch processes that is capable of optimizing batch durations and achieving the desired final product end-point specification by batch termination while minimizing the operating costs.

1.2 RESEARCH OBJECTIVES AND THESIS OUTLINE

First, we present one contribution in the area of detecting and isolating process faults. It is widely recognized that faults are ubiquitous in process systems and chemical plants, causing system upsets in other downstream process operations. As such, many process measurement variables and feedback control loops may be identified as performing poorly, even though these suspect variables are not the root cause of the fault. In Chapter 2, one novel contribution in an effort to better detect and identify process faults is presented, where we propose a novel pattern matching based process monitoring approach. Traditional multivariate statistical processes monitoring (MSPM) techniques like principal component analysis (PCA) and partial least squares (PLS) are not well-suited in monitoring non-Gaussian processes because the derivation of T^2 and SPE indices requires the approximate multivariate

Gaussian distribution of the process data. In this work, a novel pattern analysis driven dissimilarity approach is developed by integrating multidimensional mutual information (MMI) with independent component analysis (ICA) in order to quantitatively evaluate the statistical dependency between the independent component subspaces of the normal benchmark and monitored data sets. The new MMI based ICA dissimilarity index is derived from the higher-order statistics so that the non-Gaussian process features can be extracted efficiently. Moreover, the moving-window strategy is used to deal with process dynamics. The multidimensional mutual information based ICA dissimilarity method is applied to the Tennessee Eastman Chemical process. The process monitoring results of the proposed method are demonstrated to be superior to those of the regular PCA, PCA dissimilarity, regular ICA and angle based ICA dissimilarity approaches.

In Chapter 3, we consider the problem of multi-rate modeling and economic model predictive control (EMPC) of electric arc furnaces (EAF), which are widely used in the steel industry to produce molten steel from scrap metal. The two main challenges that we address are the multi-rate nature of the measurement availability, and the requirement to achieve final product of a desired characteristic, while minimizing the operation cost. To this end, multi-rate models are identified that include predictions for both the infrequently and frequently measured process variables. The models comprise local linear models and an appropriate weighting scheme to capture the nonlinear nature of the EAF. The resulting model is integrated into a two-tiered predictive controller that enables the target end-point to be achieved while minimizing the associated cost. The EMPC is implemented on the EAF process and the closed-loop simulation results subject to the limited availability of process measurements and noise illustrate the improvement in economic performance over existing trajectory-tracking approaches.

In Chapter 4, we consider the problem of variable duration economic model predictive control (EMPC) of batch processes subject to multi-rate and missing data. To this end, we first generalize a recently developed subspace-based model identification approach for batch processes to handle multi-rate and missing data by utilizing the incremental singular value decomposition technique. Exploiting the fact that the proposed identification approach is capable of handling inconsistent batch lengths, the resulting dynamic model is integrated into a tiered EMPC formulation that optimizes process economics (including batch duration). Simulation case studies involving application to the energy intensive electric arc furnace process demonstrate the efficacy of the proposed approach compared to a traditional trajectory tracking approach subject to limited availability of process measurements, missing data, measurement noise and constraints.

Finally, Chapter 5 summarizes the main contributions of the research work, and recommendations for related future work and research opportunities are presented.

CHAPTER 2

PATTERN MATCHING BASED FAULT DETECTION AND IDENTIFICATION[†]

2.1 INTRODUCTION

Process monitoring and diagnosis are crucially important for detecting abnormal operating conditions, process upsets, equipment malfunctions, sensor failures, and other faults in industrial plants in order to improve operational safety, product quality, environmental sustainability, and profit margin. More than thousands of process variables are measured and recorded continuously in industrial plants so that the process monitoring becomes a challenging task. Meanwhile, the commonly used plant historians contain huge amounts of process data that may be employed to build various kinds of models for process monitoring [1]. Traditionally, univariate statistical process control (SPC) techniques have been used for

[†]The results in this chapter have been published in:

- M. M. Rashid and J. Yu. A new dissimilarity method integrating multidimensional mutual information and independent component analysis for non-Gaussian dynamic process monitoring. *Chemometrics Intell. Lab. Syst.*, 115:44–58., 2012.

monitoring industrial processes. Nevertheless, the highly correlated process measurements in industrial plants often result in the failure of univariate methods [2].

Multivariate statistical process monitoring (MSPM) techniques like principal component analysis (PCA) and partial least squares (PLS) have been widely used for fault detection and diagnosis in industrial practice [3–6]. These kinds of methods first project the multivariate and collinear data onto a lower dimensional subspace. Then the test statistics like T^2 and SPE are developed to monitor the multivariate data [7–11]. The effectiveness of these conventional methods in detecting process abnormalities requires that the process data approximately follow a multivariate Gaussian distribution for the derivation of control limits. However, industrial data often obey a non-Gaussian distribution so that the PCA/PLS based monitoring techniques become ill-suited [12]. Moreover, the regular PCA and PLS models ignore time-varying dynamics in processes. Although dynamic PCA (DPCA) and dynamic PLS (DPLS) have been introduced, they expand time-lagged variables into the data matrices to model the time-varying process behavior [13]. The orders of time delay in process variables are thus needed and it is not a trivial task in industrial applications. Furthermore, DPCA and DPLS only consider cross-correlations and autocorrelations of process measurements via time-shifted lags while the higher-order statistics are ignored. Alternatively, Fisher discriminant analysis (FDA) is applied to distinguish between normal and faulty process operations. However, labeled training data from both normal and faulty operating conditions are required to build the initial model [14–18]. In addition, FDA may not be able to detect new faults unless they already exist in the training data set. Meanwhile, machine learning algorithms such as artificial neural networks (ANN) and support vector machines (SVM) have been used for process monitoring. These supervised monitoring techniques also require labeled data from normal and faulty operating conditions [19–21]. In industrial processes, however, the historical data often do not have known class labels and thus these supervised

monitoring methods may not be applicable. More recently, Gaussian mixture model (GMM) method is proposed to monitor non-Gaussian processes by characterizing measurement data with various multivariate Gaussian density functions. The data from the individual operating modes are still assumed to follow a multivariate Gaussian distribution [22–24]. On the other hand, independent component analysis (ICA) is adopted to decompose multivariate data into linear combinations of statistically independent components (IC). ICA imposes independency on latent variables beyond second-order statistics and thus can extract the non-Gaussian features of process data [25–27]. Moreover, ICA based monitoring statistics like I^2 and SPE have been developed to describe the variability within the independent component and residual subspaces [28]. However, those statistics do not take advantage of pattern based analytics that can improve the process fault detection capability.

As alternative solutions, unsupervised pattern matching techniques are proposed to identify similar patterns between multivariate time-series data sets. Various PCA based pattern matching methods compare PC subspaces using similarity factors, which are developed from the geometric angles between principal components [29, 30]. However, the PCA based similarity factors only incorporate second-order statistics and are thus limited in feature extraction of process data. Alternately, Eigenvalue decomposition of the covariance matrices is used to determine the dissimilarity factor between two data sets [4]. Nevertheless, this method suffers from the same issue that only the second-order statistics are taken into consideration and thus the non-Gaussian features cannot be effectively extracted. More recently, the dissimilarity method is extended to ICA for comparing two data sets using independent components [31]. However, the dissimilarity index is calculated from the angles among different ICs, which cannot efficiently characterize the non-Gaussian process features.

In this study, ICA is integrated with multidimensional mutual information (MMI) to measure the statistical independency between two IC subspaces, which represents the subspace

dissimilarity. The proposed approach does not require any assumptions regarding the relationships among measurement variables and can deal with the process data following an arbitrary probability density distribution. In contrast to the angle based dissimilarity factor, the new multidimensional mutual information based dissimilarity takes into account the higher-order statistics and thus can well capture the non-Gaussian features of process data. Furthermore, a rolling window that moves over the monitored segment incrementally ensures that the time-varying process dynamics are accounted for in the MMI based dissimilarity approach.

The remainder of the article is organized as follows. Section 2.2 reviews the conventional ICA based monitoring technique. Then the novel ICA and multidimensional mutual information based dissimilarity method are developed for process monitoring in Section 2.3. Section 2.4 demonstrates the application of the new dissimilarity approach to the Tennessee Eastman Chemical process and its comparison to the regular PCA, PCA dissimilarity, conventional ICA and angle based ICA dissimilarity methods. The conclusions of this work are summarized in Section 2.5.

2.2 Independent Component Analysis Based Process Monitoring

Independent component analysis is a statistical technique for computing hidden factors that underlies a set of measurement variables. ICA expresses n measurement variables $X = \left[x_1(k), x_2(k), \ldots, x_n(k)\right]^T$ at the k-th sampling instant as linear combinations of m unknown independent components

$$x(k) = \sum_{j=1}^{m} a_j s_j(k) = As(k) \tag{2.2.1}$$

where $A = [a_1, a_2, \ldots, a_m] \in \mathbb{R}^{n \times m}$ is an unknown mixing matrix and $S = [s_1, s_2, \ldots, s_m]^T$ are the independent components. The FastICA algorithm is used to estimate the mixing matrix A and independent components $\hat{S}$ from the original data X [32, 33]. The solution is equivalent to finding a demixing matrix W as follows

$$\hat{S} = WX \tag{2.2.2}$$

where the statistical independency between the reconstructed independent components $\hat{S}$ in terms of negentropy is maximized. The initial step in the FastICA algorithm is whitening that eliminates the cross-correlation between the measurement variables. This is expressed as

$$z(k) = Qx(k) \tag{2.2.3}$$

where Q is the whitening matrix and $z(k)$ is the whitened data at the k-th sampling instant. The transformation is given by

$$z(k) = Bs(k) \tag{2.2.4}$$

where the orthogonal matrix B is computed iteratively such that the i-th independent component has the maximized non-Gaussianity. Thus the projection of $x(k)$ into the independent component subspace can be estimated as

$$\hat{s}(k) = B^T Qx(k) \tag{2.2.5}$$

with the demixing matrix $W = B^T Q$. An optimal number of ICs are selected to capture the dominant characteristics of the process based upon the assumption that the rows of W with the highest norm have the largest effect on the variation of S.

The I^2 and SPE monitoring statistics are further defined as

$$I^2(k) = \hat{s}(k)^T \hat{s}(k) \tag{2.2.6}$$

and

$$\text{SPE}(k) = e(k)^T e(k) \tag{2.2.7}$$

where $\hat{s}(k) = Wx(k)$ and $e(k) = x(k) - \hat{x}(k)$. The prediction, $\hat{x}(k)$, is calculated as

$$\hat{x}(k) = QB^T Wx(k) \tag{2.2.8}$$

The control limits for the I^2 and SPE statistics can be computed using a kernel density estimation for monitoring multivariate data.

2.3 ICA Based Dissimilarity Approach for Process Monitoring

2.3.1 Angle Based ICA Dissimilarity Method

Conventional MSPM techniques like PCA and ICA do not specifically detect the dynamic changes of relationships among different measurement variables. In contrast, the dissimilarity

approach can be used to monitor multivariate data by comparing latent variable subspaces and extracting the hidden variable relationships.

Consider two data sets $X_1 \in \mathbb{R}^{n\times k}$ and $X_2 \in \mathbb{R}^{n\times k}$, which consist of n variables and k samples. Here X_1 serves as normal benchmark set while X_2 is the monitored set. Two different ICA models can be built on X_1 and X_2 to obtain two sets of ICs, S_1 and S_2, respectively. It is noted that the ICs are sorted in terms of L_2-norm. Firstly the geometric angle between each pair of ICs can be computed as

$$\cos(\theta_i) = \frac{(s_1^{(i)})^T (s_2^{(i)})}{\left\|s_1^{(i)}\right\| \cdot \left\|s_2^{(i)}\right\|} \tag{2.3.1}$$

where θ_i is the angle between the i-th independent components $s_1^{(i)}$ and $s_2^{(i)}$ [31]. Then, the angle part of the dissimilarity index is expressed as

$$D_\theta = \frac{1}{m}\sum_{i=1}^{m} \sin^2(\theta_i) \tag{2.3.2}$$

which is equivalent to

$$D_\theta = \frac{1}{m}\sum_{i=1}^{m}\left(1 - \left(\frac{(s_1^{(i)^T})(s_2^{(i)})}{\left\|s_1^{(i)}\right\| \cdot \left\|s_2^{(i)}\right\|}\right)^2\right) \tag{2.3.3}$$

It is possible that the independent components have similar geometric orientations but quite different magnitudes. Then a distance ratio factor for the IC subspaces is introduced as follows

$$D_{\text{dist}} = \frac{I_2^2}{I_1^2} \tag{2.3.4}$$

where I_1^2 and I_2^2 are the mean values of the I^2 test statistic for the two respective IC subspaces. Hence, the angle based dissimilarity index is defined as

$$D_{\mathrm{A}} = D_{\mathrm{dist}} \cdot D_{\theta} \tag{2.3.5}$$

which integrates both the angle and distance portions.

A statistical control limit corresponding to the above angle based dissimilarity index can be computed using the kernel density estimation for process monitoring.

2.3.2 Multidimensional Mutual Information Based ICA Dissimilarity Method

The angle based dissimilarity index is based on the cross-correlation between the independent components of the benchmark and monitored data sets. However, it does not take into full consideration the higher-order statistics. Thus the non-Gaussian features underlying the process cannot be effectively extracted. In this work, a novel method is proposed to characterize the dissimilarity through the multidimensional mutual information based statistical independency between the two IC subspaces corresponding to the benchmark and monitored sets. The merit of MMI based dissimilarity index lies in its capability to identify the non-Gaussian statistical relationship and hidden patterns of the benchmark and monitored data. In this way, any abnormal features within the monitored set can be extracted and alarmed precisely.

Mutual information is a quantitative measure of statistical dependency between two random variables estimated from entropy [34, 35]. In contrast to cross-correlation, it takes into account the higher-order statistics and is able to capture the non-Gaussianity of stochastic

systems. Firstly, the Shannon's entropy of a random variable x can be estimated as

$$H(x) = -\int_{x} p(x) \log p(x) dx \tag{2.3.6}$$

where $p(x)$ is the probability density function of x. The higher entropy value indicates that the more statistical information is contained within x. If unbiased estimates for the log probability density function $\log p(x_i)$ for each observation are available, then the entropy of the random variable x can be estimated as

$$H(x) = -\frac{1}{N} \sum_{i=1}^{N} \log p(x_i) \tag{2.3.7}$$

Moreover, the entropy of the random variable x ordered by descending magnitudes can be computed using a simple numerical technique as follows

$$H(x) \approx \frac{1}{N-1} \sum_{i=1}^{N} \log \left[x(i+1) - x(i) \right] + \psi(1) - \psi(N) \tag{2.3.8}$$

where $\psi(\cdot)$ denotes the digamma function [35]. Then, mutual information is referred to the information sharing between two random variables x_1 and x_2 and can be computed as follows

$$I(x_1, x_2) = \int_{x_1} \int_{x_2} p(x_1, x_2) \log \left(\frac{p(x_1, x_2)}{p(x_1) p(x_2)} \right) dx_1 dx_2 \tag{2.3.9}$$

where $p(x_1, x_2)$ is the joint probability density function while $p(x_1)$ and $p(x_2)$ are the marginal probability density functions of x_1 and x_2, respectively. The above mutual information index can be rewritten as

$$I(x_1, x_2) = H(x_1) + H(x_2) - H(x_1, x_2) \tag{2.3.10}$$

where $H(x_1)$ and $H(x_2)$ are the marginal entropies of x_1 and x_2 while $H(x_1, x_2)$ denotes the joint entropy of both variables as

$$H(x_1, x_2) = -\int_{x_1}\int_{x_2} p(x_1, x_2)\log p(x_1, x_2)dx_1 dx_2 \tag{2.3.11}$$

The complex integrals in Eq. (2.3.10) are difficult to solve analytically. Instead, a l-nearest neighbor based strategy can be used to estimate the mutual information numerically. Initially, an estimate of entropy based on nearest-neighbor distances in the sample space is derived for improved computational efficiency as follows

$$H(x) = \sum_{i=1}^{N}(N \cdot \rho_i) + \ln 2 + C \tag{2.3.12}$$

where ρ_i represents the distance from the i-th sample to its nearest neighbor, N is the number of points and C is the Euler-Mascheroni constant [36]. This approach of l-nearest neighbor statistics is extended to compute mutual information between high-dimensional spaces. The multidimensional mutual information between the two IC subspaces S_1 and S_2 corresponding to the benchmark and monitored data sets is expressed as follows

$$I(S_1, S_2) = \psi(l) - \frac{1}{l} - \langle\psi(n_{S_1}) + \psi(n_{S_2})\rangle + \psi(N) \tag{2.3.13}$$

where N is the size of the data sets, n_{S_1} and n_{S_2} represent the numbers of samples in proximity to the nearest neighbors within each IC subspace, l is the number of nearest neighbors identified through data clustering, $\langle\cdot\rangle$ denotes the averages over all observations in the data sets, and $\psi(\cdot)$ is the digamma function defined as

$$\psi(x) = \Gamma(x)^{-1}d\Gamma(x)/dx \tag{2.3.14}$$

with $\Gamma(x)$ denoting the Gamma function [34].

Hence, the multidimensional mutual information between the two IC subspaces can be computed to quantify the dissimilarity between the benchmark and monitored data sets. Consider the benchmark data set $X_b \in \mathbb{R}^{n\times w}$ and the monitored data set $X_m \in \mathbb{R}^{n\times r}$, both of which consist of n variables. The moving window of width w can be incremented throughout the monitored data set for the dynamic monitoring purpose. Firstly, an ICA model is built on the benchmark data with S_b denoting its corresponding IC subspace. Simultaneously, the moving-window based ICA models are developed from the subsets of monitored data with a series of IC subspaces $S_m^{(1)}, S_m^{(2)}, \ldots, S_m^{(r)}$ obtained. Fig. 2.3.1 illustrates the moving window strategy for updating the monitored IC subspaces. Then, the multidimensional mutual information based dissimilarity index D_{MMI} is defined as follows to evaluate the statistical dependency between the benchmark and monitored IC subspaces

$$D_{\text{MMI}}(i) = \frac{I_m^2(i)}{I_b^2} \cdot \frac{1}{I(S_b, S_m^{(i)})} \tag{2.3.15}$$

where i denotes the i-th moving window on the monitored data set, $I(S_b, S_m^{(i)})$ is the multidimensional mutual information between the benchmark and monitored IC subspaces while I_b^2 and $I_m^2(i)$ are the ICA based I^2 statistics of those two subspaces. The larger dissimilarity index value indicates the stronger statistical independency and the more distinct hidden patterns of the monitored set compared to the normal benchmark set. Thus the monitored operation has the higher tendency to be abnormal and in this way the process faults can be detected.

The proposed D_{MMI} index determines the statistical dependency between the independent component subspaces and then captures the non-Gaussian features in the data sets. It should be emphasized that the statistical dependency is different from the cross-correlation as

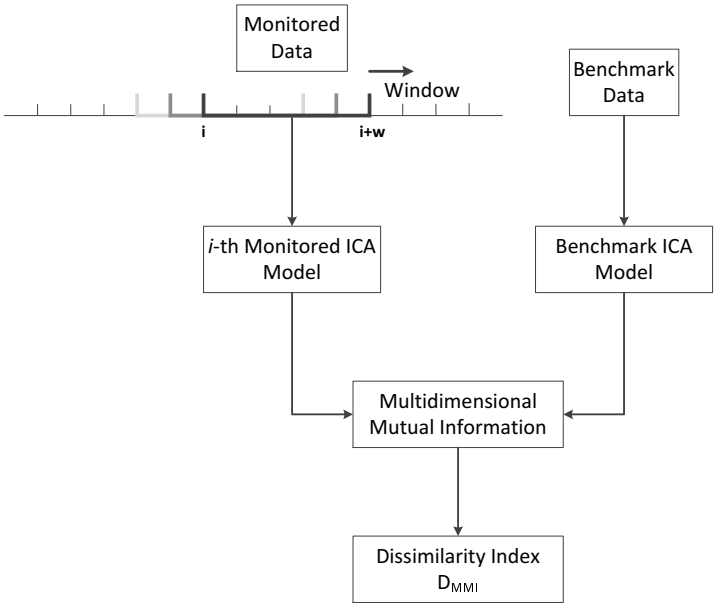

Figure 2.3.1: Illustration of Moving Window Strategy for Multidimensional Mutual Information Based ICA Dissimilarity Method

the former depends on the higher-order rather than the second-order statistics so that the process non-Gaussianity can be well characterized. With the set of moving window based dissimilarity index values computed, the kernel density estimation can be used to estimate the corresponding control limit for abnormal event detection. The kernel density estimator is defined as

$$\hat{f}_h(D_{\text{MMI}}) = \frac{1}{Nh}\sum_{i=1}^{N} K\left(\frac{D_{\text{MMI}} - D_{\text{MMI}}(i)}{h}\right) \tag{2.3.16}$$

where h is the bandwidth and K denotes the Gaussian kernel function

$$K(u) = \frac{1}{\sqrt{2\pi}} e^{\left(-\frac{1}{2}u^2\right)} \tag{2.3.17}$$

with u representing an arbitrary data point [37]. The fault alarms are triggered as long as the MMI based dissimilarity index values are above the estimated control limit. Otherwise, the

process operation is considered as normal. A schematic diagram of the proposed monitoring approach is shown in Fig. 2.3.2 and the detailed step-by-step procedure is summarized below

1) Specify the moving window width w and set the initial iteration number as $i = 1$;
2) Build ICA model on the selected benchmark data $X_b \in \mathbb{R}^{n\times w}$;
3) Extract the IC subspace S_b corresponding to the benchmark set;
4) Select the moving window based subset of the monitored data $X_m \in \mathbb{R}^{n\times r}$ as $X_m^{(i)} \in \mathbb{R}^{n\times w}$;
5) Build ICA model using current monitored data subset $X_m^{(i)}$;
6) Extract the IC subspace $S_m^{(i)}$ for the i-th monitored window;
7) Estimate the multidimensional mutual information $I(S_b, S_m^{(i)})$ between the benchmark and monitored data sets;
8) Compute the multidimensional mutual information based dissimilarity index $D_{\text{MMI}}(i)$.
9) Increment $i = i + 1$ and return to step 3). Stop the iterations at the last sampling point in the monitored set.
10) Estimate the corresponding control limit of $D_{\text{MMI}}(i)$ for continuous monitoring and fault detection

2.4 PROCESS MONITORING APPLICATION

2.4.1 TENNESSEE EASTMAN CHEMICAL PROCESS

The Tennessee Eastman Chemical process (TEP) is used in this study to evaluate the utility of the proposed monitoring method. The process flow diagram is shown in Fig. 2.4.1 and it

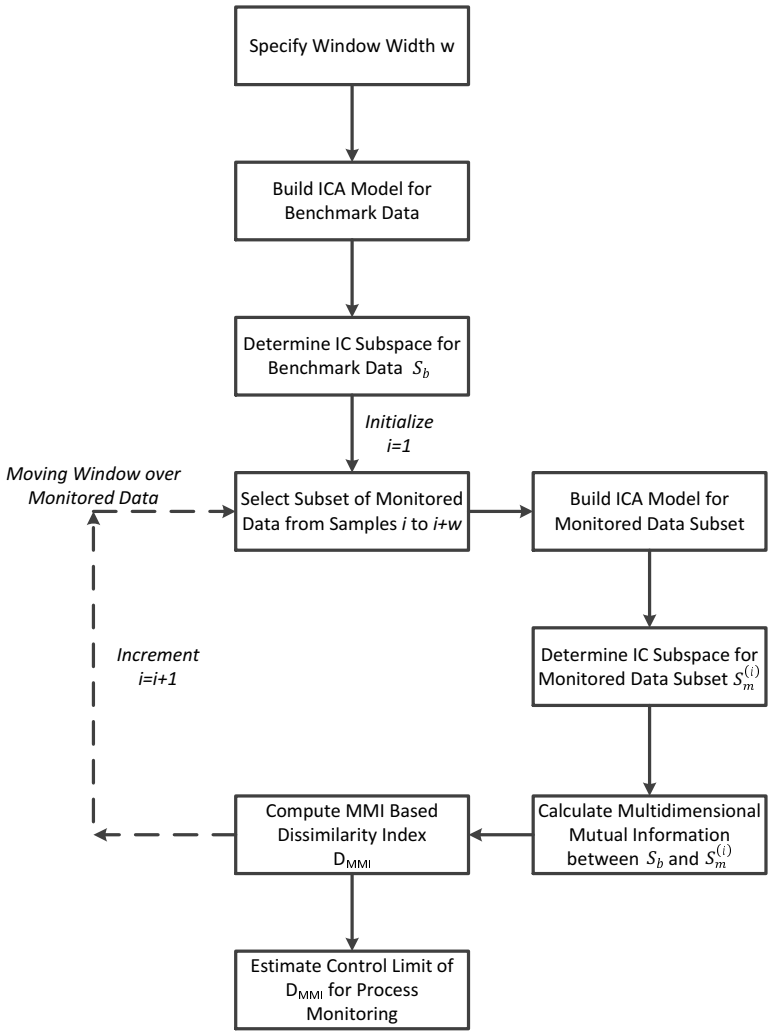

Figure 2.3.2: Schematic Diagram of Multidimensional Mutual Information Based ICA Dissimilarity Method

is composed of five major unit operations including chemical reactor, condenser, a recycle compressor, vapor/liquid separator and stripper [38]. The process produces two liquid products, G and H, from four gaseous reactants A, C, D and E along with a byproduct of F. An inert gaseous component, B, is also present in the reactant mixture and enters mainly through the C stream. The reactor product stream is cooled through a partial condenser and fed to a vapor/liquid separator for component separation. Further, the vapor stream exiting the separator is recycled to the reactor feed stream through a compressor. A fraction of the recycle stream is purged to prevent accumulation of inert and byproduct in the process. Meanwhile, the condensed components from the separator (stream 10) are pumped into a stripper. The products, G and H, exiting the stripper are further processed in the downstream operation. This process contains total 41 measured and 12 manipulated variables. In addition, the process has 20 pre-defined abnormal operation events as listed in Table 2.4.1 and consists of six operating modes given in Table 2.4.2.

In this research, the 22 continuous measurement variables as listed in Table 2.4.3 are selected for process monitoring purpose and the sampling time of 0.05h is used. Moreover, the process is essentially open-loop unstable and thus a decentralized control strategy is adopted for closed-loop operation stability [39]. A data set of 300 normal samples is generated to train the models or serve as the benchmark set. Then, four test cases mixed with various types of process faults are designed to compare different monitoring methods. The detailed test scenarios are described in Table 2.4.4. Each of the test cases contains both normal and different types of faulty operation data. In this study, the window width of the dissimilarity methods is set to 25 while the confidence level for computing the control limits of different approaches is fixed at 95%.

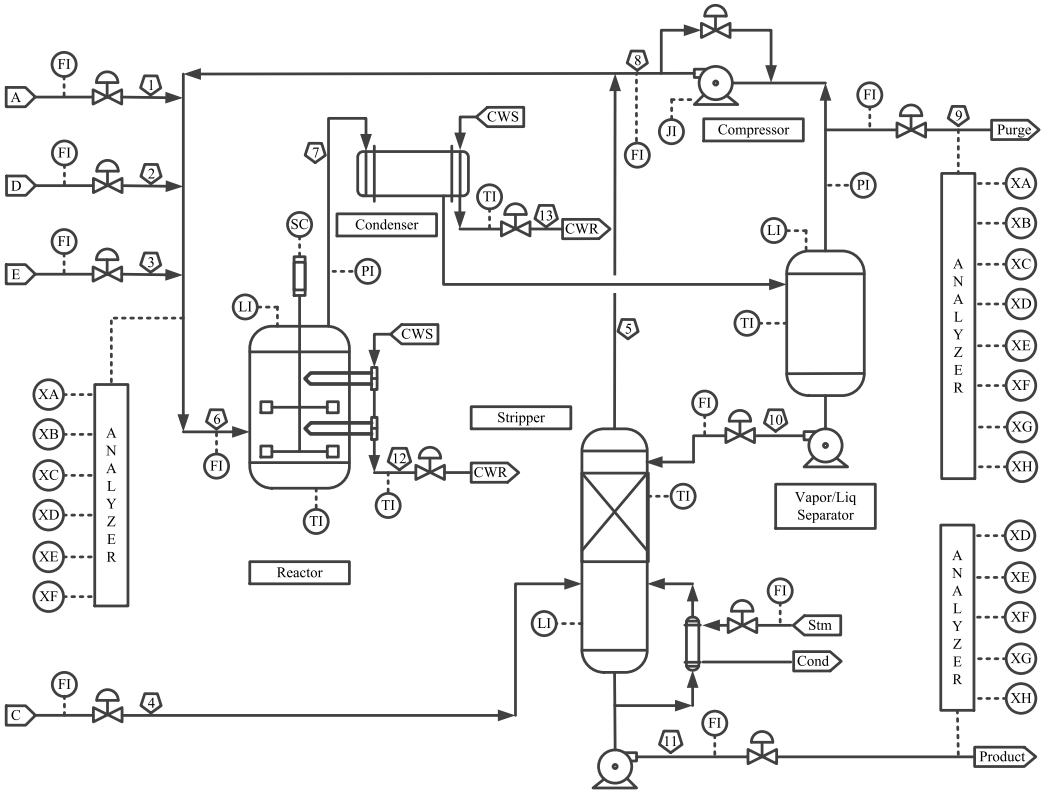

Figure 2.4.1: Process Flow Diagram of Tennessee Eastman Chemical Process

Table 2.4.1: Predefined Faults of Tennessee Eastman Chemical Process

Fault No.	Description
1	Step in A/C feed ratio, B composition constant
2	Step in B composition, A/C ratio constant
3	Step in D feed temperature (stream 2)
4	Step in reactor cooling water inlet temperature
5	Step in condenser cooling water inlet temperature
6	A feed loss (step change in stream 1)
7	C header pressure loss (step change in stream 4)
8	Random variation in A+C feed composition (stream 4)
9	Random variation in D feed temperature (stream 2)
10	Random variation in C feed temperature (stream 4)
11	Random variation in reactor cooling water inlet temperature
12	Random variation in condenser cooling water inlet temperature
13	Slow drift in reaction kinetics
14	Sticking reactor cooling water valve
15	Sticking condenser cooling water valve
16	Unknown disturbance
17	Unknown disturbance
18	Unknown disturbance
19	Unknown disturbance
20	Unknown disturbance

Table 2.4.2: Six Operation Modes of Tennessee Eastman Chemical Process

Operating Mode	G/H Mass Ratio	Production Rate (Stream 11)
1	50/50	7038 kg/h G and 7038 kg/h H
2	10/90	1408 kg/h G and 12669 kg/h H
3	90/10	10000 kg/h G and 1111 kg/h H
4	50/50	Maximum
5	10/90	Maximum
6	90/10	Maximum

Table 2.4.3: Monitored Variables of Tennessee Eastman Chemical Process

Variable No.	Variable Description
1	A Feed (stream 1)
2	D Feed (stream 2)
3	E Feed (stream 3)
4	A and C Feed (stream 4)
5	Recycle Flow (stream 8)
6	Reactor Feed (stream 6)
7	Reactor Pressure
8	Reactor Level
9	Reactor Temperature
10	Purge Rate (stream 9)
11	Separator Temperature
12	Separator Level
13	Separator Pressure
14	Separator Underflow (stream 10)
15	Stripper Level
16	Stripper Pressure
17	Stripper Underflow (stream 11)
18	Stripper Temperature
19	Steam Flow
20	Compressor Work
21	Reactor Coolant Temperature
22	Condenser Coolant Temperature

Table 2.4.4: Four Test Cases of Tennessee Eastman Chemical Process

Case No.	Test Scenario
Case 1	Normal operation from the 1st to 100th samples Step in reactor cooling water inlet temperature from the 101st to 200th samples Normal operation from the 201st to 300th samples Random variation in reactor cooling water inlet temperature from the 301st to 400th samples
Case 2	Normal operation from the 1st to 100th samples Slow drift in reaction kinetics from the 101st to 200th samples Normal operation from the 201st to 300th samples Sticking reactor cooling water valve from the 301st to 400th samples
Case 3	Normal operation from the 1st to 100th samples Step in A/C feed ratio, B composition constant from the 101st to 140th samples Normal operation from the 141st to 240th samples A feed loss from the 241st to 319th samples Normal operation from the 320th to 419th samples Slow drift in reaction kinetics from the 420th to 519th samples
Case 4	Normal operation from the 1st to 100th samples Step in B composition, A/C ratio constant from the 101st to 200th samples Normal operation from the 201st to 300th samples C header pressure loss from the 301st to 347th samples Normal operation from the348th to 447th samples Sticking condenser cooling water valve from the 448th to 532nd samples Normal operation from the 533rd to 632nd samples Unknown disturbance from the 633rd to 732nd samples

2.4.2 COMPARISON OF PROCESS MONITORING RESULTS

In the first test case, the plant starts with normal operation and then followed by the first fault of a step change in reactor cooling water inlet temperature during the period from the 101st through the 200th samples. After that, the process operation returns to the normal conditions and lasts 100 samples before the second process fault occurs with the increased random variations in the reactor cooling water inlet temperature. The process monitoring results of the various methods including PCA, angle based PCA dissimilarity, ICA, angle based ICA dissimilarity and multidimensional mutual information based ICA dissimilarity, are depicted in Figs. 2.4.2 to 2.4.6, respectively. It is observed that the PCA and angle based PCA dissimilarity methods cannot isolate the non-Gaussian features of the monitored data, resulting in low fault detection rates of below 25%, as shown in Fig. 2.4.7. It should be noted that average fault detection and false alarm rates of the T^2 and SPE statistics for the PCA method and I^2 and SPE indices for the ICA approach are used for the methodology evaluation and comparison. It can be readily seen from Fig. 2.4.4 that the ICA based I^2 and SPE statistics are unable to identify the process faults reliably. Though some of the faulty points are captured in the I^2 or SPE plot, there is a long delay in triggering the fault alarms that result in a poor average fault detection rate of only 28.0%. Meanwhile, the angle based ICA dissimilarity index, as shown in Fig. 2.4.5, has improved fault detection capability with the fault detection rate of 42.0%. However, its performance is much worse than the proposed multidimensional mutual information based ICA dissimilarity method, which results in the highest fault detection rate of 95.0%. The superior fault detection capacity of the MMI based ICA dissimilarity method is attributed to its inherent feature to account for the process non-Gaussianity through the entropy based statistical dependency instead of the essential cross-correlation. On the other hand, its false alarm rate is as low as 3.5% indicating its satisfactory performance in minimizing both the type-I and type-II errors in fault detection.

The PCA, PCA based dissimilarity and the angle based ICA dissimilarity methods have much worse false alarm rates greater than 7.0%. The high false alarm rates can be caused by the second-order statistics driven monitoring indexes that partially mismatches the non-Gaussian process patterns. The proposed MMI based dissimilarity approach demonstrates the best overall performance among the monitoring methods in terms of both fault detection and false alarm rates.

For the second test case, the normal operation of the plant is mixed with two different types of faults, which are a slow drift error in reaction kinetics from the 101-st to the 200-th samples and a sticking reactor cooling water valve from the 301-st to the 400-th samples. The rest of process data are collected under normal operating conditions. Figs. 2.4.8 and 2.4.9 show the PCA and angle based PCA dissimilarity methods. It is readily seen that the PCA method has a lengthy delay in alarming the faults while the PCA dissimilarity method cannot characterize the normal and faulty operating conditions. Thus, low fault detection rates for the PCA and PCA dissimilarity methods in comparison to the other methods are seen. The ICA based I^2 and SPE plots, as shown in Fig. 2.4.10, indicate that most of the faulty samples fall below the corresponding control limit lines resulting in an average fault detection rate of as low as 29.3%. Specifically for the drift error, the SPE index has a long delay of over 50 samples before triggering the fault alarms while the I^2 index misses a vast majority of the faulty samples. As shown in Fig. 2.4.11, the angle based ICA dissimilarity method does not appear to be much better in detecting the faulty points than the ICA method. Its fault detection rate is only 38.5% with more than 60% of faulty samples are undetected. In contrast, the monitoring result of the multidimensional mutual information based ICA dissimilarity index is shown in Fig. 2.4.12. It is obvious that the new dissimilarity method is able to accurately alarm the faulty operation with the high fault detection rate of 94.0%. Meanwhile, its false alarm rate is only 5.0% and much lower than that of the angle based ICA dissimilarity

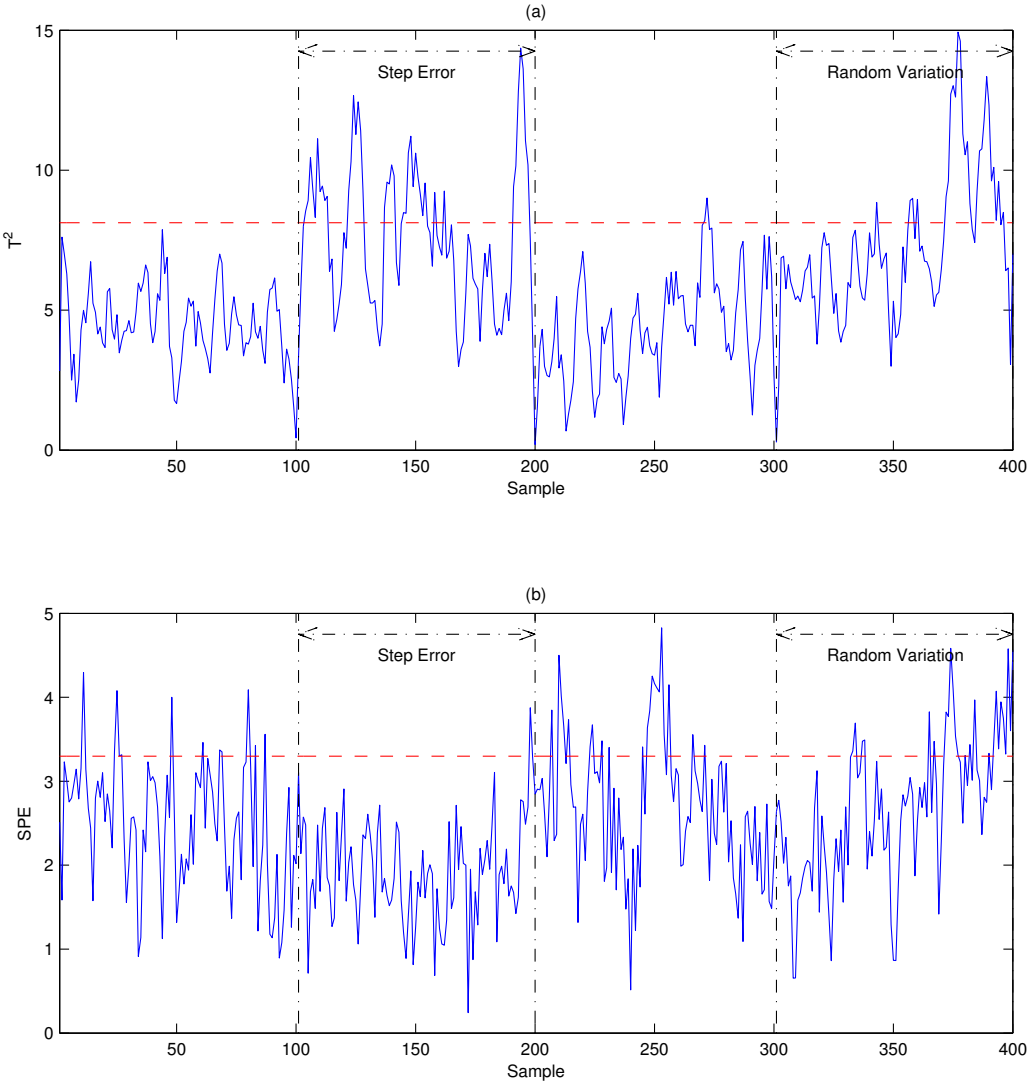

Figure 2.4.2: Monitoring Results of PCA Method in Test Case 1 of Tennessee Eastman Chemical Process

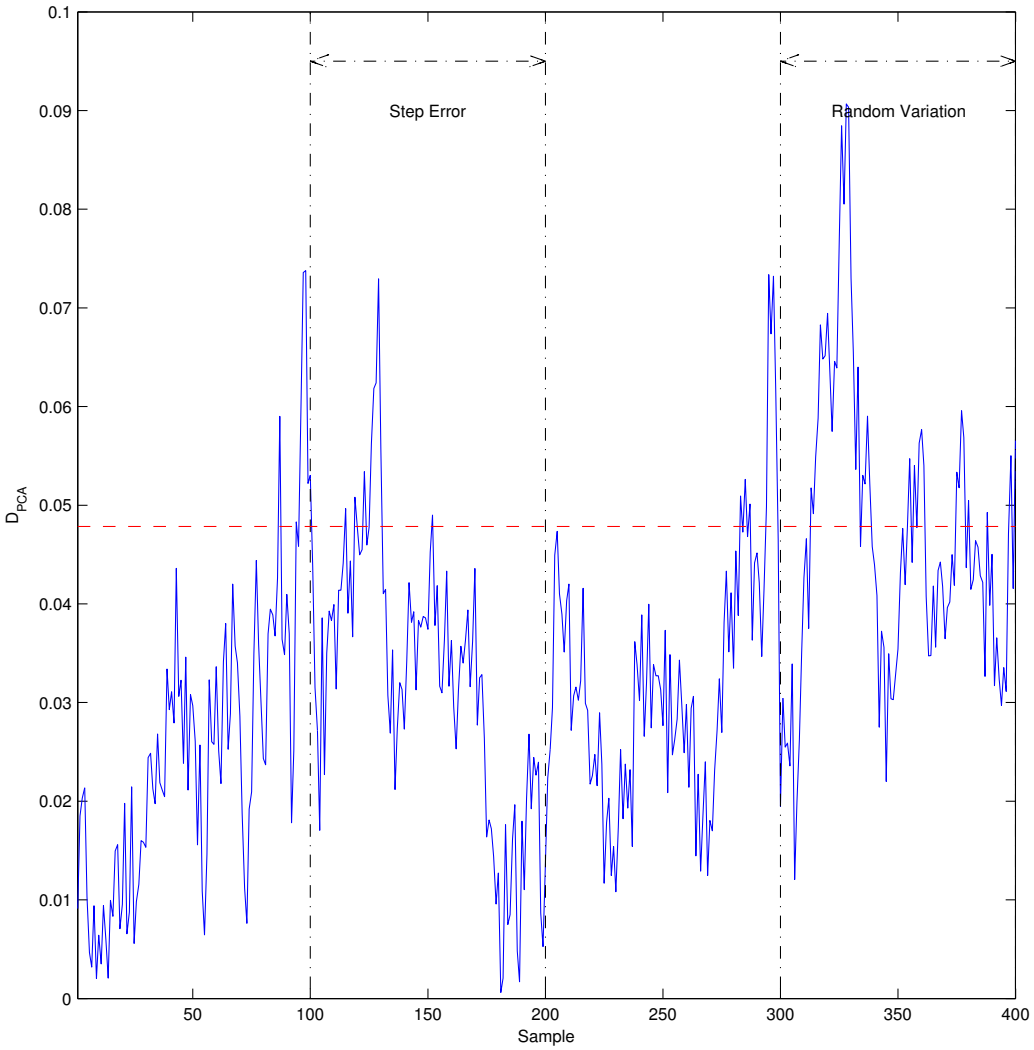

Figure 2.4.3: Monitoring Results of PCA Dissimilarity Method in Test Case 1 of Tennessee Eastman Chemical Process

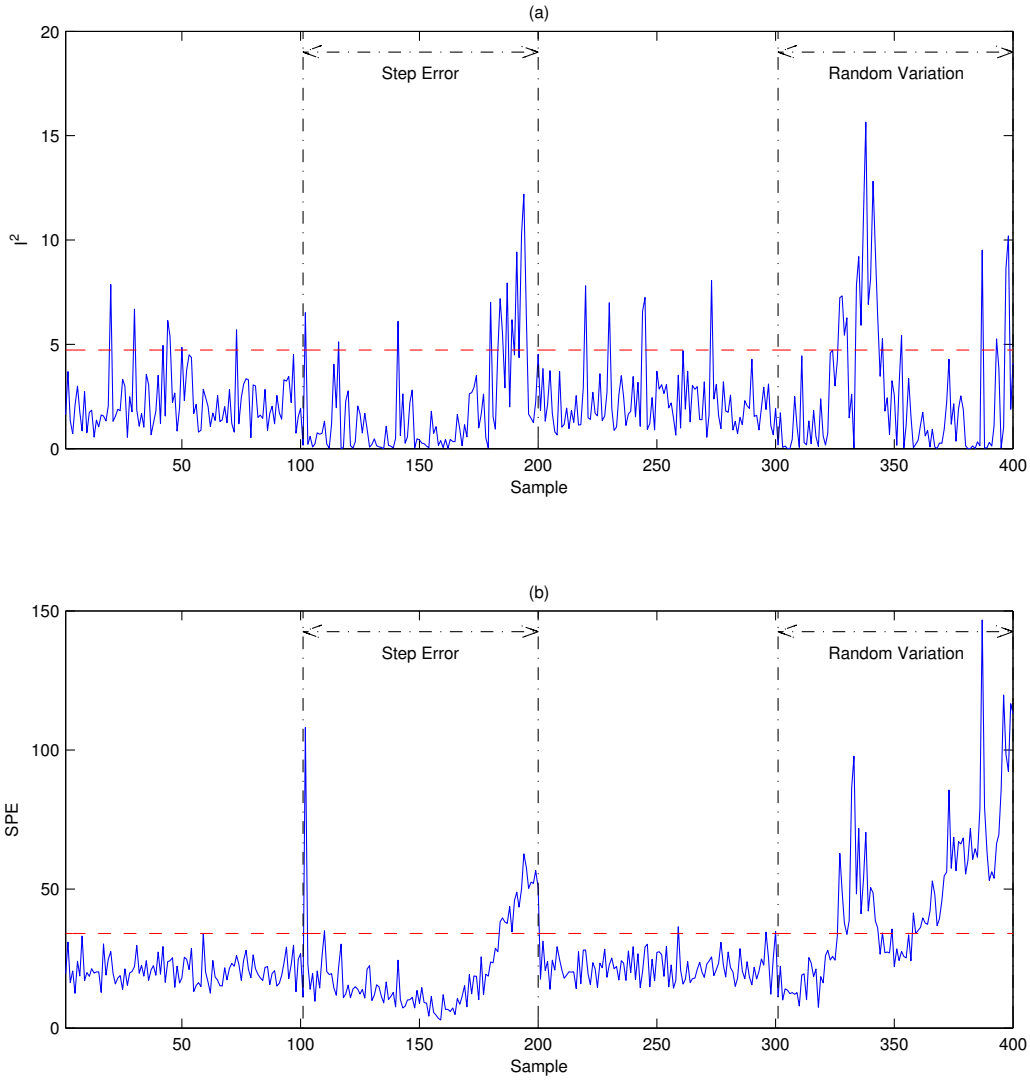

Figure 2.4.4: Monitoring Results of ICA Method in Test Case 1 of Tennessee Eastman Chemical Process

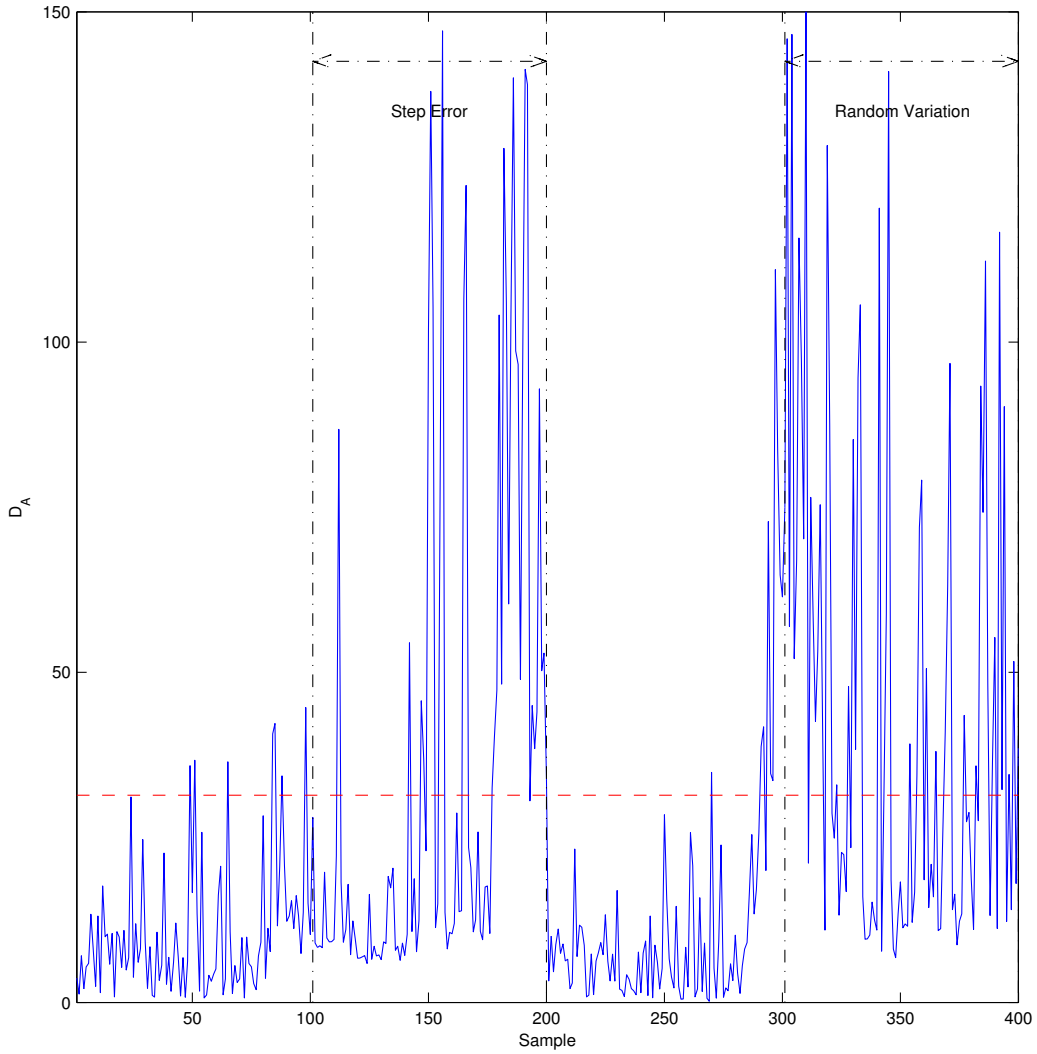

Figure 2.4.5: Monitoring Results of Angle Based ICA Dissimilarity Method in Test Case 1 of Tennessee Eastman Chemical Process

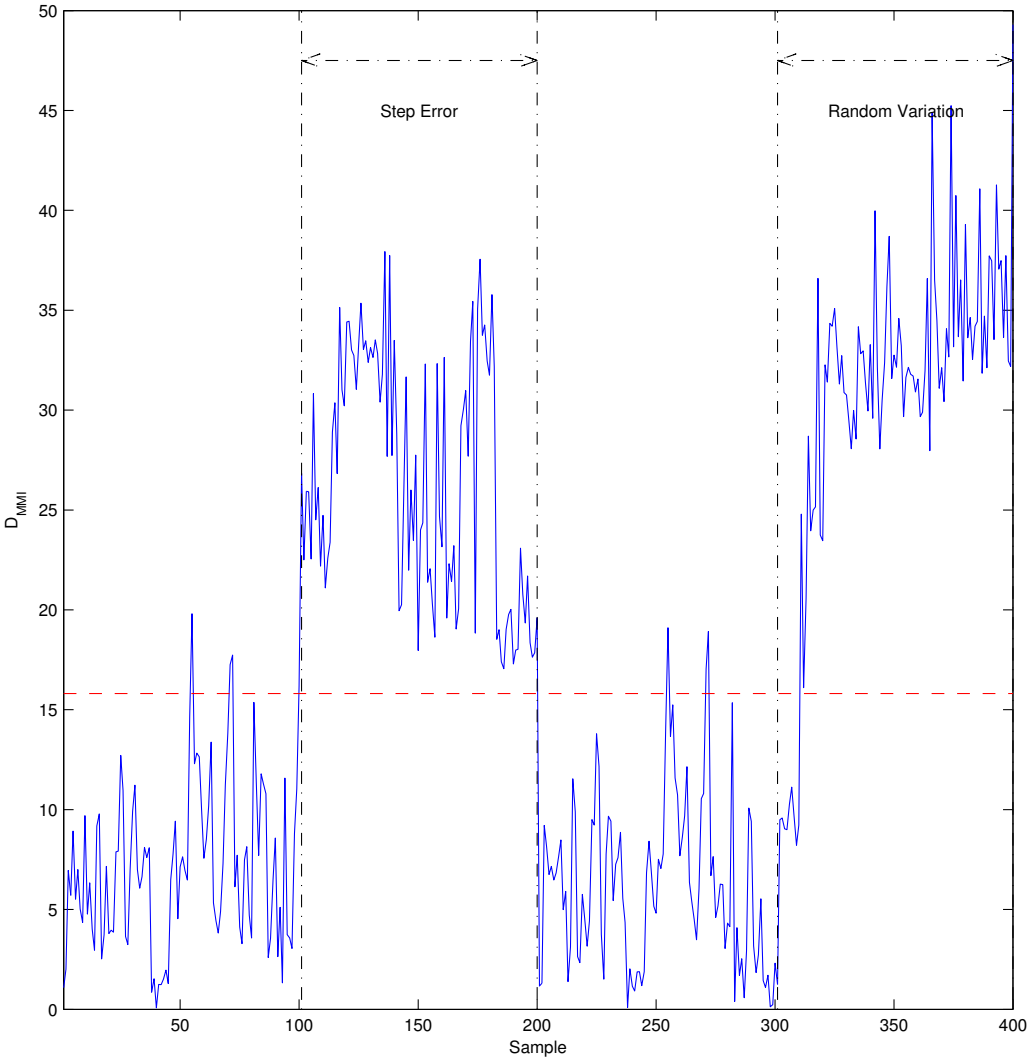

Figure 2.4.6: Monitoring Results of Multidimensional Mutual Information Based ICA Dissimilarity Method in Test Case 1 of Tennessee Eastman Chemical Process

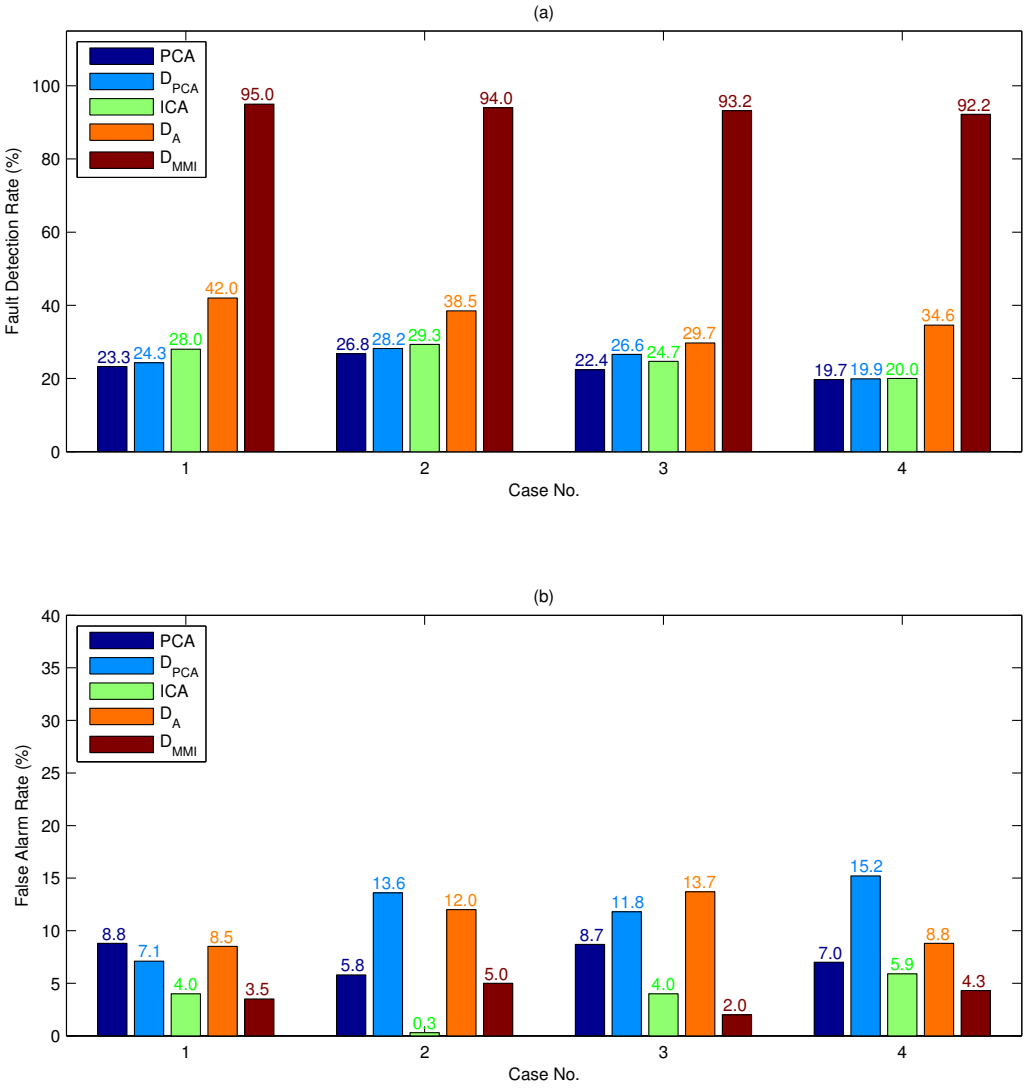

Figure 2.4.7: Comparison of Fault Detection and False Alarm Rates for PCA, PCA Dissimilarity, ICA, Angle Based ICA Dissimilarity and Multidimensional Mutual Information Based ICA Dissimilarity Methods

method (12.0%) and PCA based dissimilarity method (13.6%). It should be noted that the abnormally low false alarm rate (0.3%) of the ICA method is due to its insensitivity to the process faults. In this case, the MMI based ICA dissimilarity method still performs the best among all the monitoring approaches.

A more complex test scenario is considered in the third case, which involves three different types of process faults (a step error, a feed loss, and a slow drift error) among the normal operation periods. The fault detection results of the various process monitoring methods are shown in Figs. 2.4.13 to 2.4.17, respectively. It is seen that the T^2 and SPE statistics of the PCA based monitoring method cannot handle the dynamic and non-Gaussian data resulting in the poor monitoring performance seen. Although the feed loss fault is detectable, the fault is alarmed after nearly half the faulty samples are misclassified as normal. Similar to PCA, the PCA based dissimilarity index also cannot extract the non-Gaussian features for monitoring, resulting in a low fault detection rate of of just 26.6%. Moreover, the ICA based I^2 index misses most of the faulty samples with extremely low fault detection capacity. Though the SPE index has relatively higher sensitivity to the three types of faults, the long delays of fault detection are still unacceptable. The average fault detection rate of ICA monitoring method is only 24.7%. The angle based ICA dissimilarity method leads to a similar fault detection rate of 29.7% with many undetected faulty samples especially during the abnormal operation events of feed loss and drift error, as shown in Fig. 2.4.16. Meanwhile, its false alarm rate is as high as 13.7%. The MMI based ICA dissimilarity approach, however, shows the strongest fault detection capability along with the highest fault detection rate of 93.2% while the lowest false alarm rate of 2.0%. As easily observed from Fig. 2.4.17, the D_{MMI} index is able to distinguish between the normal and faulty operations with high accuracy, which apparently cannot be achieved by the monitoring methods.

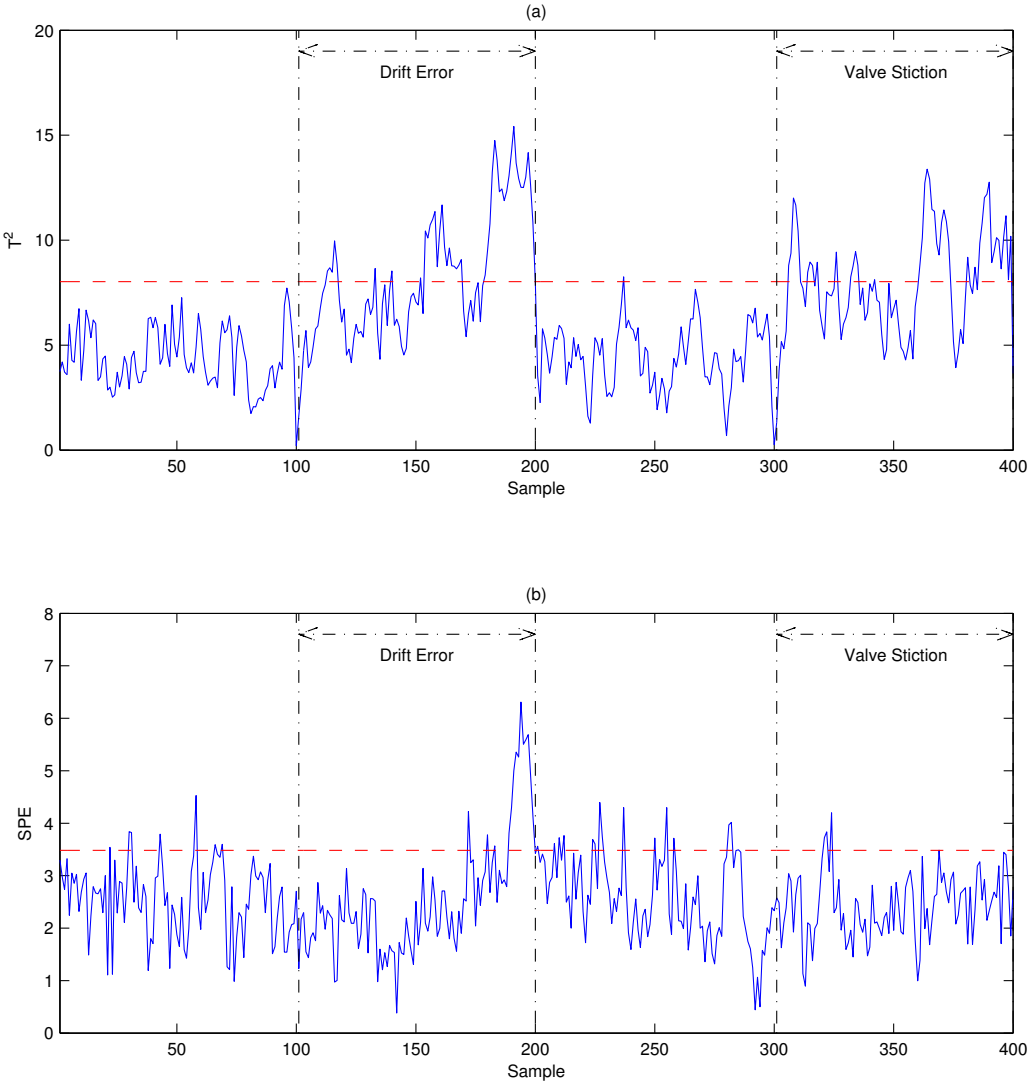

Figure 2.4.8: Monitoring Results of PCA Method in Test Case 2 of Tennessee Eastman Chemical Process

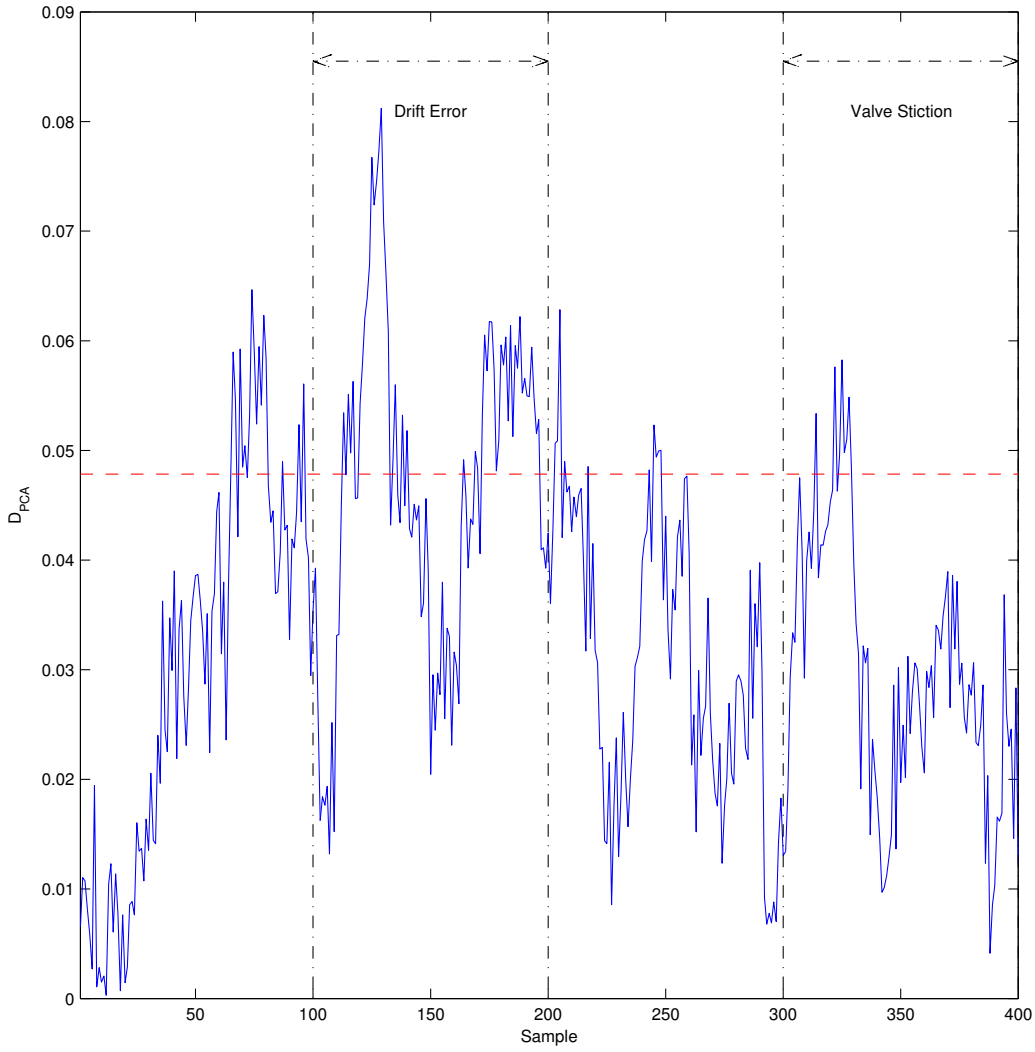

Figure 2.4.9: Monitoring Results of PCA Dissimilarity Method in Test Case 2 of Tennessee Eastman Chemical Process

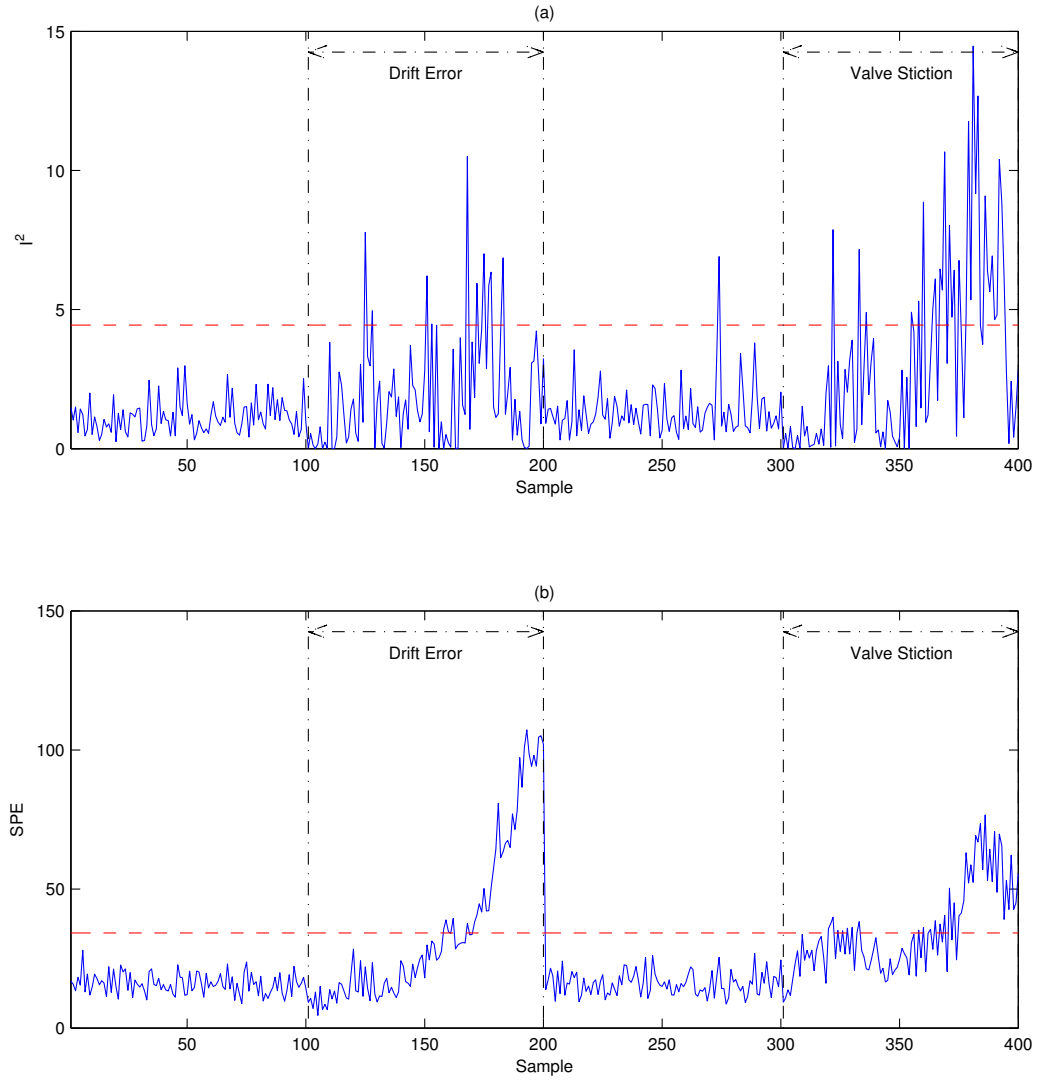

Figure 2.4.10: Monitoring Results of ICA Method in Test Case 2 of Tennessee Eastman Chemical Process

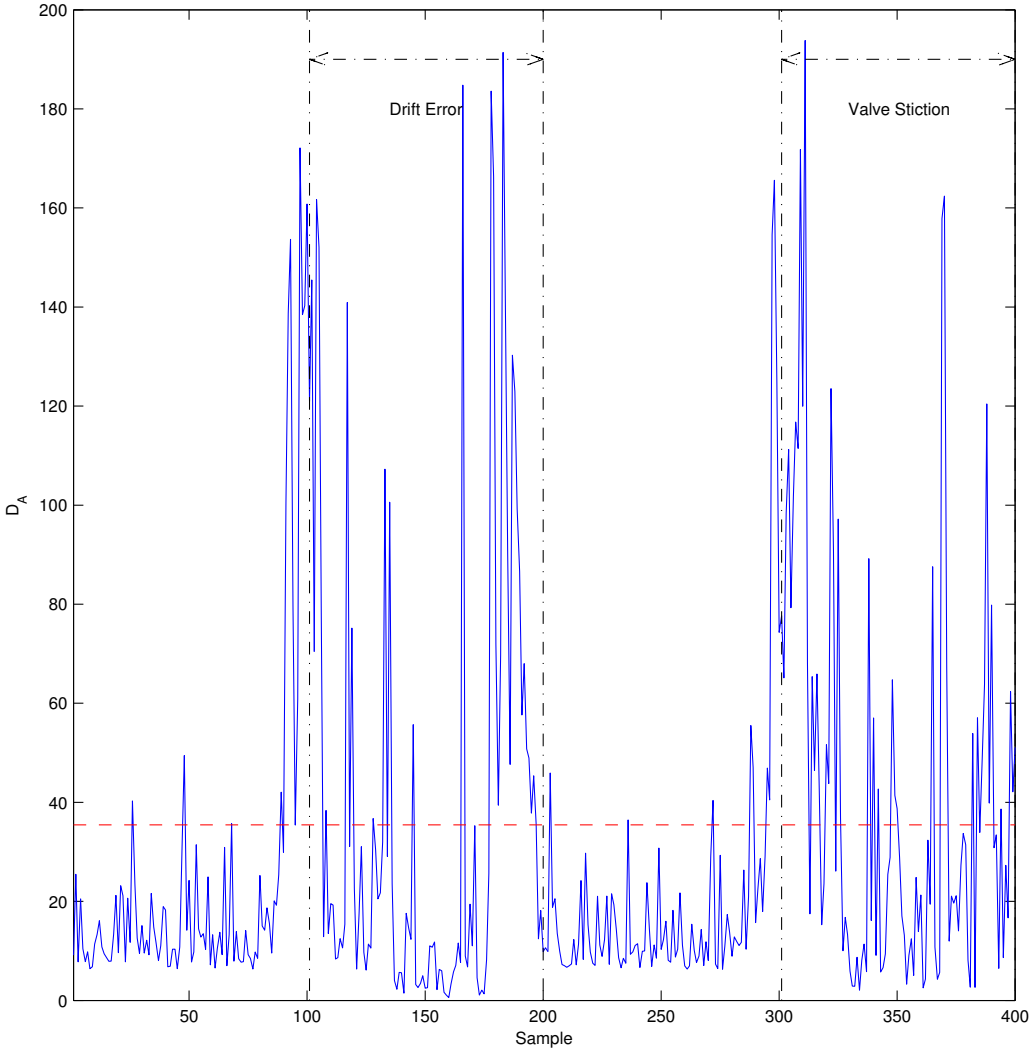

Figure 2.4.11: Monitoring Results of Angle Based ICA Dissimilarity Method in Test Case 2 of Tennessee Eastman Chemical Process

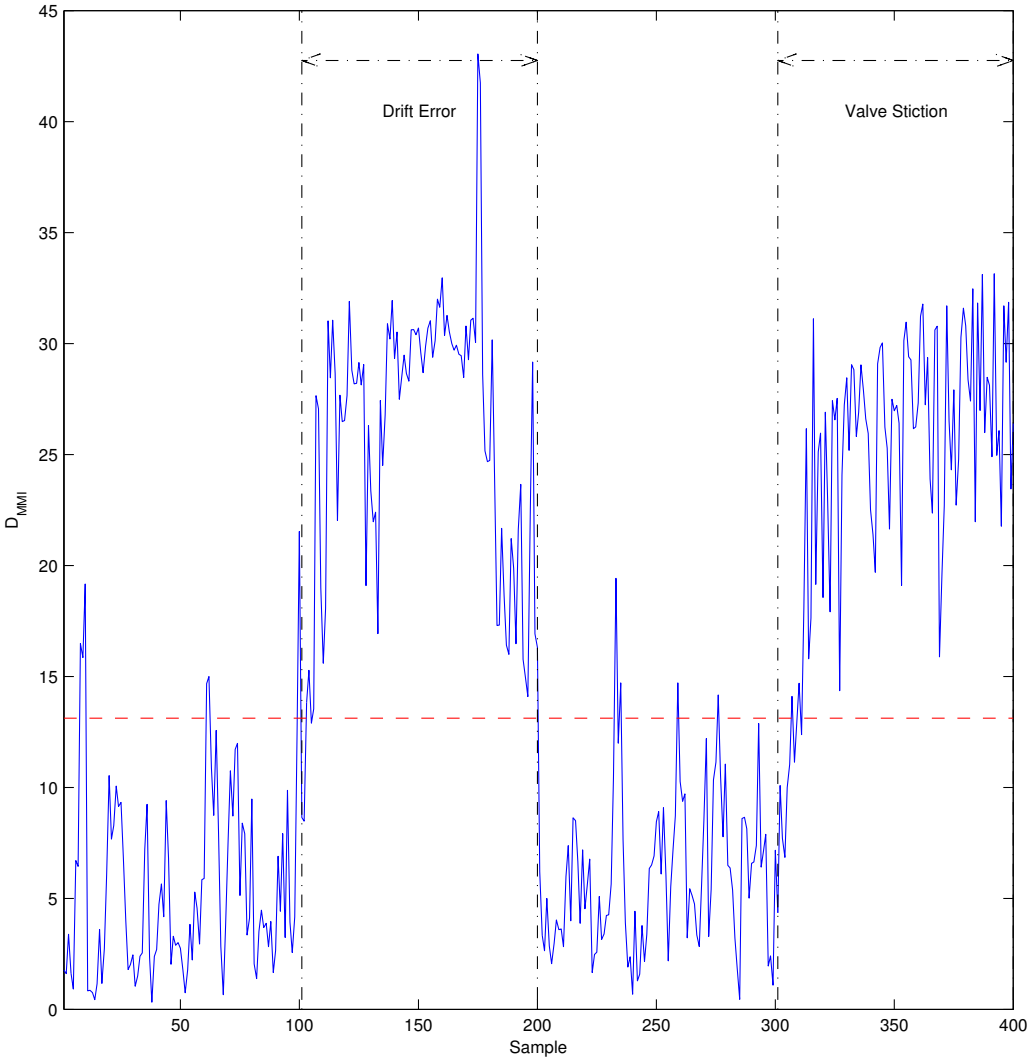

Figure 2.4.12: Monitoring Results of Multidimensional Mutual Information Based ICA Dissimilarity Method in Test Case 2 of Tennessee Eastman Chemical Process

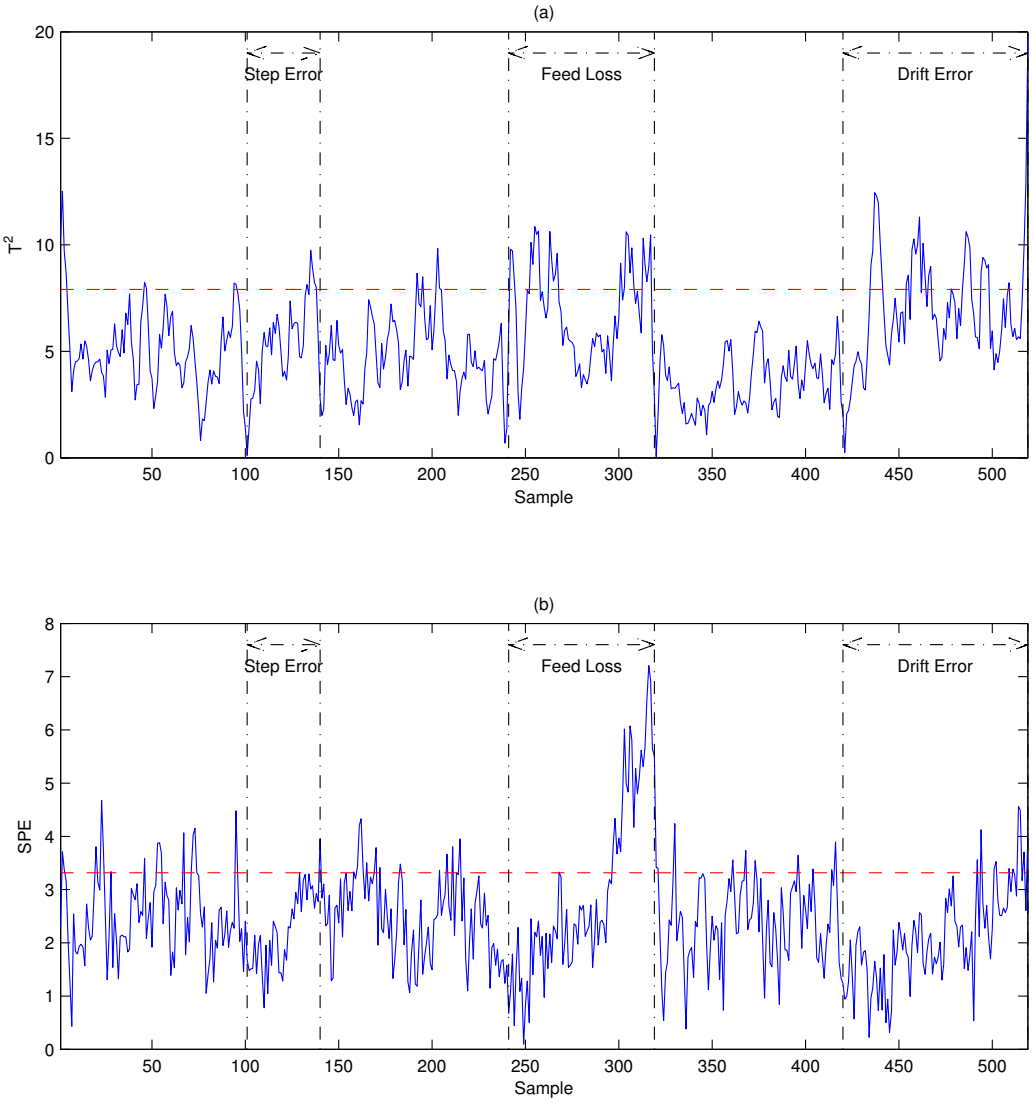

Figure 2.4.13: Monitoring Results of PCA Method in Test Case 3 of Tennessee Eastman Chemical Process

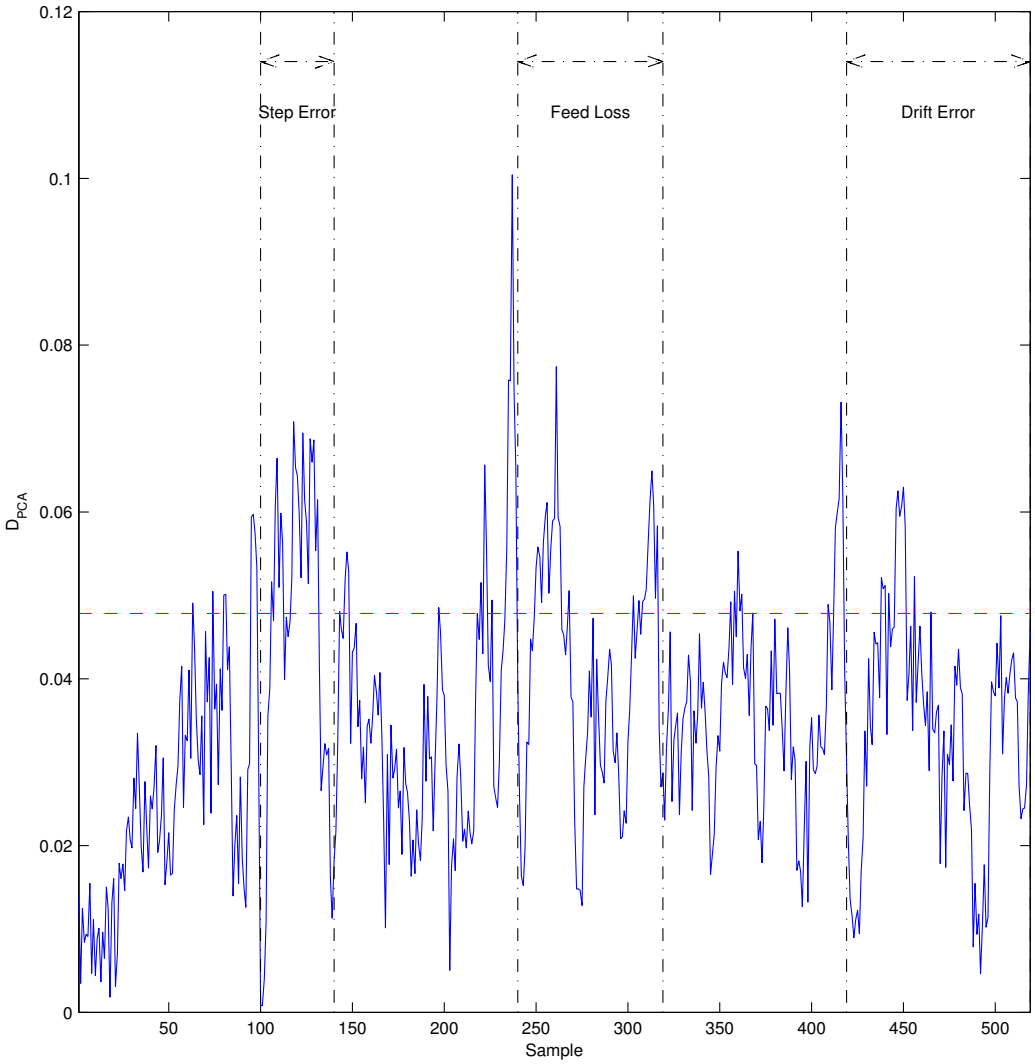

Figure 2.4.14: Monitoring Results of PCA Dissimilarity Method in Test Case 3 of Tennessee Eastman Chemical Process

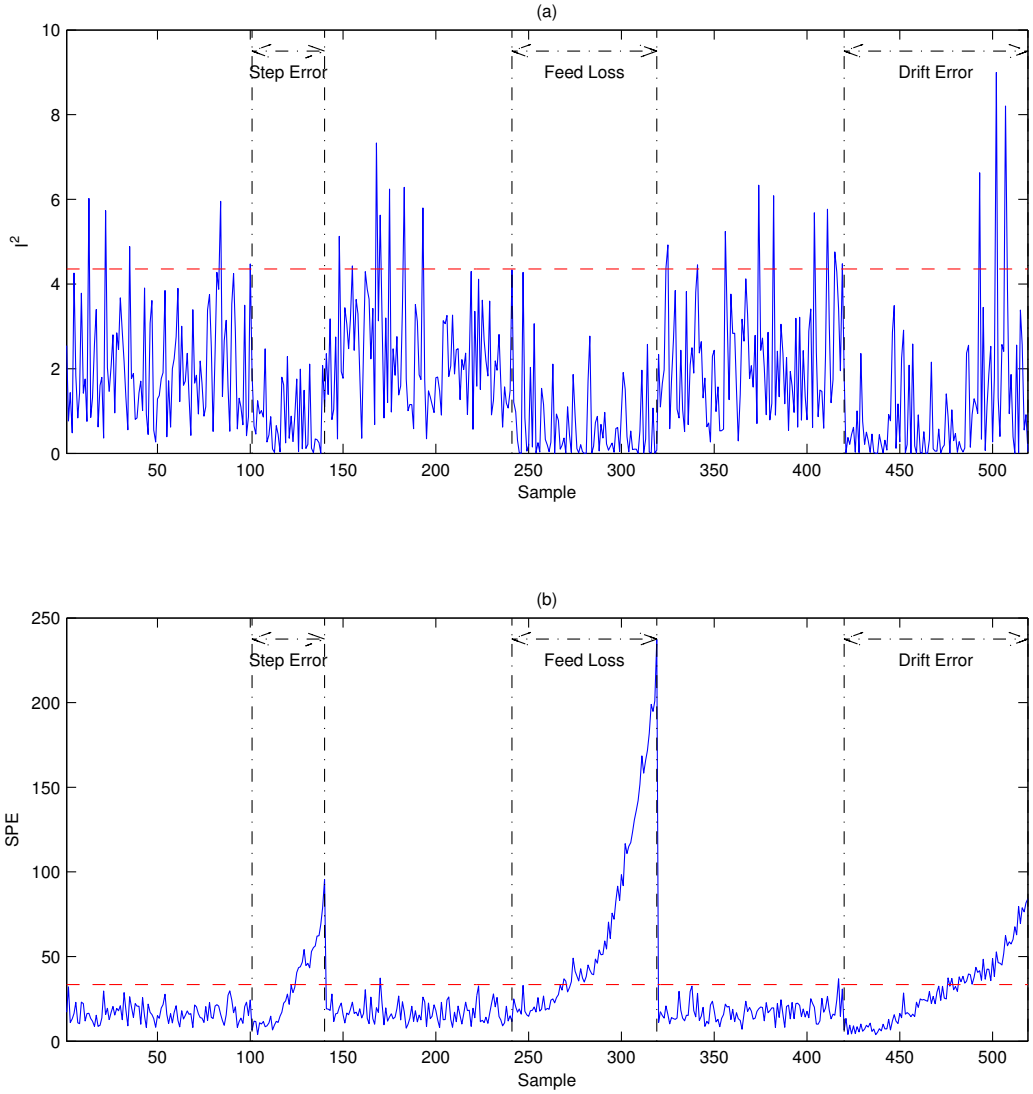

Figure 2.4.15: Monitoring Results of ICA Method in Test Case 3 of Tennessee Eastman Chemical Process

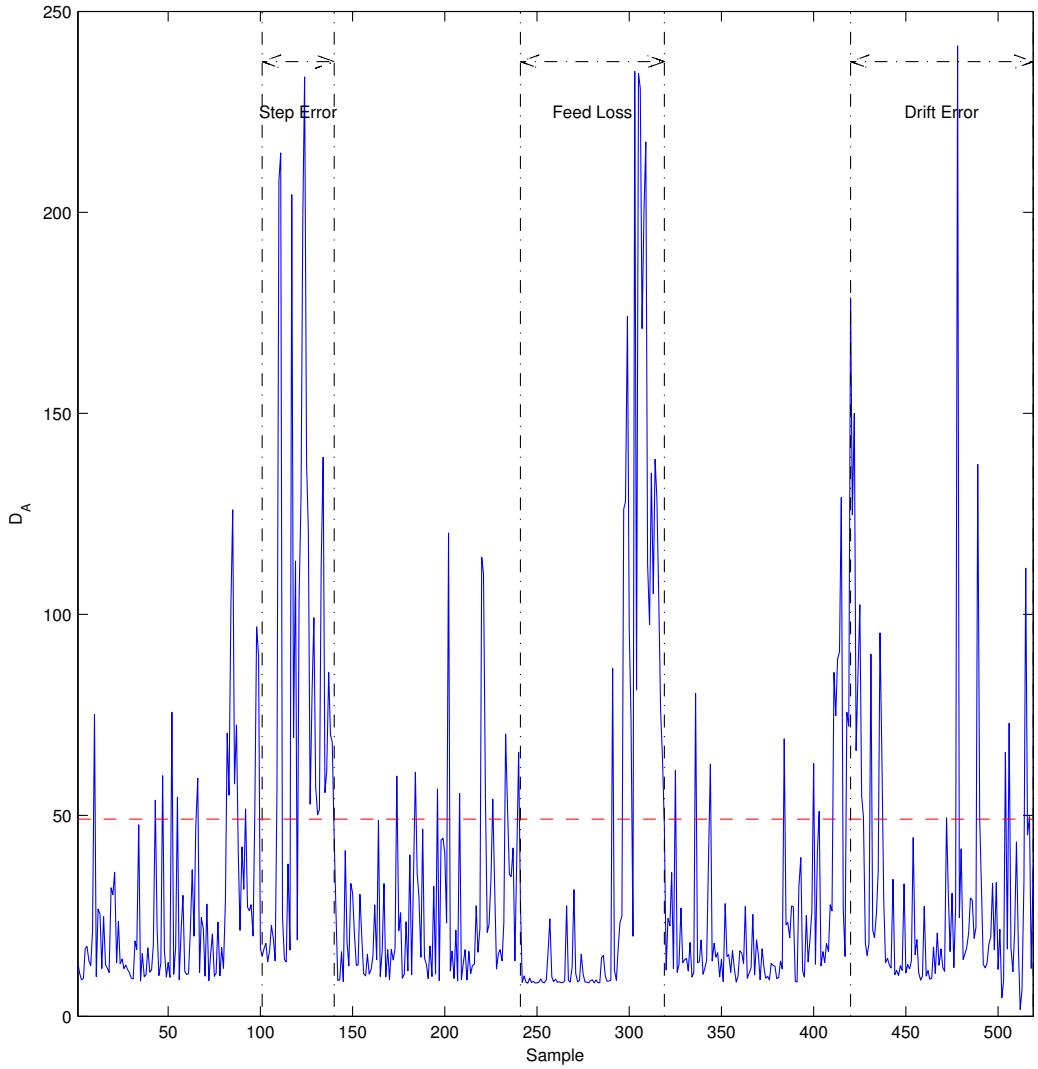

Figure 2.4.16: Monitoring Results of Angle Based ICA Dissimilarity Method in Test Case 3 of Tennessee Eastman Chemical Process

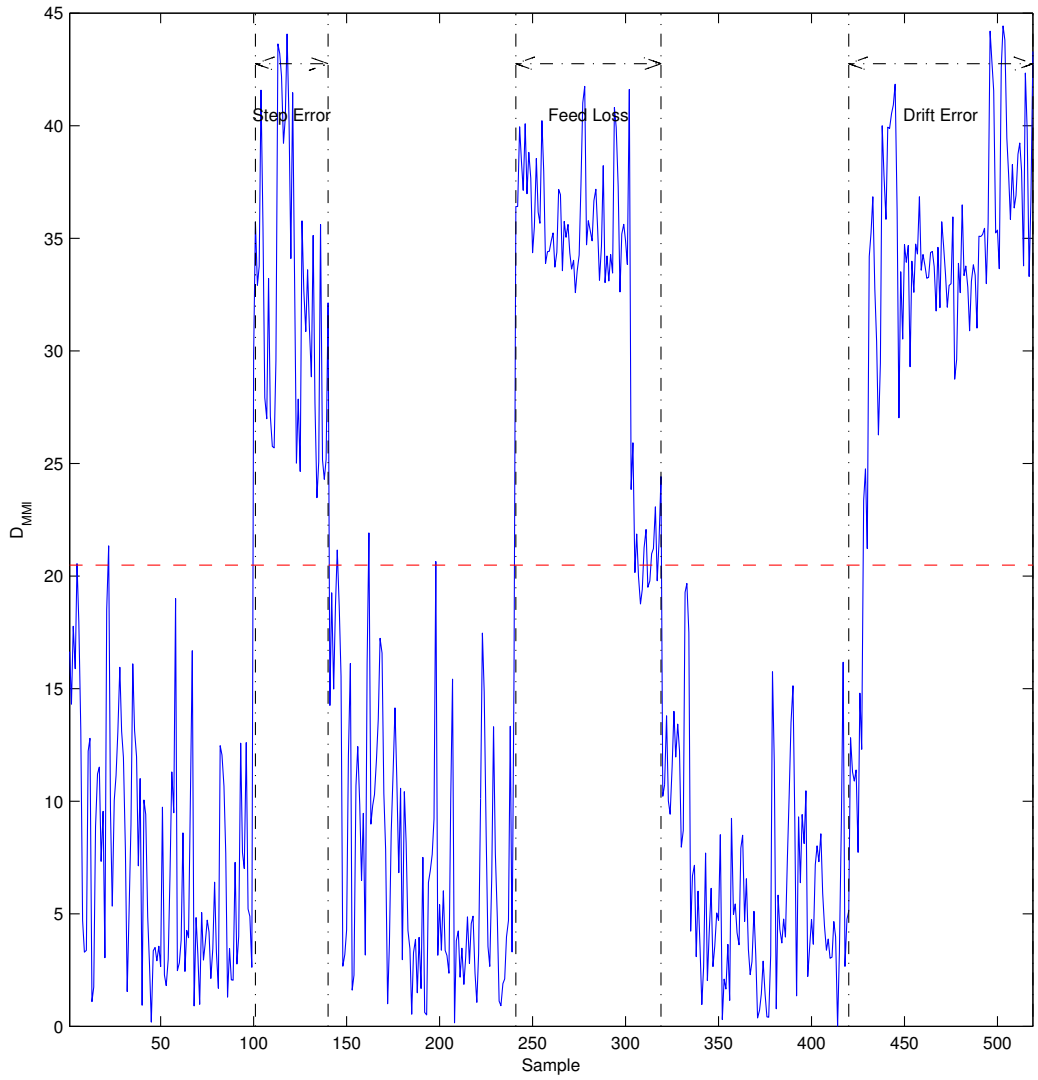

Figure 2.4.17: Monitoring Results of Multidimensional Mutual Information Based Dissimilarity Method in Test Case 3 of Tennessee Eastman Chemical Process

In the last test case, the normal process operation is mixed with four types of abnormal events, which are step change in B composition and A/C ratio, C head pressure loss, valve stiction of condenser cooling water flow, and an unknown process disturbance. Similar to the previous cases, the PCA and PCA dissimilarity methods fail to accurately detect the faulty samples, as seen in Figs. 2.4.18 and 2.4.19, respectively. The PCA based methods cannot extract the non-Gaussian features of the measurement data with only the pressure loss fault being detected with reasonable accuracy, resulting in low overall fault detection rates of below 20%. Also, it is noted that the false alarm rate of the PCA dissimilarity method is the highest among all other methods at over 15.0%. Moreover, the ICA method does not perform well in fault detection, as seen in Fig. 2.4.20. The I^2 statistic is insensitive to most types of faults except the pressure loss that is partially detected. Similarly, the SPE index can identify the pressure loss but has substantial delays in detecting valve stiction and unknown disturbance. Hence, an average fault detection rate of 20.0% is obtained from the ICA based monitoring method along with the false alarm rate of 5.9%. As a comparison, the angle based dissimilarity method does not perform significantly better than ICA method in capturing process abnormalities with only slightly higher fault detection rate of 34.6%. Despite an improvement over ICA method, the angle based dissimilarity index still misses over 60% of faulty samples without any alarms. Moreover, the false alarm rate of the angle based dissimilarity method is the second highest among the monitoring approaches. In contrast, the multidimensional mutual information based dissimilarity approach leads to much better monitoring results than the other two methods. As shown in Fig. 2.4.7, its fault detection rate reaches 92.2% while the false alarm rate is as low as 4.3% even in the most complex test scenario with four different types of faults. This case further verifies the superiority of the MMI based ICA dissimilarity method with respect to the conventional approaches in process monitoring and fault detection.

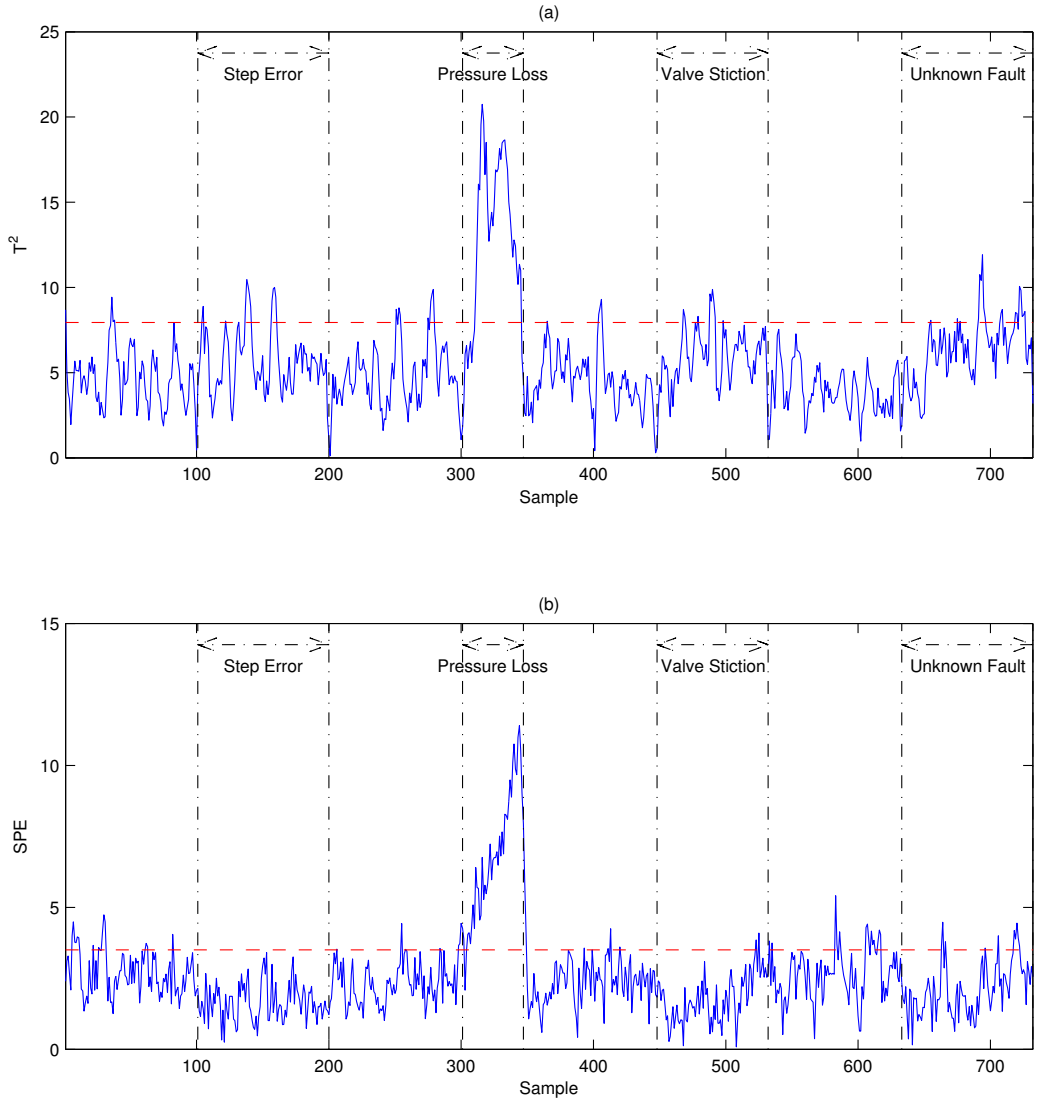

Figure 2.4.18: Monitoring Results of PCA Method in Test Case 4 of Tennessee Eastman Chemical Process

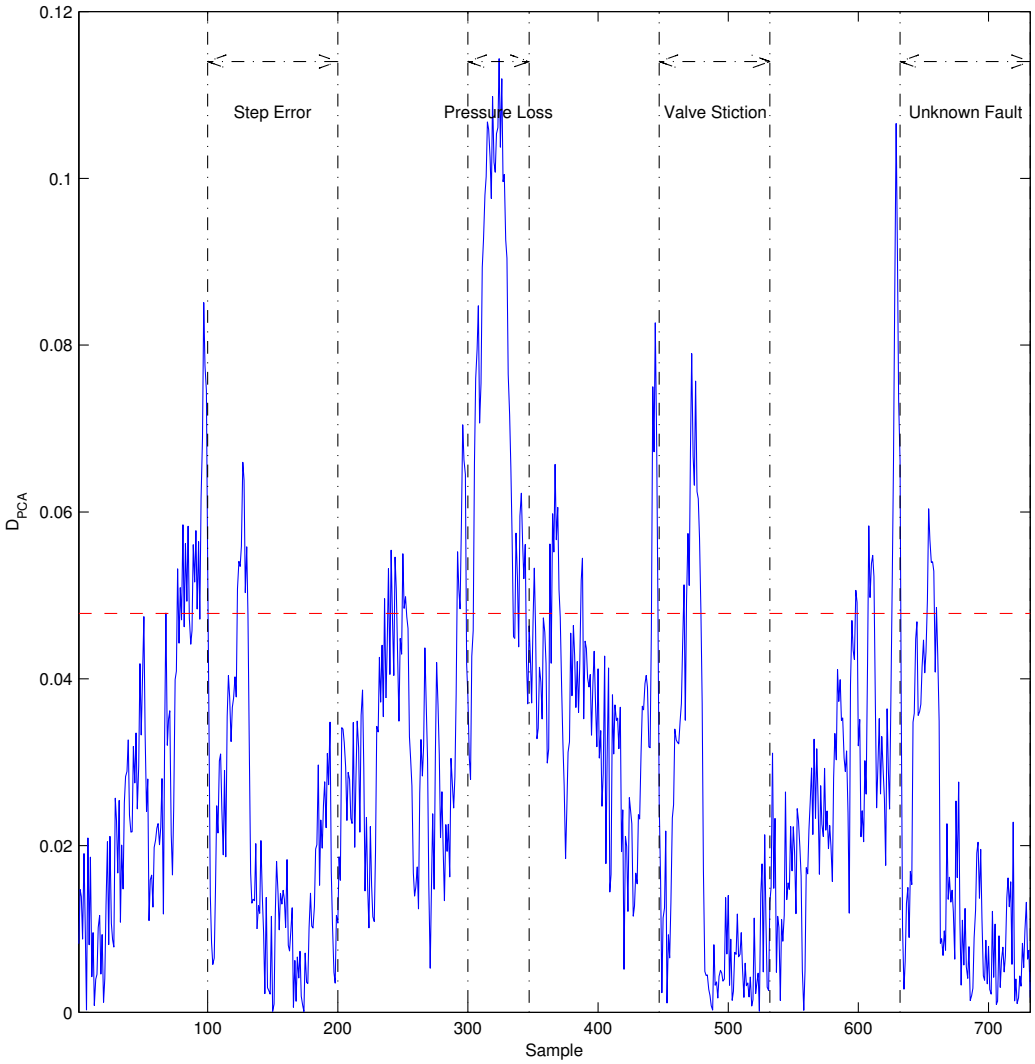

Figure 2.4.19: Monitoring Results of PCA Dissimilarity Method in Test Case 4 of Tennessee Eastman Chemical Process

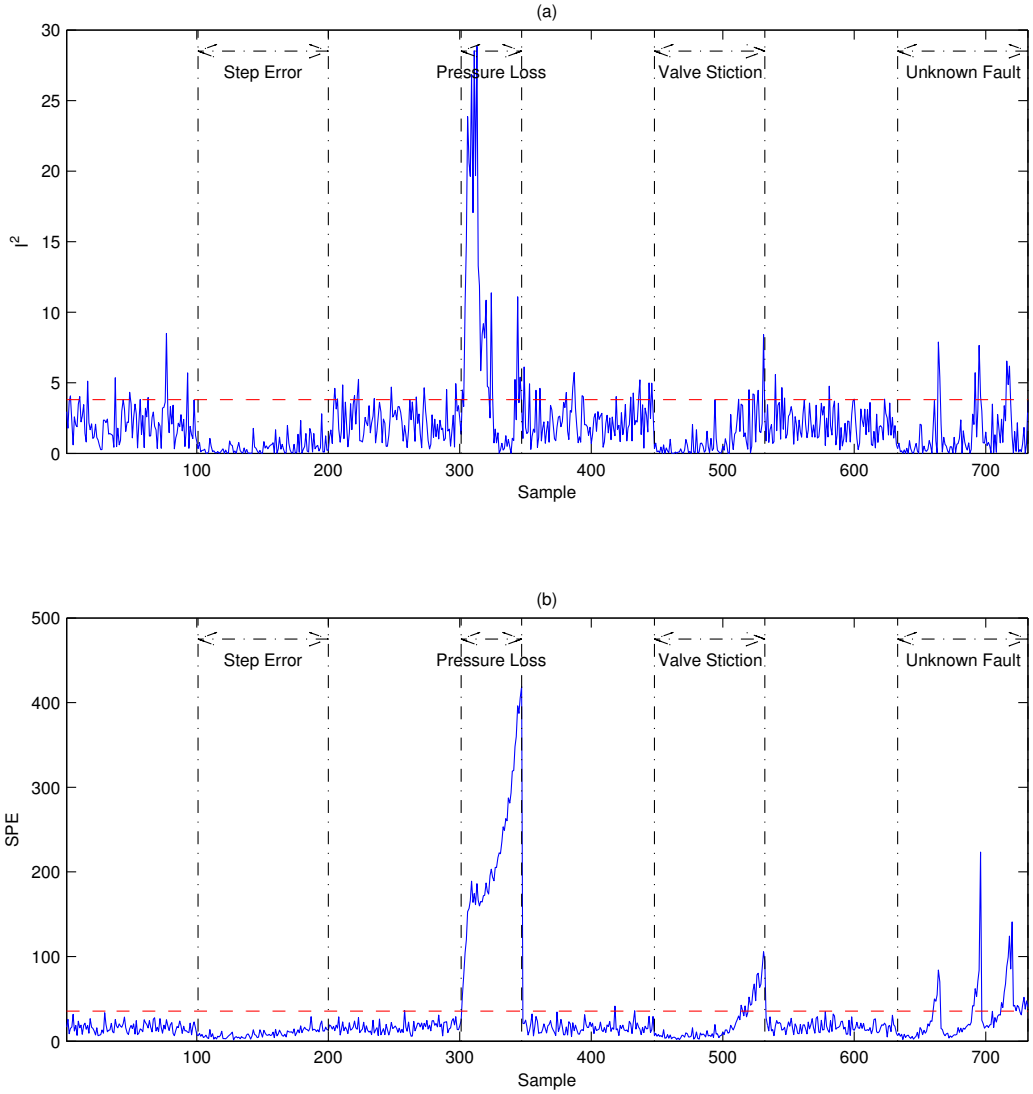

Figure 2.4.20: Monitoring Results of ICA Method in Test Case 4 of Tennessee Eastman Chemical Process

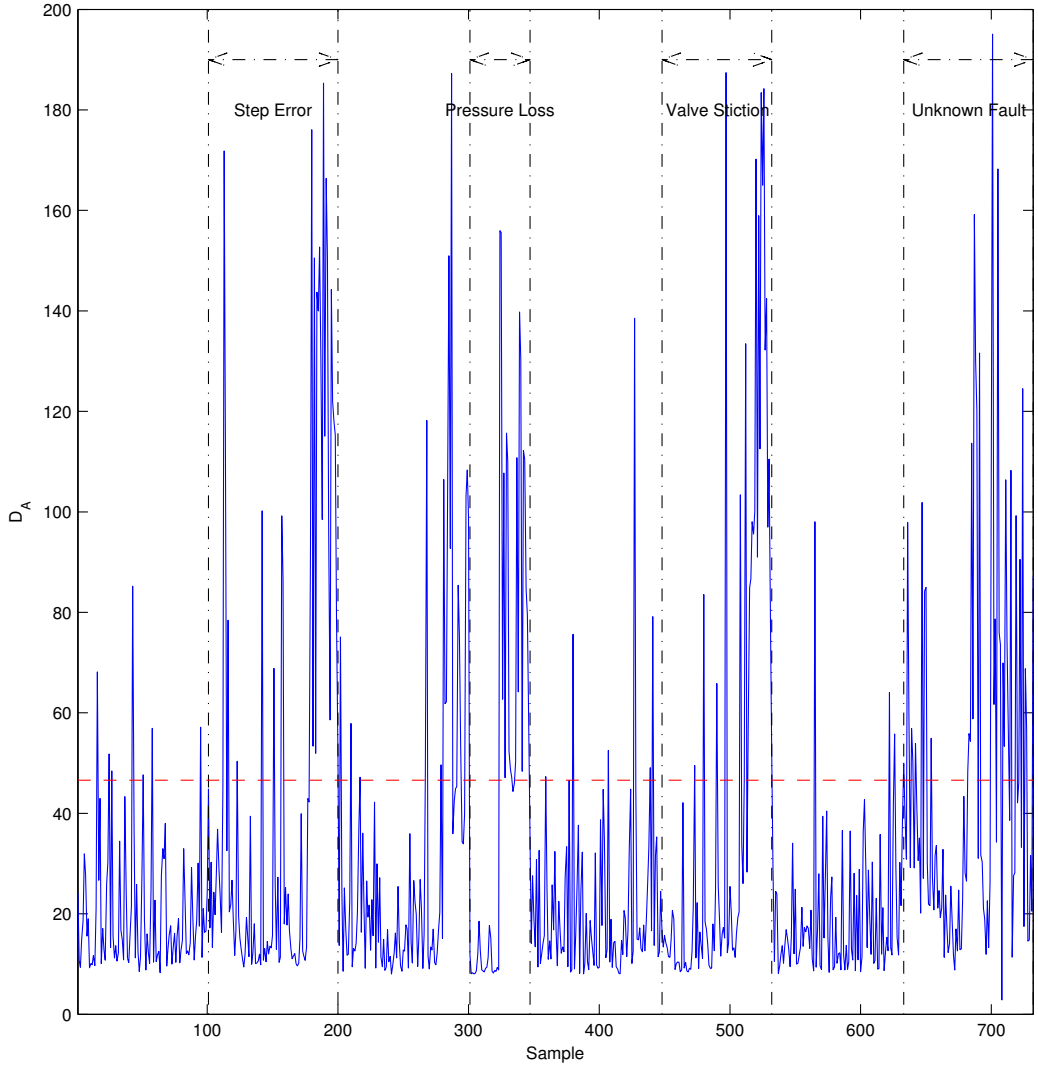

Figure 2.4.21: Monitoring Results of Angle Based ICA Dissimilarity Method in Test Case 4 of Tennessee Eastman Chemical Process

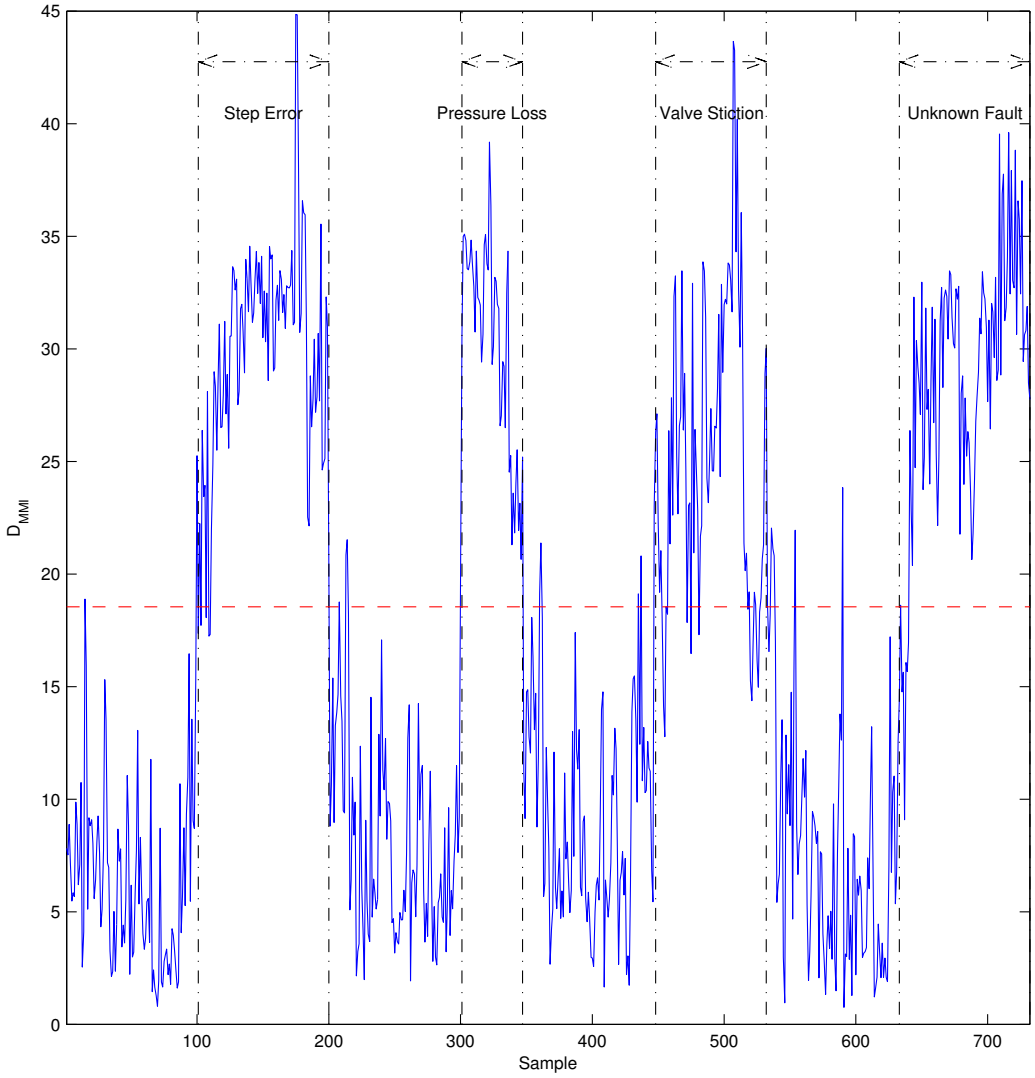

Figure 2.4.22: Monitoring Results of Multidimensional Mutual Information Based ICA Dissimilarity Method in Test Case 4 of Tennessee Eastman Chemical Process

2.5 CONCLUSIONS

A novel multidimensional mutual information based dissimilarity index is proposed and integrated with independent component analysis to monitor non-Gaussian processes in this article. The presented approach uses entropy based mutual information to assess the dissimilarity between the multidimensional independent component subspaces of the benchmark and monitored sets. The higher-order statistics underlying the dissimilarity index can help extract the non-Gaussian features and quantify the statistical dependency between IC subspaces on a moving-window basis. Thus the non-Gaussian dynamic processes can be effectively monitored through the continuous comparison between the normal benchmark and monitored data sets. The MMI based ICA dissimilarity method is applied to four test cases of the Tennessee Eastman Chemical process. The comparison of monitoring results demonstrates that the new mutual information based dissimilarity index is superior to regular PCA, angle based PCA dissimilarity, conventional ICA and angle based ICA dissimilarity methods with the most reliable fault detection capability. Future work may focus on the fault diagnosis part through the dissimilarity based pattern identification to isolate the faulty variables.

CHAPTER 3

MULTI-RATE MODELING AND ECONOMIC MODEL PREDICTIVE CONTROL[†]

3.1 Introduction

Electric arc furnaces (EAF) play a prominent role in the steel industry and are widely used for recycling scrap metal. Operated primarily as batch processes (a batch is referred to as a heat), EAFs melt the scrap and adjust the chemical composition of the molten metal to obtain steel of the desired product grade. The required melting of steel scrap results in a highly energy intensive process, necessitating efficient operation. Given that the feed to the EAF, from recycled steel, comes from diverse sources with obscure compositions that vary significantly, efficient operation can only be achieved via an online measurement and

[†]The results in this chapter have been published in:

- M. M. Rashid, P. Mhaskar, and C. L. E. Swartz. Multi-rate modeling and economic model predictive control of the electric arc furnace. *J. Proc. Cont.*, 40:50–61, 2016.
- M. M. Rashid, P. Mhaskar, and C. L. E. Swartz. Economic model predictive control of the electric arc furnace using data-driven multi-rate models. In *Proceedings of the 2016 American Control Conference*, Boston, MA, 2016.

feedback control strategy. Closed-loop control of the EAF, however, presents a challenging problem due to the lack of on-line measurements of key process variables. This complicates both the model development and control implementation steps.

One approach to modeling and control of the EAF process in particular [40–44], and batch processes [45, 46] in general, is to develop first-principles/mechanistic models, and use them for the purpose of optimization. Note that while a first-principles model provides excellent predictive capabilities when sufficient measurements are available to uniquely estimate the associated parameters, the resultant optimization problem is often quite computationally complex, and difficult to solve and implement in real-time. To address these challenges, recent results have exploited the structure of the optimization problem to identify the shape of the optimal constraints, which can then be parameterized and readily updated online [47, 48]. More recently, the concept of reachability regions is used to implement model predictive control strategies where the controller, instead of trying to drive the process to the desired end-point at all computation times, guides the process through the reachability regions (computed off-line) [49, 50]. Another effort to shift the computational effort to an offline step includes design of explicit model predictive control involving multi-parametric programming, where the state of the system is represented as a vector of parameters so that the optimal solution for all possible realizations of the state vector can be pre-computed as explicit functions [51, 52]. While these approaches mitigate the online computation aspect of the problem, the problem of developing and implementing a first-principles model-based controller remains a challenging task.

The first-principles model-based control approaches typically require initialization of the nonlinear process models using an effective state estimator so that the necessary feedback control actions can be applied. However, inferring the states of the EAF process based on the available process data is not a trivial task due to the lack of frequent on-line measurements.

Furthermore, the fast convergence of the state estimator from initialization errors and the ability to handle measurement noise are critical, and may not be achieved with the limited, infrequent sampling rate for the EAF process variables.

One approach to address these practical problems is through use of simpler, data-driven model-based controller. However, in developing data-driven models, the identification experiments traditionally utilized to build empirical models, while suitable for identification at steady-state operating conditions, are often too expensive to justify for batch systems. In particular, identification techniques that require the implementation of a pseudo-random binary sequence (PRBS) on the process, may result in off-spec product, and thus wastage of expensive batches, making them economically infeasible. Thus, for batch systems, the available plant data is essentially limited to the historical databases comprised of prior batches (possibly augmented with a limited number of identification experiments). Furthermore, the process dynamics of batch systems are typically highly nonlinear, and they are not operated around an equilibrium point, thus making conventional system identification approaches, where a single linear model is identified, ill-suited for identifying an accurate dynamic model.

One general strategy to describe nonlinear behavior while retaining the simplicity of linear models is to partition/cluster the training data into a number of different regions, identify local linear models for each region, and combine them with appropriate weights in an attempt to describe the global nonlinear behavior. This idea has been formalized in piece-wise affine (PWA) [53], Takagi, Sugeno, and Kang (TSK) [54], and operating-regime based [55] modeling. Recently, a new multi-model approach, specific to batch processes, was proposed that unifies the concepts of dynamic modeling, latent variable regression techniques, fuzzy c-means clustering, and multiple local linear models in an integrated framework to capture the nonlinear nature of batch data [56]. The key delineating aspects of the work are the integration of the clustering algorithm used to partition the training data, the use of latent variable tools

to estimate the model parameters, and the utilization of a generalized continuous weighting function that is entirely data dependent and does not require precise process knowledge [56]. Additionally, the resulting model is readily applicable in an online optimization framework [57]. The model development in these approaches, however, assumes the process measurements to be available at the same sampling rate, motivating the need to generalize these results for the case of the EAF process, where measurements are available at different sampling rates.

Regardless of the nature of the model used, the control problem can benefit from utilizing notions of economic control recently proposed for continuous processes [58–62]. The key idea in these developments is that the controller determines the set-point internally to satisfy the prescribed economic objective, and requires a rigorous analysis to ensure stability is preserved. In contrast, the batch control problem requires driving the process to a target that is often not a steady-state, but is the desired end-point. Online control of EAF processes therefore stands to gain from incorporation of economic considerations in the control implementation. Motivated by the above considerations, this work addresses the problem of economic model predictive control (EMPC) of the electric arc furnace using data-driven models. To this end, we first review the electric arc furnace process, and present a first-principles model that we utilize as a test-bed to implement and validate the proposed approach. We also review the existing data-driven multi-model approach for batch process control in Section 3.2. Subsequently, multi-rate models are proposed in Section 3.3.1 that incorporate infrequent and frequent measurements to improve the predictions of the process variables. In Section 3.3.2, multi-rate models for the EAF process are computed. In Section 3.4.1 a two-tiered economic MPC is developed. In the first tier, the best achievable product (in terms of meeting product specifications) is determined by penalizing the deviation of the end-point variables from the desired target, while accounting

for the input constraints in the optimization problem. Then, in the second layer, the optimal inputs are computed where the best achievable end-point (computed using the first layer) is imposed as a constraint, with economic requirements specified in the objective function. The proposed two-tiered economic MPC method and the closed-loop simulation results demonstrating its effectiveness are presented in Section 3.4.2. The conclusions of this work are summarized in Section 3.5.

3.2 PRELIMINARIES

A description of the electric arc furnace process is provided below, followed by the description of the test-bed model, and the aspects of the simulation designed to replicate practical application issues. Then a review of an existing data-driven multi-model approach for batch process control is presented.

3.2.1 ELECTRIC ARC FURNACE PROCESS

The EAF is a batch process that involves a series of distinct operating phases that include the initial charging of the batch, followed by preheating, melting and tapping of the furnace. The scrap charge is generally comprised of a variety of sources selected based on a number of factors such as the availability of each scrap source and the desired product grade. Typically, two or three loads of scrap are charged in each batch depending on the bulk density of the scrap and the volume of the furnace. The furnace charge may also be supplemented with some direct reduced iron (DRI) or pig iron for chemical balance and to improve production yields. Once the batch is charged, the EAF is preheated through natural gas combustion to raise the temperature of the steel. Subsequent to preheating, electrodes are lowered into the furnace and the electric power is turned on to an intermediate voltage while the electrodes bore into

the scrap. The voltage is increased once a sufficient amount of molten steel is formed at the base of the arc and the electrodes are submerged into the melt to avoid damage to the furnace walls. During the initial stages of the meltdown, a high voltage is selected that allows for more energy to be transferred to the surrounding scrap. As the batch approaches completion, a lower voltage arc is preferred to avoid damage to the exposed furnace walls. Moreover, slag is foamed during the EAF operation by lancing carbon and oxygen to form carbon monoxide gas that bubbles through the slag layer. The foaming slag cloaks the arc, thereby protecting the furnace walls from arc radiation and improving the energy efficiency. During the batch operation, impurities such as phosphorus, sulfur, aluminum, silicon, manganese and carbon are removed from the steel as they react with oxygen and float into the slag. After a predefined batch duration, the temperature and carbon content of the steel are measured to determine whether further inputs are needed to reach the desired end-point specifications [43, 44]. Once the desired steel composition and temperature are obtained, the vessel is tapped and the molten steel is poured into a ladle for transport to the downstream units for further processing.

In this work, we focus on the melting process (see Fig. 3.2.1 for a schematic of an EAF during the melting stage). To this end, we utilize a first-principles model as a test-bed [41, 63]. The model describes the melting process by using a total of 14 state variables and six manipulated variables. The model parameters were estimated using operating data from an industrial EAF [63]. While the model is focused on the melting process, and does not capture all the details of the EAF process, it is sufficiently detailed and validated through real plant data, making it an excellent candidate to adapt and utilize as a test-bed to implement and evaluate the proposed approach.

In the steel industry, accurate, reliable and low-maintenance sensors for continuous on-line measurement are typically not available for many of the EAF process variables because of

the harsh operating environment, extreme temperatures and highly corrosive nature of the molten steel. Recognizing the limited availability of process measurements in practice, in this work the measurements available to build the data-driven model and to implement the proposed control approach include infrequent and frequent measurement variables where the infrequent measurements related to the slag and molten steel are available with a sampling time of 11 min while the frequent measurements corresponding to the off-gas composition are available with a sampling time of 1 min. A list of the infrequent and frequent process measurement variables are given in Tables 3.2.1 and 3.2.2, respectively, and the manipulated inputs are listed in Table 3.2.3. In keeping with typical EAF batch runs, each batch of the test-bed simulation is run for a duration of 66 min, which results in 7 infrequent measurements and 67 frequent measurements.

Another important feature necessary to make the test-bed application realistic is to recognize the significant variability of the feed caused by the various scrap sources of diverse steel grades. To replicate this variability across the batches, the initial concentrations of the species within the molten steel are assumed to have a variance of 50% with respect to the nominal values. On the other hand, the EAF processes are run by utilizing lime and dolime that is bought from suppliers, thus the resulting slag formed has lesser variability. Therefore, the initial conditions for the concentrations of the species within the slag are assumed to have a variance of 10% with respect to the nominal values (note though that as the EAF

Table 3.2.1: List of Infrequent Measurement Variables of the EAF Process

Variable	Description	Units
T	Temperature of Molten Steel	K
x_{Fe}	Mass Fraction Iron in Molten Steel	kg/kg
x_{C}	Mass Fraction Carbon in Molten Steel	kg/kg
x_{Slag}	Mass Fraction Lime/Dolime in Slag	kg/kg
x_{FeO}	Mass Fraction Iron Oxide in Slag	kg/kg
x_{SiO_2}	Mass Fraction Silicon Dioxide in Slag	kg/kg

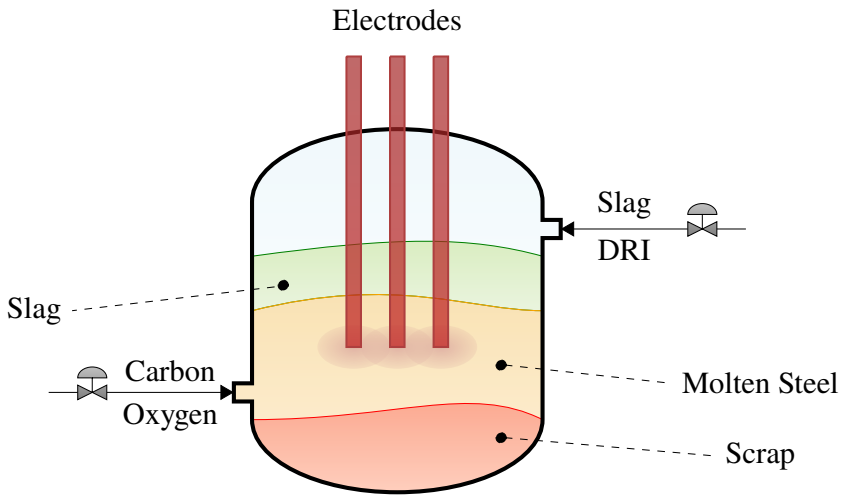

Figure 3.2.1: An Illustrative Diagram of the EAF Process

Table 3.2.2: List of Frequent Measurement Variables of the EAF Process

Variable	Description	Units
P	Relative Pressure	Pa
x_{CO}	Mass Fraction Carbon Monoxide in Gas	kg/kg
x_{CO_2}	Mass Fraction Carbon Dioxide in Gas	kg/kg
x_{N_2}	Mass Fraction Nitrogen in Gas	kg/kg

batch progresses, the slag composition does vary significantly owing to the variance in the molten metal composition). Finally, the initial temperatures of the molten steel and scrap during the nascent period of the EAF are highly dependent on the tightly controlled pre-processing steps taken prior to the commencing of the melting phase. The initial values of the temperatures are thus assumed to have a modest variance of 10% with respect to the nominal initial conditions.

Additionally, to ensure the EAF test-bed is characteristic of real industrial processes, the measurements are assumed to be corrupted by uncorrelated noise that is Gaussian distributed with zero-mean and appropriate variances. The noise variances are established such that the average signal-to-noise ratio in the measurements is approximately 30 dB, representative of

Table 3.2.3: List of Manipulated Variables and Corresponding Input Costs for the EAF Process

Variable	Description	Units	Costs	Units of Cost
m_{gas}	Off-gas Turbine Flow	kg/s	4.6296×10^{-5}	$\$ \cdot \text{kg}^{-1}$
m_{O_2}	Oxygen Lanced	kg/s	0.01749	$\$ \cdot \text{kg}^{-1}$
m_{DRI}	DRI Additions	kg/s	0.0900	$\$ \cdot \text{kg}^{-1}$
m_{Slag}	Slag Additions	kg/s	0.0600	$\$ \cdot \text{kg}^{-1}$
E	Electric Arc Power	kW	0.0625	$\$ \cdot \text{kWh}^{-1}$
m_{C}	Carbon Injected	kg/s	0.2500	$\$ \cdot \text{kg}^{-1}$

the typical measurement noise encountered in industrial practice due to random errors in the instrumentation.

From a control standpoint, the objective in EAF processes is to achieve a desired end-point, which like many batch processes typically corresponds to a non-equilibrium point, by batch termination. In industrial practice, the EAF process is typically operated until the carbon content is reduced below the desired level and the molten steel temperature is greater than the required temperature for pouring into ingot molds or casting. In addition, it is necessary to maintain the slag at the proper chemical composition to minimize over-oxidation of the bath. These primary targets are often used by plant operators to evaluate the EAF batch maturity [64]. In this work, we determine the desired end-points based on the attributes of the molten steel product obtained using the EAF simulation test-bed and standard operating policies. To this end, we explicitly characterize the end-point targets through the melt temperature ($\text{T}_{t_f} \geq 1830$ K), mass fraction of carbon in the molten steel ($x_{\text{C},t_f} \leq 0.0047$ kg/kg) and the mass fraction of iron oxide in the slag ($x_{\text{FeO},t_f} \leq 0.475$ kg/kg). Moreover, the architecture of industrial EAFs usually incorporate water-cooled furnace walls and roof panels to avoid damage due to overheating. Path constraints that limit the maximum achievable temperature of the molten steel ($\text{T}_t \leq 1950$ K, $t \in [0, t_f]$) ensure that the furnace temperature is within an operating region that takes safety considerations into account. In addition, the relative

pressure within EAFs is typically maintained to be negative ($P_t \leq 0$ Pa, $t \in [0, t_f]$) so as to prevent exposure of harmful chemicals to plant operators and retain the hazardous gaseous emissions within the furnace.

As with many industrial batch processes, the commonly used operating policy involves limited feedback applied primarily by experienced plant operators and typically does not take into account end-point projections or explicit economic considerations. Another less commonly used operating strategy is through tracking suitable trajectories of the measurable process variables, where the variable trajectories to be tracked are the ones that historically generated on-spec product. As an experienced plant operator is untenable in this study, trajectory-tracking control is implemented as a surrogate to the operator in order to mimic typical industrial EAF operation where reference profiles of the measurement variables are closely followed to ensure the constraints are satisfied during normal batch operation. The tracking objective is traditionally accomplished for a set of measurable process variables related to the desired end-point targets using local controllers that invoke classic (linear) control approaches such as local proportional-integral (PI) controllers. In this work, to generate the database of historical batches, four PI control loops are used to track the melt temperature, mass fraction of carbon in the molten steel, the mass fraction of iron oxide in the slag and the relative pressure inside the reactor. In keeping with the frequency of measurement of three of these variables, and for the sake of consistency, PI control calculations are done at the same frequency (i.e., corresponding to the times that the infrequent measurements become available). A detailed breakdown regarding the PI control loops, the manipulated variables that are paired with the controlled variables and the corresponding controller parameters are given in Table 3.2.4. The trajectories to be tracked are the conventional operating profiles that if closely followed result in steel product that meets the desired end-point targets. Nevertheless, PI controllers remain inherently based on a decentralized

(single-input-single-output) framework that is not well suited to account for the complex multivariable interactions among the various control loops, process constraints, economic objectives and optimality.

In contrast to trajectory-tracking control, an industrially relevant cost functional that explicitly takes the process economics (e.g., operating cost or profit) into consideration can be used to determine the control actions that not only satisfy the desired end-point targets but also obtain economic optimality. As such, the economic objective we formulate in this work represents the total operating expense of an EAF run, thus penalizing energy and resource consumption over the entire batch duration to operate the EAF in an economically optimal fashion while ensuring the constraints are satisfied. The nominal costs for the manipulated inputs are given in Table 3.2.3 [65]. We also take into account input bounds due to the physical limitations of the system, such as the maximum arc voltage or oxygen lanced into the melt.

3.2.2 DATA-BASED BATCH PROCESS MODELING AND CONTROL

For the proposed data-driven modeling and control approach, we generalize a recently developed multi-model approach that incorporates multiple local dynamic linear models and fuzzy c-means clustering based MPC [56, 57], where it is assumed that the measurements

Table 3.2.4: List of PI Control Loop Pairings and the Corresponding Controller Parameters for the EAF Process

Controlled Variable	Manipulated Variable	Parameters	
		K_C	τ_I
T	E	50.0	20.0
x_{C}	m_{C}	2.0	10.0
x_{FeO}	$m_{\mathrm{O_2}}$	3.0	5.0
P	m_{gas}	0.5	3.0

are all available with the same frequency. We next review the modeling approach in Section 3.2.2.1, and the control design in Section 3.2.2.2.

3.2.2.1 Multi-model Approach

The modeling approach in [56, 57] is predicated on the idea that a nonlinear process can be approximated by appropriately combining linear models that are valid around the point of linearization. To this end, local linear models are first developed. As one choice of the local linear models, the following form is used:

$$\hat{y}_k = \sum_{i=1}^{n_y} A_i y_{k-i} + \sum_{j=1}^{n_u} B_j u_{k-j} + \nu \tag{3.2.1}$$

where A and B are coefficient matrices for the output and input variables denoted by $y \in \mathbb{R}^p$ and $u \in \mathbb{R}^m$ with corresponding lag orders n_y and n_u, respectively, and ν is a bias term. The model can be written in a concatenated form as follows

$$\hat{y}_k = C \begin{bmatrix} x_k^* \\ 1_{p\times 1} \end{bmatrix} \tag{3.2.2}$$

where $1_{p\times 1}$ denotes a vector of ones with length p and

$$C = \begin{bmatrix} A_1 & \dots & A_{n_y} & B_1 & \dots & B_{n_u} & \nu \end{bmatrix} \tag{3.2.3}$$

with

$$x_k^* = \begin{bmatrix} y_{k-1}^T & \dots & y_{k-n_y}^T & u_{k-1}^T & \dots & u_{k-n_u}^T \end{bmatrix}^T \tag{3.2.4}$$

The matrix of model coefficients in Eq. (3.2.2) can be determined using ordinary least squares (OLS) [56, 57]. However, OLS may not precisely determine robust regression

coefficients when the process data is highly correlated or co-linear, which leads to ill-conditioning problems and imprecise model coefficients. The drawbacks of OLS regression can be addressed by using latent variable regression techniques such as principal component regression or partial least squares (PLS) regression.

In PLS regression, the regressor matrix (X) of the measurement variables and response matrix (Y) are mean centered and scaled to unit variance and then projected onto orthogonal subspaces comprised of n_A-pairs of latent variables. The pre-processing gives each variable equal importance during model identification while the bias term becomes redundant. Mathematically, PLS regression involves the decomposition of the regressor and response matrices into a summation of the outer products of the n_A score and loading vectors as follows

$$\begin{aligned} X &= \sum_{i=1}^{n_A} t_i p_i^T + E_X \\ &= TP^T + E_X \end{aligned} \tag{3.2.5}$$

$$\begin{aligned} Y &= \sum_{i=1}^{n_A} r_i q_i^T + E_Y \\ &= RQ^T + E_Y \end{aligned} \tag{3.2.6}$$

where t and r are the scores for the projection of the input and output data matrices onto the respective subspaces whose orientation is defined by the vectors p and q. Moreover, the matrices T, P, R and Q succinctly express the PLS decomposition with E_X and E_Y as the residual matrices, resulting in estimated model coefficients $C = f(P, T, Q)$.

Although PLS-based approaches to building dynamical models enables utilizing sound statistical techniques in the model parameter estimation, as a standalone model, it yields

a good, but local linear model. To characterize the process behavior over the entire range of operation, the inclusion of multiple models in an integrated approach is necessary. One such approach involves the partitioning of the historical database of training batches into n_L clusters so that the corresponding linear models can be identified for each cluster [56]. Using fuzzy c-means clustering, the dataset can be partitioned into clusters by assigning an arbitrary i-th data sample the membership values $\mu_{l,i}$, which represents the degree to which the i-th sample belongs to the l-th cluster. The membership values must satisfy the following conditions

$$\mu_{l,i} \in [0, 1] \; \forall \; l \in [1, n_L] \tag{3.2.7}$$

$$\sum_{l=1}^{n^L} \mu_{l,i} = 1 \; \forall \; i \in [1, n_{\text{obs}}] \tag{3.2.8}$$

where n_{obs} represents the total number of observations within the training dataset. The majority of fuzzy clustering algorithms is based on reducing the total variance in the data from cluster centers, which is expressed by minimizing the following nonlinear objective function

$$\min_{c_l} \; \mathcal{J} = \sum_{i=1}^{n_{\text{obs}}} \sum_{l=1}^{n_L} \mu_{l,i}^2 \left\| x_i^* - c_l \right\|^2 \tag{3.2.9}$$

where c_l denote the cluster center vectors to be determined. The membership values $\mu_{l,i}$ are then related to the cluster centers c_l as follows

$$\mu_{l,i} = \frac{\left\| x_i^* - c_l \right\|^{-2}}{\sum_{l'=1}^{n_L} \left\| x_i^* - c_{l'} \right\|^{-2}} \tag{3.2.10}$$

which shows that the degree to which the data sample x_i^* belongs to the cluster l is inversely proportional to the squared distance between the respective point and the cluster center. Therefore, a fuzzy c-means clustering based continuous weighting function can be developed

and incorporated with the dynamic modeling approach to integrate multiple local linear models into a global nonlinear model as follows

$$\hat{y}_k = \sum_{l=1}^{n_L} \omega_{l,k} \left(\sum_{i=1}^{n_y} A_{l,i} y_{k-i} + \sum_{j=1}^{n_u} B_{l,j} u_{k-j} + \nu_l \right) \tag{3.2.11}$$

$$= \sum_{l=1}^{n_L} \omega_{l,k} C_l \begin{bmatrix} x_k^* \\ 1_{p\times 1} \end{bmatrix} \tag{3.2.12}$$

where the weighting $\omega_{l,k}$ are given by

$$\omega_{l,k} = \frac{\left\| x_k^* - c_l \right\|^{-2}}{\sum_{l'=1}^{n_L} \left\| x_k^* - c_{l'} \right\|^{-2}} \tag{3.2.13}$$

The final form of the model combines the local linear models with weights to effectively describe the global nonlinear dynamics [56, 57], under the assumption of measurements available at the same frequency. A nonlinear model of this type is well suited to predict the dynamic process behavior and thus can be used for variable trajectory-tracking applications in predictive controllers.

3.2.2.2 Trajectory-tracking Predictive Control

A predictive controller for tracking reference trajectories for batch processes is presented in this section. The control action at each sampling instance is computed by solving the following optimization problem

$$\min_{u\in\mathcal{U}} \quad \mathcal{J} = \sum_{k=1}^{n_P} \left\| \hat{y}_k - y_k^{\text{ref}} \right\|_{Q_w}^2 + \| \Delta u_k \|_{R_w}^2 \tag{3.2.14}$$

$$\text{s.t.} \begin{cases} \hat{y}_k = \sum_{l=1}^{n_L} \omega_{l,k} \left(\sum_{i=1}^{n_y} A_{l,i} \hat{y}_{k-i} + \sum_{j=1}^{n_u} B_{l,j} u_{k-j} + \nu_l \right) \\ \hat{y}_0 = y_t \end{cases} \tag{3.2.15}$$

where $u \in \mathbb{R}^m$ denotes the vector of constrained input variables, taking values in a nonempty convex set $\mathcal{U} \subseteq \mathbb{R}^m$. The first term in the objective function penalizes discrepancies between the predicted output trajectories $\hat{y}$ and the reference trajectories y^{ref} over the prediction horizon n_P and the second term is a move suppression term that penalizes the magnitude of input changes [56, 57]. Further, Q_w is a positive semi-definite symmetric matrix used to penalize the deviations of the outputs from their nominal values and R_w is a strictly positive definite symmetric matrix to penalize changes in the manipulated variables. The predictive model in the MPC formulation, specifically the nonlinear weighting function, makes this optimization problem a nonlinear program. While the trajectory-tracking control paradigm has been successfully applied in many applications, the primary objective in batch processes is to reach a desired end-point by batch termination. In many instances, the initially optimal state variable trajectories to be tracked may be rendered suboptimal in the presence of measurement noise or process disturbances. On the other hand, directly accounting for process economics to compute the control actions can achieve economic optimality that may not be readily attainable through traditional tracking control techniques.

3.3 Data-driven Multi-rate Model

In this section, we propose a multi-rate modeling framework and apply it to the EAF process.

3.3.1 Multi-rate Model Formulation

To model multi-rate sampled systems, we propose a novel formulation in which the frequent process measurements are used along with the infrequent measurements for developing effective and reliable multi-rate models. To this end, consider a multi-input multi-output nonlinear system where $y^{\wp_1} \in \mathbb{R}^{p_1}$ and $y^{\wp_2} \in \mathbb{R}^{p_2}$ denote the vector of infrequent and frequent measurement variables, respectively, and $u \in \mathbb{R}^m$ denotes the vector of constrained input variables. Typically, the number of infrequent measurement variables are greater than the frequent measurement variables ($p_1 \geq p_2$). Further, given that in-between an infrequent sampling interval, there are γ frequent sampling instances, let k_1 and k_2 be the indexes for the sampling instances of the infrequent and frequent measurements with n_K as the final infrequent sampling instance. Along the lines of Eqs. (3.2.11) and (3.2.12), local linear models for the infrequent measurement variables can be developed as follows

$$\begin{aligned}\hat{y}^{\wp_1}_{k_1|k_2-1} = \sum_{l=1}^{n_L^{\wp_1}} \omega^{\wp_1}_{l,k_1} \Bigg(& \sum_{i=1}^{n_y^{\wp_1}} A^{\wp_1}_{l,i} y^{\wp_1}_{k_1-i} + \sum_{i_s=1}^{\gamma k_1-k_2} A^{s,\wp_2}_{l,i_s} \hat{y}^{\wp_2}_{\gamma k_1-i_s} \\ & + \sum_{i'_s=\gamma k_1-k_2-1}^{\gamma k_1-n_y^{s,\wp_2}} A^{s,\wp_2}_{l,i'_s} y^{\wp_2}_{\gamma k_1-i'_s} + \sum_{j=1}^{n_u^{\wp_1}} B^{\wp_1}_{l,j} u_{k_1-j} + \nu^{\wp_1}_l \Bigg)\end{aligned} \tag{3.3.1}$$

where $\hat{y}^{\wp_1}_{k_1|k_2-1}$ denotes the predicted vector of infrequent measurements at the k_1-th sampling instant given the frequent measurement variables until the (k_2-1)-th frequent sampling instance for $k_2 - 1 \in \big(\gamma k_1, \gamma\,(k_1-1)\big]$, u_{k_1} is the vector of inputs, $\omega^{\wp_1}_{l,k_1}$ is the weight given to the l-th model of the $n_L^{\wp_1}$ total models for predicting the infrequent measurements, $A^{\wp_1}_{l,i}$ and $A^{s,\wp_2}_{l,i_s}$ denote the model coefficients for incorporating information from the infrequently and frequently sampled measurements, $B^{\wp_1}_{l,j}$ denotes the model coefficients for the input variables and $\nu^{\wp_1}_l$ the bias term for the l-th model. Further, $n_y^{\wp_1}$ is the lag order for the infrequent measurement variables, $n_y^{s,\wp_2}$ is the lag order for the supplementary frequent

measurement variables used in predicting the infrequent measurement variables and $n_u^{\wp_1}$ is the lag order for the manipulated variables. Since measurements are only available until the (k_2-1)-th frequent sampling instance, predicting the future infrequently sampled variables requires either estimates or measurements, or both (depending on the respective infrequent and frequent sampling instances in consideration), of the frequently sampled variables, which is incorporated through the respective summations over the estimated and measured frequently sampled variables. The weights $\omega_l^{\wp_1}$ for predicting the infrequent measurements are dependent on the cluster centers $c_l^{\wp_1}$ and given by

$$\omega_{l,k_1}^{\wp_1} = \frac{\left\| x_{k_1}^{\wp_1,*} - c_l^{\wp_1} \right\|^{-2}}{\sum_{l'=1}^{n_L^{\wp_1}} \left\| x_{k_1}^{\wp_1,*} - c_{l'}^{\wp_1} \right\|^{-2}} \tag{3.3.2}$$

with

$$x_{k_1}^{\wp_1,*} = \left[{y_{k_1-1}^{\wp_1}}^T \ \cdots \ {y_{k_1-n_y^{\wp_1}}^{\wp_1}}^T \ {y_{\gamma k_1-1}^{\wp_2}}^T \ \cdots \ {y_{\gamma k_1-n_y^{s,\wp_2}}^{\wp_2}}^T \ {u_{k_1-1}}^T \ \cdots \ {u_{k_1-n_u^{\wp_1}}}^T \right]^T \tag{3.3.3}$$

and the cluster centers can be determined using the $n_{\text{obs}}^{\wp_1}$ samples by solving the nonlinear optimization problem

$$\min_{c_l^{\wp_1}} \ \mathcal{J} = \sum_{i=1}^{n_{\text{obs}}^{\wp_1}} \sum_{l=1}^{n_L^{\wp_1}} \left(\mu_{l,i}^{\wp_1} \right)^2 \left\| x_i^{\wp_1,*} - c_l^{\wp_1} \right\|^2 \tag{3.3.4}$$

where the membership of the samples is defined by

$$\mu_{l,i}^{\wp_1} = \frac{\left\| x_i^{\wp_1,*} - c_l^{\wp_1} \right\|^{-2}}{\sum_{l'=1}^{n_L^{\wp_1}} \left\| x_i^{\wp_1,*} - c_{l'}^{\wp_1} \right\|^{-2}} \tag{3.3.5}$$

Estimates of the infrequent measurements variables, however, require either estimates or measurements of both the infrequent and frequent variables as formalized in Eq. (3.3.1).

Modeling the infrequent measurements alone without considering the frequent measurements can result in a model with inadequate predictive performance because of the long delays between sampling instances during which the operating dynamics can vary significantly. In this work, the proposed data-driven multi-rate models are developed such that all the available process measurements are used to obtain the most accurate predictions. In particular, while past frequently measured variables are used to predict future frequently measured variables, the future infrequently measured variables are predicted using both the past infrequently measured variables, and the past frequently measured variables (see Fig. 3.3.1 for an illustration). Since the key process variables are typically measured infrequently, accurate predictions and effective output-feedback control significantly benefits from the integrated modeling approach.

Therefore, another model that predicts the frequent measurement variables can be developed as follows

$$\hat{y}^{\wp_2}_{k_2|k_2-1} = \sum_{l=1}^{n_L^{\wp_2}} \omega^{\wp_2}_{l,k_2} \left(\sum_{i=1}^{n_y^{\wp_2}} A^{\wp_2}_{l,i} y^{\wp_2}_{k_2-i} + \sum_{j=1}^{n_u^{\wp_2}} B^{\wp_2}_{l,j} u_{k_2-j} + \nu^{\wp_2}_l \right) \tag{3.3.6}$$

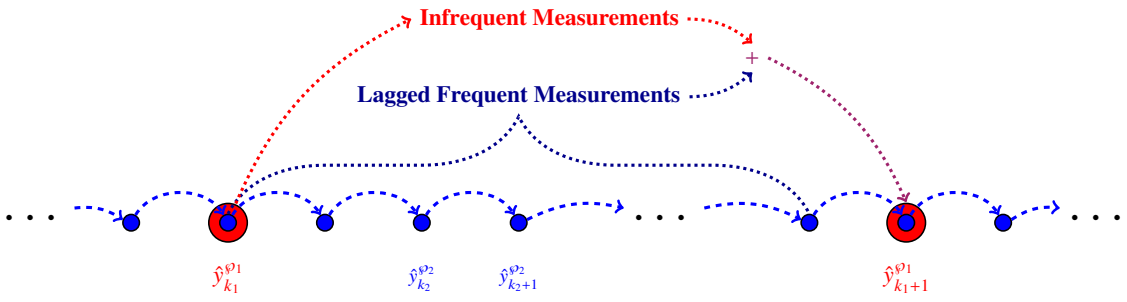

Figure 3.3.1: An Illustration of the Multi-rate Modeling Approach for Infrequent and Frequent Variables

where $\hat{y}^{\wp_2}_{k_2|k_2-1}$ denotes the predictions of the frequent measurements given past measurements and $\omega^{\wp_2}_{l,k_2}$ is the weight given to the l-th model of the $n^{\wp_2}_L$ total models for predicting the frequent measurements, $A^{\wp_2}_{l,i}$ and $B^{\wp_2}_{l,j}$ are the model coefficients and $\nu^{\wp_2}_l$ the bias term for the l-th model with $n^{\wp_2}_y$ as the lag order for the frequent measurement variables and $n^{\wp_2}_u$ as the lag order for the manipulated variables. The weights $\omega^{\wp_2}_l$ are dependent on the cluster centers $c^{\wp_2}_l$ and given by

$$\omega^{\wp_2}_{l,k_2} = \frac{\left\| x^{\wp_2,*}_{k_2} - c^{\wp_2}_l \right\|^{-2}}{\sum_{l'=1}^{n^{\wp_2}_L} \left\| x^{\wp_2,*}_{k_2} - c^{\wp_2}_{l'} \right\|^{-2}} \tag{3.3.7}$$

with

$$x^{\wp_2,*}_{k_2} = \left[{y^{\wp_2}_{k_2-1}}^T \ \cdots \ {y^{\wp_2}_{k_2-n^{\wp_2}_y}}^T \ {u_{k_2-1}}^T \ \cdots \ {u_{k_2-n^{\wp_2}_u}}^T \right]^T \tag{3.3.8}$$

and the cluster centers can be determined using the $n^{\wp_2}_{\text{obs}}$ samples by solving the nonlinear optimization problem

$$\min_{c^{\wp_2}_l} \ \mathcal{J} = \sum_{i=1}^{n^{\wp_2}_{\text{obs}}} \sum_{l=1}^{n^{\wp_2}_L} \left(\mu^{\wp_2}_{l,i} \right)^2 \left\| x^{\wp_2,*}_i - c^{\wp_2}_l \right\|^2 \tag{3.3.9}$$

where the membership of the samples is defined by

$$\mu^{\wp_2}_{l,i} = \frac{\left\| x^{\wp_2,*}_i - c^{\wp_2}_l \right\|^{-2}}{\sum_{l'=1}^{n^{\wp_2}_L} \left\| x^{\wp_2,*}_i - c^{\wp_2}_{l'} \right\|^{-2}} \tag{3.3.10}$$

The model coefficients in Eqs. (3.3.1) and (3.3.6) can be determined using PLS regression (see Remark 3.1 on the identification aspects of the model parameters and Remark 3.2 for comparison with principal component analysis based models). A formulation of a general approach is presented here for handling multi-rate measurements that takes advantage of both infrequent and frequent measurements to improve the prediction accuracy of the models. It should be noted that between two infrequent measurements, several frequent measurements

become available and help with the prediction of the infrequent measurement. However, no infrequent measurement becomes available between two frequent measurements, therefore there is no benefit in incorporating these infrequent measurements in the model for predicting the frequent measurements.

Remark 3.1. *The accurate estimation of the model parameters often requires a select number of identification batches where a suitable excitation signal is added onto the nominal inputs to establish a measured response. Due to their prevalence, digitally generated signals that can be readily implemented are attractive for identification purposes. However, the optimal amount of stimulus required to receive an appropriately excited output response and the adequate number of excited response data samples is an important issue for further consideration and outside the scope of the present work. In the present work, the predictive ability of models is verified by k-fold cross-validation.*

Remark 3.2. *In contrast to the principal component analysis based approaches where a single linear time-varying model is built (around nominal trajectories), the proposed formulation focuses on developing multiple local linear models that are not indexed with time. One benefit of the proposed approach therefore is that batches of the same duration (or identifying a variable that can be used for indexing) are not needed. Furthermore, when identifying linear time varying models (even in the latent variable space), the number of matrices that need to be identified equals the number of sampling instances. In the present approach, on the other hand, the number of models is not necessarily equal to the number of sampling points, but can be picked via the process of cross-validation.*

Remark 3.3. *The first-principles-based model that is used as a test-bed to collect process data only describes the melting phase of the EAF process [41]. Therefore, the model has only one distinct dynamic phase and the state variables evolve throughout the batch operation because of the changing operating dynamics. More detailed models that cover a wider duration of the EAF process operation are currently in development. Future modeling and*

control work will focus on explicitly handling the discrete nature of the process dynamics and its application to the detailed process model.

3.3.2 ELECTRIC ARC FURNACE MODELING RESULTS

To develop the multi-rate models for the EAF process measurements, a database of historical batches was initially generated. To this end, the deterministic EAF process model was simulated to generate 23 normal operation batches from different initial conditions. In addition to the normal operation batches, seven identification batches are used to augment the database. For five of these batches, a low-amplitude pseudo-random binary sequence (PRBS) signal is added to the input value computed by the PI controller, except for the last actuation. In the last two, batches, the PRBS signal was added all the way through. In the identification batches, not adding the PRBS to the final actuation allows the last input actuation to be able to compensate for disturbances in the system and achieve product that meets the desired end-point target specifications, which enables many of the identification batches to result in on-spec product. The PRBS signal added to the manipulated inputs, shown in Fig. 3.3.2, consisted of varying amplitude through the course of the batch. This identification approach was observed to result in good input signal excitation for developing accurate models. It was also verified that all seven identification batches still resulted in on-spec product. Note that unlike conventional batch processes, identification batches of the EAF process do not necessarily result in wasted product because after the identification experiments are completed, further input actions can be made to correct for the end-point targets and recover the product, thus mitigating the drawbacks of running identification batches.

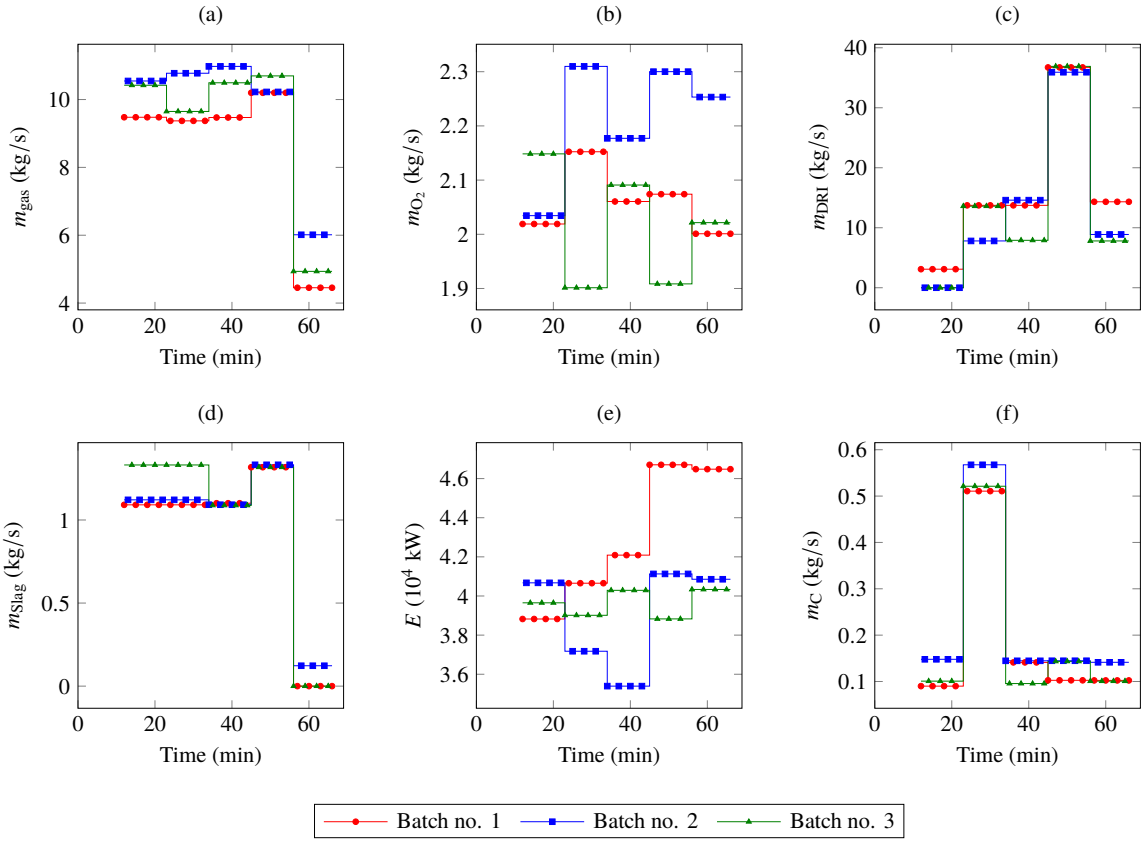

Figure 3.3.2: Manipulated Variables of the EAF Process for Selected Identification Batches with a Low-amplitude Pseudo-random Binary Sequence Signal

The identification procedure for the local linear models was as follows. For a given lag structure, the number of clusters was varied from $n_L = 1$ to 40. For each choice of n_L, the batch data was partitioned into regressor X and regressed Y matrices, decomposed using PLS, and clustered using fuzzy c-means clustering. Since the model weights were then known, multiple ARX models were estimated simultaneously using PLS. The models were built using k-fold cross-validation with $k = 7$. The goodness of each fit was judged using the weighted root-mean-square error (RMSE) in predicting back the validation samples, where the weights for the controlled variables (variables with end-point constraints) are twice the weights for the other variables.

The proposed multi-rate models are compared against a single model, identified using the multi-model approach reviewed in Section 3.2.2.1, that predicts all available process variables at only the infrequent sampling instances. The minimum weighted RMSE values obtained using the cross-validation are provided in Table 3.3.1. The lag structure, number of clusters and the number of latent variables (n_A) for the multi-rate models and the single model that yielded the lowest weighted RMSE values are also presented. It should be noted that all the frequent measurements available between infrequent sampling instances are used to augment the regressor matrix for predicting the infrequent variables. In contrast, the single model only predicts future variables using the past variables at only the infrequent sampling instances without incorporating any of the frequent measurements available between infrequent sampling instances. Moreover, 10 new batches (not used during the model development) are simulated for validation purposes. The model validation results for the infrequent and frequent variables are shown in Tables 3.3.2 and 3.3.3 (respectively) and the corresponding output of the multi-rate models, single model and actual profile trajectories from the mechanistic model for a set of new initial conditions are shown in Figs. 3.3.3 and 3.3.4.

The prediction by the data-based model is an open-loop prediction where the predictions throughout the batch are not corrected and the model errors are allowed to accumulate over the entire batch duration. It is readily observed that the single model that predicts all the process variables at only the infrequent sampling instances does not predict the variables well, resulting in higher weighted RMSE values. Additionally, since the model validation results involved open-loop predictions, the multi-rate models are expected to further improve accuracy over the single model when predictions of the frequent variables are substituted for the preferred available measurements. Accordingly, the single model will not be considered further as its capability, and that of a predictive controller derived from it, will falter in relation to the multi-rate models. Overall, the proposed multi-model approach captured the nonlinear nature of the EAF and provided relatively reliable predictions.

3.4 ECONOMIC MODEL PREDICTIVE CONTROL

In this section, we propose a two-tiered economic model predictive control algorithm and then implement it on the EAF process test-bed.

Table 3.3.1: Data-driven Modeling Results for Both Single and Multi-rate Model

Model	Type	Weighted RMSE	Variable Lags			n_L	n_A
			Infrequent	Frequent	Manipulated		
Single	-	0.3721	1	1	1	22	7
Multi-rate	Infrequent	0.2882	1	1	1	29	5
	Frequent	0.0150	-	1	1	3	13

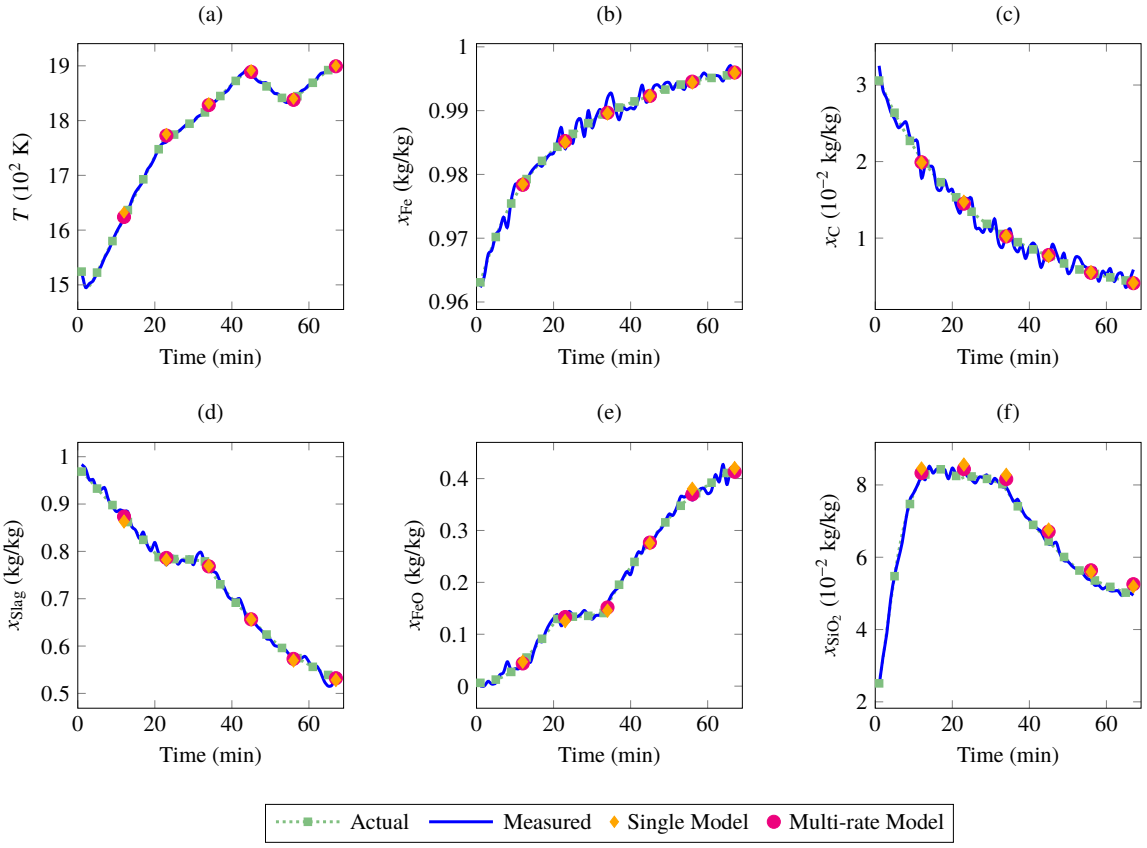

Figure 3.3.3: Model Validation Results for the Infrequent Measurement Variables of the EAF Process

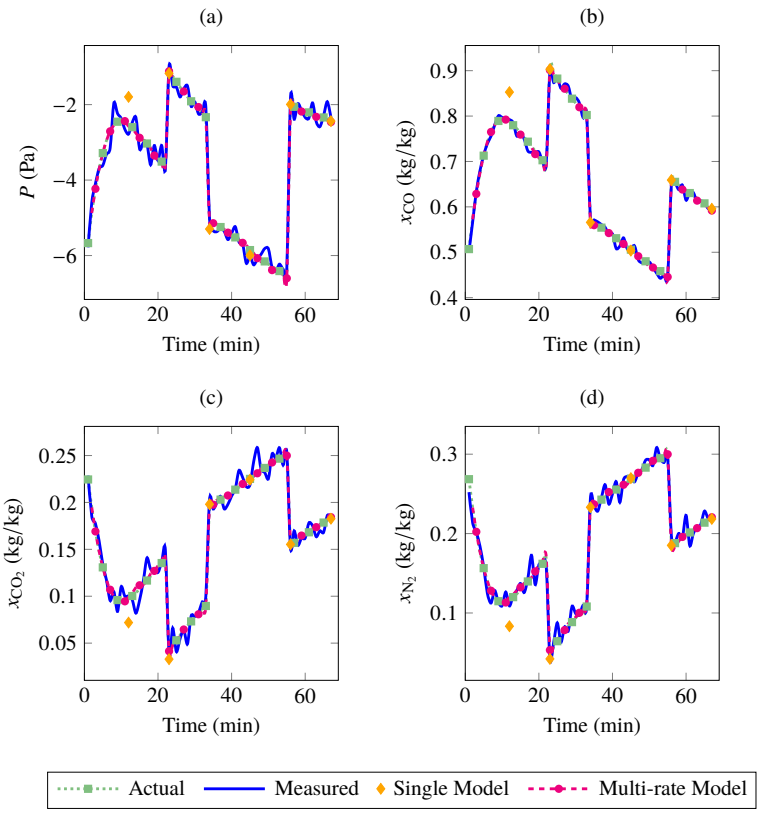

Figure 3.3.4: Model Validation Results for the Frequent Measurement Variables of the EAF Process

Table 3.3.2: Model Validation Results for the Infrequent Measurement Variables of the EAF Process

Variable	Weighted RMSE		Units
	Single Model	Multi-rate Model	
T	19.0585	12.6981	K
x_{Fe}	0.0016	0.0012	kg/kg
x_{C}	0.0027	0.0024	kg/kg
x_{Slag}	0.0124	0.0087	kg/kg
x_{FeO}	0.0296	0.0133	kg/kg
x_{SiO_2}	0.0033	0.0024	kg/kg

Table 3.3.3: Model Validation Results for the Frequent Measurement Variables of the EAF Process

Variable	Weighted RMSE		Units
	Single Model	Multi-rate Model	
P	3.6173	0.2269	Pa
x_{CO}	0.0404	0.0092	kg/kg
x_{CO_2}	0.0219	0.0103	kg/kg
x_{N_2}	0.0232	0.0103	kg/kg

3.4.1 ECONOMIC MODEL PREDICTIVE CONTROL FORMULATION

The key idea of the proposed economic MPC is to use a tiered economic model predictive control framework to achieve an acceptable (on-spec) end-point while optimizing an economics-based cost function. To this end, let y_{des} be the desired product end-point. In the first tier, the EMPC computes the best (in terms of satisfaction of product specifications) achievable end-point at each infrequent sampling instance by solving the following optimization problem

$$\min_{u \in \mathcal{U}} \quad \mathcal{J}_1 = \left\| \hat{y}_e - y_{\text{des}} \right\|_{\Psi}^2 \tag{3.4.1}$$

$$
\text{s.t.} \begin{cases}
\hat{y}^{\wp_1}_{k_1|k_2-1} = \sum_{l=1}^{n_L^{\wp_1}} \omega^{\wp_1}_{l,k_1} \left(\sum_{i=1}^{n_y^{\wp_1}} A^{\wp_1}_{l,i} y^{\wp_1}_{k_1-i} + \sum_{i_s=1}^{\gamma k_1 - k_2} A^{s,\wp_2}_{l,i_s} \hat{y}^{\wp_2}_{\gamma k_1 - i_s} \right. \\
\qquad \left. + \sum_{i'_s=\gamma k_1 - k_2 - 1}^{\gamma k_1 - n_y^{s,\wp_2}} A^{s,\wp_2}_{l,i'_s} y^{\wp_2}_{\gamma k_1 - i'_s} + \sum_{j=1}^{n_u^{\wp_1}} B^{\wp_1}_{l,j} u_{k_1-j} + \nu^{\wp_1}_l \right) \\
\hat{y}^{\wp_2}_{k_2|k_2-1} = \sum_{l=1}^{n_L^{\wp_2}} \omega^{\wp_2}_{l,k_2} \left(\sum_{i=1}^{n_y^{\wp_2}} A^{\wp_2}_{l,i} y^{\wp_2}_{k_2-i} + \sum_{j=1}^{n_u^{\wp_2}} B^{\wp_2}_{l,j} u_{k_2-j} + \nu^{\wp_2}_l \right) \\
\hat{y}^{\wp_1} \in \mathcal{Y}_{\wp_1}, \quad \hat{y}^{\wp_2} \in \mathcal{Y}_{\wp_2} \\
\hat{y}_e = g\left(\hat{y}^{\wp_1}_{n_K} \right) \\
y^{\wp_1}_{k_1-1} = y^{\wp_1}_t, \quad y^{\wp_2}_{k_2-1} = y^{\wp_2}_t
\end{cases} \tag{3.4.2}
$$

where $\hat{y}_e = g\left(\hat{y}^{\wp_1}_{n_K}\right)$ defines the batch end-point characteristics through the estimates of the measurement variables at the last sampling instant, $u \in \mathbb{R}^m$ denotes the vector of constrained input variables, taking values in a nonempty convex set $\mathcal{U} \subseteq \mathbb{R}^m$ with $\mathcal{U} := \{u \in \mathbb{R}^m : u_{\min} \leq u \leq u_{\max}\}$, $u_{\min} \in \mathbb{R}^m$ and $u_{\max} \in \mathbb{R}^m$ denote the lower and upper bounds on the manipulated input, respectively, and Ψ is a positive definite matrix used to penalize the squared deviation of the end-point variables with respect to the desired end-point values. Further, $\mathcal{Y}_{\wp_1} \in \mathbb{R}^{\wp_1}$ and $\mathcal{Y}_{\wp_2} \in \mathbb{R}^{\wp_2}$ denote the constraints on the infrequent and frequent measurement variables, respectively, and $y^{\wp_1}_t$ and $y^{\wp_2}_t$ provide the initialization of the optimization problem at the current process conditions. The multi-rate models utilize the available process measurements to predict the variables at the next sampling instance, while latter sampling instances incorporate estimates of the process measurements to predict the entire process variable trajectories over the prediction horizon.

Subsequent to obtaining the end-point that best satisfies the product specifications, $\hat{y}^*_e$, the next tier computes the optimal (from an economic perspective) input moves, albeit with the constraint that the best product specifications should still be achieved. The second tier

of the EMPC solves an optimization problem to determine the optimal input trajectory by minimizing an economic objective function at the infrequent sampling instances as follows

$$\min_{u\in\mathcal{U}} \quad \mathcal{J}_2 = \delta \cdot \sum_{i=k_1-1}^{n_K-1} \lambda^T u_i \tag{3.4.3}$$

$$\text{s.t.} \begin{cases} \hat{y}^{\wp_1}_{k_1|k_2-1} = \sum_{l=1}^{n_L^{\wp_1}} \omega^{\wp_1}_{l,k_1} \left(\sum_{i=1}^{n_y^{\wp_1}} A^{\wp_1}_{l,i} y^{\wp_1}_{k_1-i} + \sum_{i_s=1}^{\gamma k_1-k_2} A^{s,\wp_2}_{l,i_s} \hat{y}^{\wp_2}_{\gamma k_1-i_s} \right. \\ \qquad \left. + \sum_{i'_s=\gamma k_1-k_2-1}^{\gamma k_1-n_y^{s,\wp_2}} A^{s,\wp_2}_{l,i'_s} y^{\wp_2}_{\gamma k_1-i'_s} + \sum_{j=1}^{n_u^{\wp_1}} B^{\wp_1}_{l,j} u_{k_1-j} + \nu^{\wp_1}_l \right) \\ \hat{y}^{\wp_2}_{k_2|k_2-1} = \sum_{l=1}^{n_L^{\wp_2}} \omega^{\wp_2}_{l,k_2} \left(\sum_{i=1}^{n_y^{\wp_2}} A^{\wp_2}_{l,i} y^{\wp_2}_{k_2-i} + \sum_{j=1}^{n_u^{\wp_2}} B^{\wp_2}_{l,j} u_{k_2-j} + \nu^{\wp_2}_l \right) \\ \hat{y}^{\wp_1} \in \mathcal{Y}_{\wp_1}, \quad \hat{y}^{\wp_2} \in \mathcal{Y}_{\wp_2} \\ h\left(\hat{y}^{\wp_1}_{n_K}, \hat{y}^*_e\right) \leq 0 \\ y^{\wp_1}_{k_1-1} = y^{\wp_1}_t, \quad y^{\wp_2}_{k_2-1} = y^{\wp_2}_t \end{cases} \tag{3.4.4}$$

where $h\left(\hat{y}^{\wp_1}_{n_K}, \hat{y}^*_e\right) \leq 0$ denotes end-point constraints that are appropriately relaxed as an interval with $\hat{y}^*_e$ as a bound (see Remark 3.4 for more details on the end-point constraint relaxation), δ is the hold-time for the control action and $\lambda \in \mathbb{R}^m$ are the operating costs associated with the manipulated variables. The two-tiered economic MPC approach allows for a framework that can handle distinct and competing objectives and deal with the trade-off between them without resorting to using arbitrary penalty weights (see Remark 3.5). In both tiers of the proposed approach, the models used and the process constraints are identical, while the objective function for the first tier is end-point optimization and for the second tier is economic MPC with the optimal end-point as an additional constraint. The feasibility of this optimization problem is in general not guaranteed, but hard constraints are incorporated so even if the target end-point may not be reached, no safety violations will

occur. Additionally, if the optimization problem is infeasible, it suggests that for the current batch, safety constraints cannot be satisfied, and thus may require an earlier termination of the batch to avoid safety issues. On the other hand, if it is possible to meet the safety requirements, the first tier computes the solution that best achieves the desired target. The second tier is then guaranteed to be feasible, and in the worst case scenario be as economic as the first tier solution.

In summary, the two-tiered EMPC strategy uses the data-driven multi-rate models to predict the behavior of the batch dynamics over a receding horizon. The control problem is solved at each infrequent sampling instance to determine the best achievable end-point target (the nearest to the desired end-point) and the economically optimal path to reach the optimal end-point using the identified multi-rate models and the process constraints, and only the control action of the current infrequent sampling interval is implemented with the calculation repeated at subsequent sampling instances using new measurements and updated plant information. A block diagram of the two-tiered economic MPC approach is shown in Fig. 3.4.1.

Remark 3.4. *Recognizing that the optimal end-point from the first layer is the best end-point that we can reach, we implement the constraint as an interval that is bounded on one end by the best achievable end-point (as given by the first tier) and bound on the other end by the extreme limit the variable can obtain. Thus the constraints always include a target known to be feasible. The added flexibility of the relaxed end-point constraints, however, allows achieving a better economic optimum if at all possible while ensuring the constraints are satisfied.*

Remark 3.5. *The typical control objective in batch processes is to minimize the deviation between the product end-point and the desired target within the finite batch duration. Another control objective routinely involved in batch process control is to optimize the process*

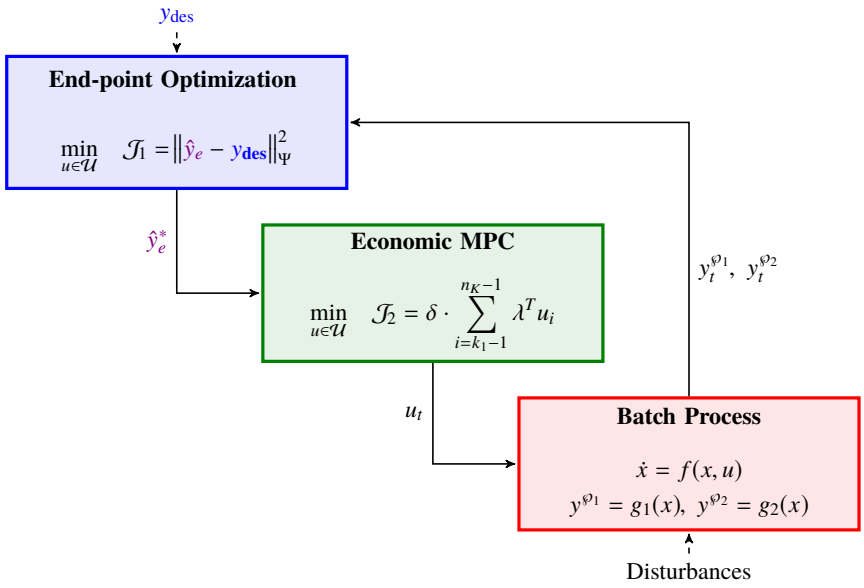

Figure 3.4.1: A Flow Diagram of the Two-tiered Economic Model Predictive Control Approach

economics while constraining the end-point to satisfy the desired specifications. These two competing objectives (minimize end-point deviation and optimize economics) when considered simultaneously result in a multi-objective optimization problem with inherent complexities in negotiating the possible trade-offs between the competing objectives. To address this issue without resorting to the compromise of using arbitrary penalty weights, the two-tiered EMPC approach is proposed that is capable of first determining the best attainable end-point and then subsequently optimizing the operating economics of reaching that optimal achievable end-point. Similar tiered optimization approaches were used in [66] in a hierarchical supervisory control scheme and in [67] in optimal operation under partial plant shutdown.

Remark 3.6. *The two-tiered EMPC framework using the proposed data-driven multi-rate models is relatively tractable in contrast to the first-principles model-based control designs. Nevertheless, for embedded systems with fast dynamics where the sampling times are in milli- or nanoseconds and thus the computational time can be prohibitive, the two-tiered EMPC*

can be implemented such that the first-tier is only solved occasionally in order to update the best achievable end-point, as appropriate, to assist with the computation time.

Remark 3.7. *Existing EMPC formulations [58–62] have shown promising results in the context of continuous systems. However, the fact that the desired end-point in batch processes is typically not an equilibrium point precludes the direct implementation of these EMPC techniques. Note also that any economic benefits achieved through the proposed two-tier formulation rely on the ability to reach (or get close to) the process specification by following different paths (and thus following different manipulated input trajectories). If the process dynamics are such that there exists only one unique path to the desired end-point, then the first and second tier optimization problems will both yield identical results, but no worse than the solution obtained at the first tier.*

3.4.2 ECONOMIC MODEL PREDICTIVE CONTROL RESULTS

Closed-loop simulations for ten new initial conditions were performed using the proposed two-tired economic MPC design, and the performance was compared against the standard EAF operating approach involving PI controllers described in Section 3.2. The two-layers of the EMPC were executed consecutively at every infrequent sampling instance. All new initial conditions for the closed-loop results were obtained from the same distribution as the initial conditions in the training data. A representative set of closed-loop simulation results (batch no. 3) is presented in Figs. 3.4.2 and 3.4.3 for the infrequent and frequent process measurements, respectively. The closed-loop trajectories of the end-point constrained variables and the corresponding intervals of the end-point constraints are shown in Fig. 3.4.2 as well. For instance, the end-point constraint for the temperature in Fig. 3.4.2(a) is represented as an interval with the lower limit as the optimal end-point obtained from the first tier of the EMPC and the upper limit as the path constraint for the temperature imposed for safety

considerations. Similarly, the end-point constraints for the mass fractions of carbon and iron oxide in Fig. 3.4.2(c) and (e), respectively, are represented as intervals with the upper limits obtained from the first tier of the EMPC and the lower limits as zero, which are the minimum physically realizable values of the concentration measurements. The desired end-points were selected based on desired attributes of the steel product as discussed in Section 3.2.1. Although both the EMPC and the standard control approaches are able to meet the desired product quality, the proposed economic MPC controller offered a significant cost advantage of approximately $\$5.7372 \times 10^3$ compared to $\$6.2020 \times 10^3$ for the standard approach, an average savings of \$464.75 per batch or approximately 7.49% improvement per batch. The poor performance of the PI controllers can be attributed to the fact that they are inherently based on a decentralized (single-input, single-output) framework that does not account for interactions among the various control loops. Furthermore, the conventional PI control also does not explicitly take into consideration process constraints and optimality.

The proposed economic MPC design was efficiently solvable with the average CPU time required to solve the two-tired MPC optimization problem with the longest prediction horizon as 3.9983 s (maximum 9.2665 s) using `GAMS` with `IPOPT` as the solver on an Intel Dual Core machine with 4 GB RAM. The closed-loop input profiles are shown in Fig. 3.4.4 and it is readily observed that the EMPC approach recognizes that in certain instances, the end-point constraints can still be achieved while maintaining the manipulated variables close to their lower bounds, due to which the operating costs of the EMPC approach are significantly lower. Overall, the simulation results demonstrated the advantages of implementing the proposed two-tiered economic predictive controller over standard operating policies.

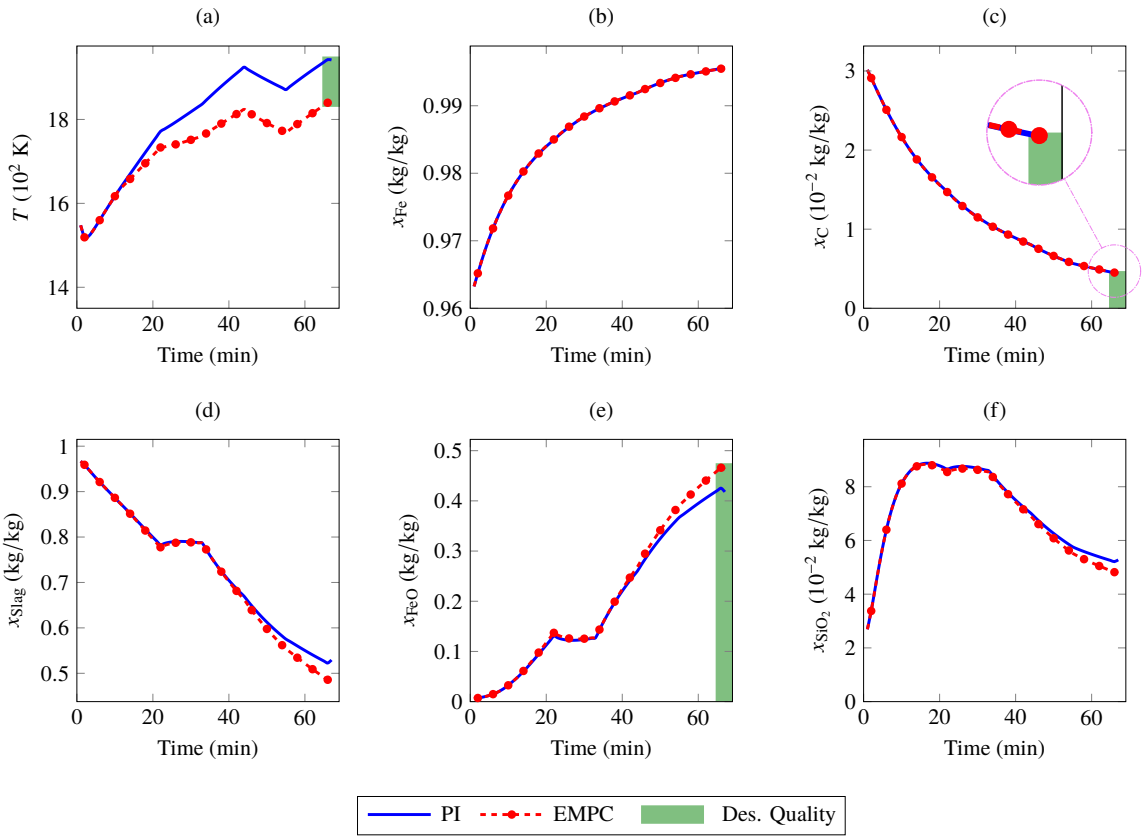

Figure 3.4.2: Comparison of the Trajectories for the Infrequent Measurement Variables Obtained from the Proposed Economic MPC and Conventional Method (The inset in subplot (c) zooms in to show the end-point constraint is satisfied)

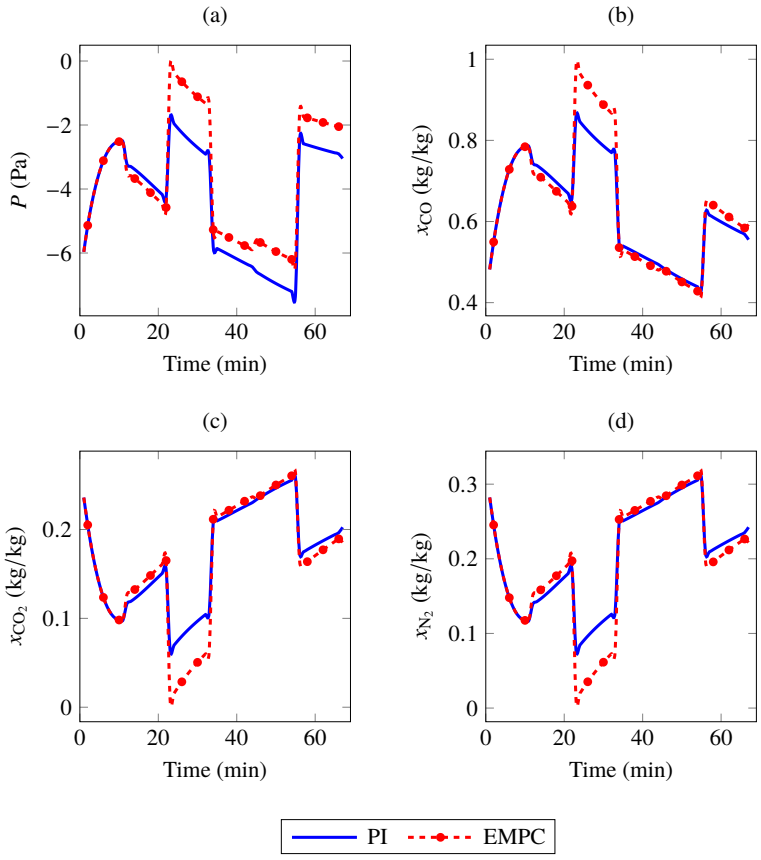

Figure 3.4.3: Comparison of the Trajectories for the Frequent Measurement Variables Obtained from the Proposed Economic MPC and Conventional Method

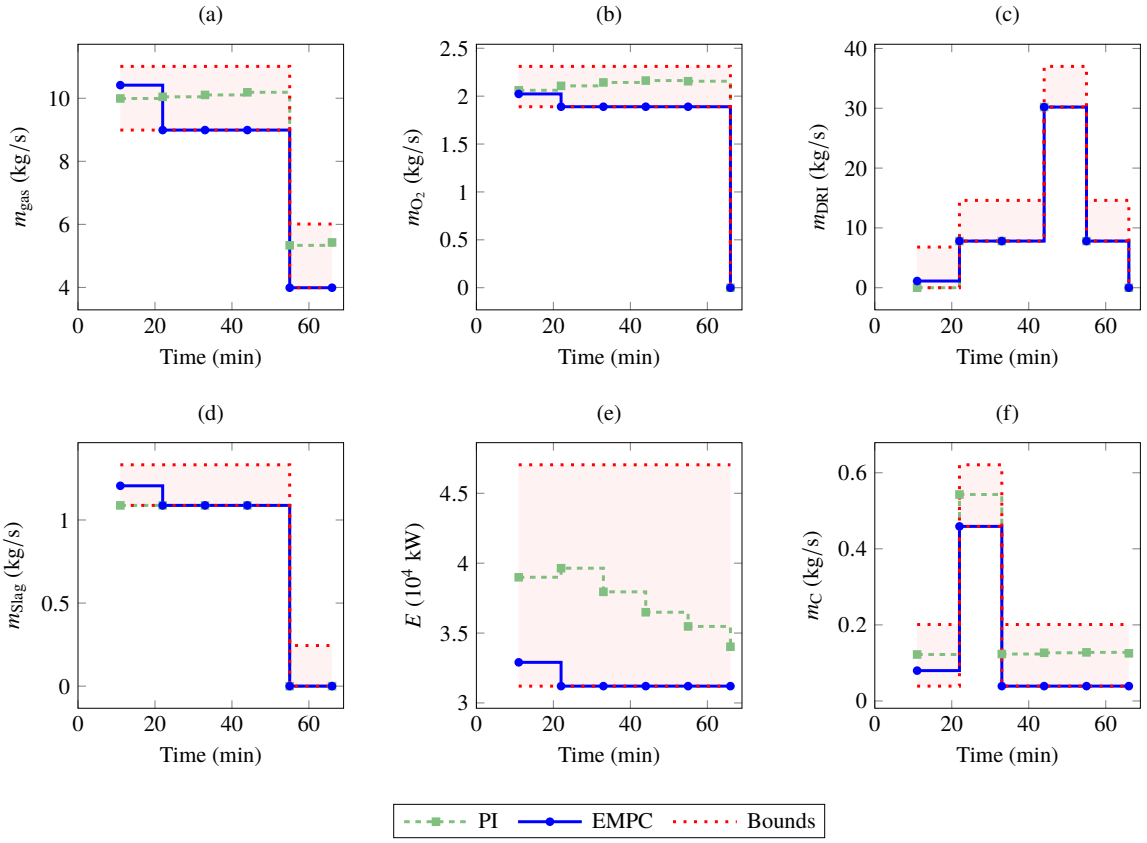

Figure 3.4.4: Closed-loop Profiles of the Manipulated Variables Obtained from the Proposed Economic MPC and Conventional Method for a Selected Batch of the EAF Process

3.5 CONCLUSION

This work considers the problem of data-based model development and economic model predictive control of the electric arc furnace. To this end, a multi-rate modeling approach is developed for the infrequent and frequent process measurements that efficiently incorporates the available measurements, the simplicity of local linear models, the data extraction capabilities of latent variable methods, and the use of appropriate clustering and weighting techniques to capture the nonlinear time-varying dynamics of the EAF process. By exploiting the enhanced capability of multi-rate data-driven models, a two-tiered economic MPC is proposed that ensures the desired product end-point specifications are satisfied and minimizes an economics-based cost function. The implementation of the multi-rate data-driven modeling approach and the economic MPC framework subject to measurement noise, constraints and desired end-point targets is illustrated on a electric arc furnace test-bed simulation process.

CHAPTER 4

MULTI-RATE SUBSPACE-BASED SYSTEM IDENTIFICATION AND ECONOMIC MODEL PREDICTIVE CONTROL[†]

4.1 Introduction

The competitive economic climate has compelled the chemical and manufacturing industries in most industrialized countries to pursue improved economic margins through the production of low volume, higher-value added specialty chemicals and materials, such as advanced alloys, polymers, herbicides, insecticides, pharmaceuticals and biochemicals, that are manufactured predominantly in batch processes. Managing and regulating the operation of these batch processes is essential to ensure their safe and reliable function, and to guarantee that they produce consistent and high-quality products. Nevertheless, the control and optimization

[†]The results in this chapter have been submitted for publication in:

- M. M. Rashid, P. Mhaskar, and C. L. E. Swartz. Handling multi-rate and missing data in variable duration economic model predictive control of batch processes. *AIChE J.*, (*submitted*).
- M. M. Rashid, P. Mhaskar, and C. L. E. Swartz. Handling multi-rate and missing data in system identification. In *Proceedings of the 2017 American Control Conference*, Seattle, WA, 2017., (*submitted*).

of batch processes through the application of mathematical programming problems, such as model predictive control (MPC) and optimization in general, is complicated by the lack of on-line sensors for measuring critical process variables, the finite duration of the process operation, the presence of significant nonlinear dynamics, the absence of equilibrium operation, and the challenges associated with developing accurate models that can characterize all the complex physical and chemical phenomena occurring in these processes. While several of these have been addressed to varying degrees in the recent past, handling missing data in process modeling and exploiting variable batch duration for improved process economics remains an opportunity for further research as discussed below.

One approach for modeling of batch processes involves the development of first-principles or mechanistic models that can then be used for the purposes of optimization and control [43–45]. While advancements in hardware and software (for instance, efficient numerical algorithms for optimizing dynamic systems and new implementation paradigms) are continuously increasing the available computational power and efficiency, thereby improving the tractability of the fundamental model-based optimization problems, the development and implementation of first-principles model-based controllers remains challenging. Compared to first-principles models, increased availability of historical process data make it amenable to develop data-driven models that are simple enough to make model-based control design practical. One successful and widely adopted approach is that of causal dynamic models identified using latent variable [68, 69] methods that can be readily integrated into an on-line optimization framework, where at each sampling instant a finite horizon optimal control problem is solved, yielding an optimal control sequence that achieves desired closed-loop performance. However, the latent variable approaches available in the literature can not readily deal with batches of variable duration (especially in the context of control) due to the inherent time-varying nature of the underlying models.

In recent contributions, a multi-model approach is proposed [56] and extended to multi-rate sampled data [70] that unifies concepts of dynamic modeling, latent variable regression techniques, fuzzy clustering and multiple local linear models in an integrated framework to capture the nonlinear nature of batch data, albeit using time-invariant models. More recently, subspace-based system identification methods that offer numerically reliable state-space models for complex systems directly from measured data [71–74] have been adapted for the purpose of model identification and control for batch processes [75].

The fundamental operation in subspace model identification is projection, which may emanate from prudent numerical techniques like singular value decomposition (SVD) or even QR factorization [71, 72, 74, 76–78]. However, an adverse consequence of their convenience is that the algorithms are incapable of directly handling the multi-rate nature of the measurement availability, missing data and incongruous batch process data. Although recent work has studied the problem of system identification of linear time-invariant models under non-ideal sampling conditions with missing input and output data, the resulting approaches typically involve solving complicated optimization problems such as nuclear norm-based structural rank minimization [78, 79] and maximum likelihood estimation through expectation-maximization algorithms [80]. The area of batch process control thus stands to gain from a computationally tractable alternative that retains the strengths of the of subspace identification modeling approach.

Predictive control algorithms that make explicit use of a (deterministic first-principles-based or empirical data-driven) process model in the optimization of a cost function to obtain the optimal control signal have been widely proposed and successfully implemented in the process industries. One excellent approach for the application of MPC in regulating batch processes utilizes time-indexed latent variable methods for trajectory tracking, where the correlation between subsequent measurement samples are employed to predict the dynamic

evolution of the process through the use of a missing data algorithm [68, 69]. As stated earlier, the time indexed model necessitates that all batches are of equal duration, which is often enforced through data alignment algorithms. While possible for monitoring, alignment of variables for an ongoing batch remains an unaddressed problem. Another method is based on tracking the necessary conditions of optimality, where an optimality criteria-based parameterization of the input profiles is used to design a multivariable feedback scheme along with model adaptation to track the first-order optimality conditions, thereby driving the system towards optimality [81, 82]. More recently, the concept of reachability regions is used to implement model predictive control strategies where the controller, rather than driving the process to the desired end-point at all computation times, guides the process through a set of precomputed states that ensure the end-point is satisfied at batch termination [49, 50]. Existing batch control approaches, especially those based on data driven models, have thus far not utilized batch duration as a decision variable.

An energy intensive batch process where both the challenge of multi-rate and missing data, and the opportunity of variable duration control is exemplified is the electric arc furnace (EAF) process that is widely employed in steelmaking, using electricity to melt post-consumer scrap metal to produce new steel. The process provides significant reductions in the labor, energy and environmental costs of steelmaking over conventional blast furnaces that forge steel out of iron ore, coal and natural gas. Despite these efficiency gains, the EAF process requires generating tremendous amounts of heat to recycle the scrap steel, while the industrial sector struggles with electricity costs that are exorbitantly high [43]. The energy efficiency and economics of the EAF process can hence be improved by leveraging new technologies in optimization and advanced control systems. However, the harsh environment and high corrosiveness of molten steel mean that on-line measurements of the molten steel temperature and chemical composition are often disrupted with unmeasured process

variables and missing data, thus making many prior existing modeling and control approaches inapplicable. Note that the control objective of the arc furnace, analogous to other batch processes, deals with the effective allocation of a set of limited resources over a finite time duration [83, 84]. When considering competing criteria and from an industrial perspective where the prevailing incentive is of an economic nature (often stated in terms such as cost, revenue, profit or investment payback time or rate of return), the multi-objective optimization problem for the EAF process is to economically reach the desired product end-point target at the termination of the batch. While recent contributions have demonstrated the advantages of economic model predictive control of the EAF process under the assumption that all batches are of equal durations [70], using a data-driven model that is capable of handling variable batch lengths opens new and beneficial possibilities of optimizing the operation of batches with variable durations.

Motivated by the above considerations, in this chapter we develop a system identification method that handles multi-rate and missing data for variable duration economic model predictive control (EMPC) and apply it to the EAF process. The remainder of the chapter is organized as follows. In Section 4.2, we briefly define the class of multi-rate sampled batch processes considered in this work, and review the conventional subspace-based system identification technique and representative MPC approach for completeness. Following the preliminaries, in Section 4.3 we present the novel subspace-based system identification approach for identifying a dynamic model with incomplete measurements and missing data. The system identification method is based on a subspace formulation and uses the incremental singular value decomposition approach, as opposed to conventional SVD, to compute a state realization and identify a dynamic model of the process from measurements complicated by missing and multi-rate data. In Section 4.4, the resulting dynamic model is integrated into a tiered economic model predictive control formulation for optimizing process economics

with varying batch durations, where solutions to computationally tractable mixed-integer quadratic programming problems achieve the desired final product end-point specifications by batch termination while minimizing the operating costs. Following the proposed multi-rate modeling and variable duration EMPC formulation, in Section 4.5 we describe the electric arc furnace process, and present the model development and validation simulation results. Furthermore, we present the corresponding closed-loop simulation results that illustrate the use and effectiveness of the proposed multi-rate subspace-based system identification technique and EMPC framework through implementation on the EAF process, subject to the limited availability of process measurements, missing data, measurement noise and constraints. Finally, we conclude this article with some remarks in Section 4.6.

4.2 PRELIMINARIES

In this section we first provide a brief description of the general class of batch processes that are considered in the study. Then, we succinctly review the conventional subspace-based system identification and economic model predictive control approach for batch processes.

4.2.1 PROBLEM STATEMENT

In this work, we consider a class of multi-rate sampled batch processes, such as the EAF process, that have measurements available at different sampling frequencies. For notational convenience, consider that the variables $y^{\phi_1} \in \mathbb{R}^{p^{\phi_1}}$ and $y^{\phi_2} \in \mathbb{R}^{p^{\phi_2}}$ denote the vector of frequent and infrequent measurements, respectively, and $u \in \mathbb{R}^m$ denotes the vector of constrained input variables, taking values in a nonempty convex set $\mathcal{U} \subseteq \mathbb{R}^m$ with $\mathcal{U} := \{u \in \mathbb{R}^m : u_{\min} \leq u \leq u_{\max}\}$, $u_{\min} \in \mathbb{R}^m$ and $u_{\max} \in \mathbb{R}^m$ denote the lower and upper bounds on the manipulated input, respectively. The sets $\mathbb{K}^{\phi_1}$ and $\mathbb{K}^{\phi_2}$ are the sampling

instances where either the frequent or infrequent measurements are available. Note that the infrequent measurements typically also include all the output variables available at the frequent sampling instances. The specific problem we address in the manuscript is the subspace-based model identification for batch processes that handles multi-rate and missing data and variable duration batch control.

4.2.2 SUBSPACE IDENTIFICATION

In this subsection, we briefly review the conventional subspace-based state-space system identification [76, 77] methods used to determine the system matrices of a discrete-time state-space model using synchronous data, where a model of the following form is identified:

$$\begin{aligned} x_{k+1} &= Ax_k + Bu_k \\ y_k &= Cx_k + Du_k \end{aligned} \tag{4.2.1}$$

The subspace-based system identification techniques utilize Hankel matrices constructed from the process measurements and manipulated inputs. To establish these Hankel matrices, define a $pi \times 1$ vector of stacked output measurements as

$$y_{k|i} = \begin{bmatrix} y_k^T & y_{k+1}^T & \cdots & y_{k+i-1}^T \end{bmatrix}^T \tag{4.2.2}$$

where i is a user-specified parameter greater than the observability index or, for simplicity, the system order n. Similarly, define a vector of stacked input variables as $u_{k|i}$. Through the repeated iterative application of the state equations (Eq. (4.2.1)), it is straightforward to verify the expression for the stacked quantities:

$$y_{k|i} = \Gamma_i x_k + \Phi_i u_{k|i} \tag{4.2.3}$$

where:

$$\Gamma_i = \begin{bmatrix} C \\ CA \\ \vdots \\ CA^{i-1} \end{bmatrix}$$

$$\Phi_i = \begin{bmatrix} D & 0 & \cdots & 0 \\ CB & D & \cdots & 0 \\ \vdots & \vdots & \ddots & \vdots \\ CA^{i-2}B & CA^{i-3}B & \cdots & D \end{bmatrix}$$

Consider the block Hankel matrix for the outputs

$$Y_i = \begin{bmatrix} y_{1|i} & y_{2|i} & \cdots & y_{n_s|i} \end{bmatrix}$$

and similarly define U_i as a block Hankel matrix of inputs [72, 74, 77, 78]. Then, it is clearly evident that Y_i is given by

$$Y_i = \Gamma_i X_i + \Phi_i U_i \tag{4.2.4}$$

where

$$X_i = \begin{bmatrix} x_1 & x_2 & \cdots & x_{n_s} \end{bmatrix}$$

The next step in the system identification methods is to estimate either the extended observability matrix or the state sequence, followed by computing the system matrices [76, 85]. We first review the conventional approach where the extended observability matrix is identified to estimate the system matrices, and subsequently we provide a brief overview of the later approach where the state sequence is identified to estimate the model.

4.2.2.1 Extended Observability Matrix Approach

The basic underlying idea of some common system identification methods is the orthogonal projection matrix on the null space of U_i as

$$\Pi^{\perp}_{U_i^T} = I - U_i^T \left(U_i U_i^T\right)^{-1} U_i \tag{4.2.5}$$

Multiplying Eq. (4.2.4) by the projection matrix $\Pi^{\perp}_{U_i^T}$ yields

$$Y_i \Pi^{\perp}_{U_i^T} = \Gamma_i X_i \Pi^{\perp}_{U_i^T} \tag{4.2.6}$$

where $Y_i \Pi^{\perp}_{U_i^T}$ can be readily computed using prudent numeral algorithms such as LQ factorization. An efficient implementation of this scheme is the multi-input, multi-output output-error state-space (MOESP) algorithm, where an estimate of Γ_i is obtained through the dominant left singular vectors of $Y_i \Pi^{\perp}_{U_i^T}$. Moreover, numerous variations of this approach (for instance, multiplying the matrix $Y_i \Pi^{\perp}_{U_i^T}$ with instrumental variables and/or nonsingular weight matrices before computing the SVD) are proposed to improve the consistency of the estimate. Four major variants of this method are PO-MOESP (past outputs MOESP), N4SID (numerical algorithms for subspace state-space system Identification), IVM (instrumental variable method) and CVA (canonical variate analysis) approach, which differ by the choice of weight matrices that pre- and post-multiply the matrix $Y_i \Pi^{\perp}_{U_i^T} \Psi^T$, where $\Psi = \begin{bmatrix} U_j^T & Y_j^T \end{bmatrix}^T \in \mathbb{R}^{2j \times n_s}$ is the instrumental variable matrix constructed by combining the Hankel matrices of 'past' inputs and outputs [72, 74, 77, 78]. Once an estimate of Γ_i has been determined from the dominant left singular vectors of $W_1 Y_i \Pi^{\perp}_{U_i^T} \Psi^T W_2$, where W_1 and W_2 denote the weight matrices, a system realization can be calculated in a multitude of ways. One approach for computing the system realization involves retrieving estimates of

system matrices A and C from Γ_i, while estimates of B and D can be computed by solving a least-squares problem [77, 78].

The key step in the classical subspace methods described above is the SVD of the matrix $W_1 Y_i \Pi^{\perp}_{U_i^T} \Psi^T W_2$ to estimate the extended observability matrix (Γ_i). However, the rank of the matrix Γ_i may not be equal to the order of the system, a phenomenon known as rank cancellation. Although the estimate of the extended observability matrix Γ_i is correct and consistent as the number of data samples tends to infinity, for a finite number of data samples, as is the case in batch data where a sufficient quantity data may not be available, there is no guarantee of optimality [78, 79]. Furthermore, the classical system identification approaches are limited to measurements sampled at the same frequency and can not readily handle missing or unmeasured data. Consequently, in this work we use an alternative subspace approach that first estimates the state sequence and then computes the system matrices in order to model the multi-rate sampled batch processes.

4.2.2.2 State Sequence Approach

We now review one particular example of a system identification approach that first estimates the matrix of states [71]. In this approach, the input and output data are divided into 'past' and 'future' measurements as follows

$$U_{2i} = \begin{bmatrix} U_p \\ U_f \end{bmatrix}, \quad Y_{2i} = \begin{bmatrix} Y_p \\ Y_f \end{bmatrix}$$

where the matrices $U_p \in \mathbb{R}^{mi \times n_s}$ and $U_f \in \mathbb{R}^{mi \times n_s}$ are referred to as the past and future input Hankel matrices, and $Y_p \in \mathbb{R}^{pi \times n_s}$ and $Y_f \in \mathbb{R}^{pi \times n_s}$ are referred to as the past and future output

Hankel matrices, respectively. It is readily shown that Y_f and Y_p are given by the relations

$$Y_f = \Gamma_i X_f + \Phi_i U_f$$

$$Y_p = \Gamma_i X_p + \Phi_i U_p$$

where X_p and X_f are the past and future states that are yet to be identified. One approach to estimating the state sequence involves computing the intersection between the past and future data given by

$$\text{span}\left(X_f\right) \coloneqq \text{row space}\left(\begin{bmatrix} Y_f \\ U_f \end{bmatrix}\right) \cap \text{row space}\left(\begin{bmatrix} Y_p \\ U_p \end{bmatrix}\right)$$

which provides an estimate of the future states X_f [71]. Once an estimate of X_f is known, it is straightforward to calculate a system realization through solving a least-squares problem since X_f, Y_f and U_f are all known. More details on the derivation of this result and the application of this system identification approach to batch processes are provided in the next section.

Remark 4.1. *Beyond the non-iterative subspace-based state-space system identification techniques that are readily implemented using efficient algorithms such as SVD and QR-decomposition, other system identification techniques for modeling uniformly sampled processes include the maximum likelihood estimation (MLE) approach and the closely related prediction error methods (PEM). These MLE and PEM approaches solve a (possibly) non-convex optimization problem to identify a system realization. Furthermore, they have well-established theoretical properties including asymptotically achieving the Cramér-Rao lower bound, and extensively studied theoretical underpinnings for practical considerations such as variance and bias distributions [80, 86, 87]. Their theoretical advantages in*

addressing important practical issues such as error analysis and performance trade-offs notwithstanding, the practical implementation of MLE methods is not always straightforward due to the embedded non-convex optimization problem (which may be poorly conditioned as a result of the chosen model parametrization) [77, 80, 86]. Moreover, the identification approach involving MLE is more meaningful for continuous processes because sufficient data collected around a nominal operating point enables the estimators to achieve consistency and asymptotic efficiency [80, 86]. In contrast, batch processes are typically not operated around an equilibrium operating point and a sufficient quantity of data may not be available for the finite duration of batch processes, making consistency and efficiency difficult to achieve under the limited data conditions of batch processes.

Remark 4.2. *The multi-rate model structure for batch processes that we identify in this work is similar to the form considered by Raghavan et al. [86] in the context of continuous processes through maximum likelihood estimation. In this work, we extend the multi-rate modeling problem to the application of batch processes through subspace-based system identification techniques that avoid solving complex and possibly non-convex optimization problems. Furthermore, the multi-rate state-space realization obtained through the subspace-based system identification techniques can be employed as an initialization for a batch specific MLE formulation to obtain a solution with possibly strong theoretical properties including consistency and asymptotic efficiency.*

4.2.3 MODEL PREDICTIVE CONTROL

In this subsection, we provide a standard formulation of a representative MPC to illustrate the paradigm of end-point control for batch processes. In a typical batch MPC, the control action at each sampling instance is computed by solving an optimization problem of the

following form:

$$\min_{u \in \mathcal{U}} \quad \mathcal{J} = \delta \cdot \sum_{i=k}^{n_t-1} c^T u_i \tag{4.2.7}$$

$$\text{s.t.} \begin{cases} x_{k+1} = Ax_k + Bu_k \\ \hat{y}_k = Cx_k + Du_k \\ \hat{y} \in \mathcal{Y} \\ \hat{y}_{n_t} = y_{\text{des}} \end{cases}$$

where $u \in \mathbb{R}^m$ denotes the vector of constrained input variables, taking values in a nonempty convex set $\mathcal{U} \subseteq \mathbb{R}^m$. The objective function minimizes the costs of the manipulated inputs, thus penalizing resource usage. While the end-point-based economic model predictive controllers have demonstrated improved economic operation in various applications, the control paradigm typically does not consider batches of varying durations. This is due to the fact that the model utilized in the above predictive control framework often originates from system identification techniques that can not handle multi-rate sampled measurements and missing data.

4.3 Multi-rate System Identification with Missing Data

In this section, we propose a novel multi-rate subspace-based system identification algorithm for batch processes that uses the incremental singular value decomposition (iSVD) to compute a realization of the state sequence since regular SVD is inapplicable in subspace-based system identification from Hankel matrices composed of multi-rate measurements with missing data. Recognizing the multi-rate nature of the data, we pose the problem as one of identifying a

discrete-time, linear time-invariant state-space model of the following form:

$$\begin{aligned} x_{k+1} &= Ax_k + Bu_k \\ \hat{y}_k^{\phi_1} &= C^{\phi_1} x_k + D^{\phi_1} u_k, \ \forall k \in \mathbb{K}^{\phi_1} \\ \hat{y}_k^{\phi_2} &= C^{\phi_2} x_k + D^{\phi_2} u_k, \ \forall k \in \mathbb{K}^{\phi_2} \end{aligned} \tag{4.3.1}$$

where $x \in \mathbb{R}^n$ denotes the state vector of the identified model. Consider that there are n_b batches of varying durations and define a vector of stacked multi-rate sampled output measurements as

$$y_{k|i} = \begin{bmatrix} y_k^{\phi_2 T} & y_{k+1}^{\phi_1 \ T} & \cdots & y_{k+i-1}^{\phi_1 \ T} \end{bmatrix}^T \tag{4.3.2}$$

Then for an arbitrary batch b of the n_b total batches, with $n_s^b + 2i - 1$ input and output data samples, we develop the output Hankel matrices for the b-th batch as follows

$$Y_f^b = \begin{bmatrix} y_{i+1|i} & y_{i+2|i} & \cdots & y_{i+n_s^b|i} \end{bmatrix} \tag{4.3.3}$$

$$Y_p^b = \begin{bmatrix} y_{1|i} & y_{2|i} & \cdots & y_{n_s^b|i} \end{bmatrix} \tag{4.3.4}$$

where i is a user-specified parameter that is greater than the observability index or the system order. It should be noted that $y_{k|i}$ in this case is composed of vectors of stacked output measurements that include both the infrequent and frequent measurements, as shown in Eq. (4.3.2). Each output Hankel matrix for an arbitrary batch (batch no. b of n_b total batches) is of size $pi \times n_s^b$ where the entries in the block Hankel matrices corresponding to unmeasured variables at the frequent sampling instances are left empty. The partitioning of the data into Y_p^b and Y_f^b is sometimes referred to as past and future. Define U_f^b and U_p^b as input block Hankel matrices similar to Eqs. (4.3.3) and (4.3.4), respectively. The individual block

Hankel matrices of the various batches are then assembled together as

$$Y_f = \begin{bmatrix} Y_f^1 & Y_f^2 & \cdots & Y_f^{n_b} \end{bmatrix} \tag{4.3.5}$$

and similarly to create Y_p, U_f and U_p. It was proposed by Moonen et al. [71], who showed that a realization of the unknown system states can be obtained through computing the intersection of the past input-output and the future input-output spaces via the application of singular value decomposition, as we will show below.

From Moonen et al. [71], it is readily shown that Y_f and Y_p are given by the relations

$$Y_f = \Gamma_i X_f + \Phi_i U_f \tag{4.3.6}$$

$$Y_p = \Gamma_i X_p + \Phi_i U_p \tag{4.3.7}$$

where

$$X_f = \begin{bmatrix} x_{i+1}^{(1)} & \cdots & x_{i+n_s^{(1)}}^{(1)} & x_{i+1}^{(2)} & \cdots & x_{i+n_s^{(2)}}^{(2)} & x_{i+1}^{(n_b)} & \cdots & x_{i+n_s^{n_b}}^{(n_b)} \end{bmatrix}$$

$$X_p = \begin{bmatrix} x_1^{(1)} & \cdots & x_{n_s^{(1)}}^{(1)} & x_1^{(2)} & \cdots & x_{n_s^{(2)}}^{(2)} & x_1^{n_b} & \cdots & x_{n_s^{n_b}}^{(n_b)} \end{bmatrix}$$

Note that Γ_i and Φ_i are defined in terms of the full output measurement vector available at the infrequent sampling times using the multi-rate state-space model of Eq. (4.3.1) as

$$\Gamma_i = \begin{bmatrix} C^{\phi_1} \\ C^{\phi_1} A \\ \vdots \\ C^{\phi_1} A^{i-1} \end{bmatrix}$$

$$\Phi_i = \begin{bmatrix} D^{\phi_1} & 0 & \cdots & 0 \\ C^{\phi_1}B & D^{\phi_1} & \cdots & 0 \\ \vdots & \vdots & \ddots & \vdots \\ C^{\phi_1}A^{i-2}B & C^{\phi_1}A^{i-3}B & \cdots & D^{\phi_1} \end{bmatrix}$$

while keeping the missing data at the frequent sampling instances as empty entries in the block Hankel matrices. This ensures that the equations are properly specified and that the resulting state sequence is uninterrupted and congruous, a necessary requirement for estimating the system realization. Further, X_f can be related to X_p as follows

$$X_f = A^i X_p + \Delta_i U_p \tag{4.3.8}$$

where Δ_i is the reversed extended controllability matrix given by

$$\Delta_i = \begin{bmatrix} A^{i-1}B & A^{i-2}B & \cdots & AB & B \end{bmatrix}$$

Solving for X_f in Eq. (4.3.6) yields

$$X_f = \begin{bmatrix} \Gamma_i^\dagger & -\Gamma_i^\dagger \Phi_i \end{bmatrix} \begin{bmatrix} Y_f \\ U_f \end{bmatrix} \tag{4.3.9}$$

where $\Gamma_i^\dagger$ denotes the Moore-Penrose matrix inverse of Γ_i. Eq. (4.3.9) implies that the row space of X_f is contained within the row space of $\begin{bmatrix} Y_f^T & U_f^T \end{bmatrix}^T$. Similarly, solving for X_p in Eq. (4.3.7) and substituting into Eq. (4.3.8) gives

$$X_f = \begin{bmatrix} A^i \Gamma_i^\dagger & \Delta_i - A^i \Gamma_i^\dagger \Phi_i \end{bmatrix} \begin{bmatrix} Y_p \\ U_p \end{bmatrix} \tag{4.3.10}$$

which implies that the row space of X_f is equally contained within the row space of $\begin{bmatrix} Y_p^T & U_p^T \end{bmatrix}^T$. Therefore, the intersection between the past and future data given by

$$\text{span}\left(X_f\right) \coloneqq \text{row space}\left(\begin{bmatrix} Y_f \\ U_f \end{bmatrix}\right) \cap \text{row space}\left(\begin{bmatrix} Y_p \\ U_p \end{bmatrix}\right) \tag{4.3.11}$$

For the present case of multi-rate sampled measurements as well as missing data, however, traditional SVD of the Hankel matrices can not be determined because the Hankel matrices are composed of multi-rate sampled output measurements, and thus this intersection cannot be computed using singular value decomposition of the two spaces as is done in traditional subspace identification to compute an estimate of the states X_f [71]. Therefore, in this work, we propose the use of incremental singular value decomposition algorithm to compute the intersection between Hankel matrices, and thus the estimate of the states X_f, where the Hankel matrices are composed of multi-rate sampled measurements with missing data.

Remark 4.3. *The conventional subspace model, based on the underlying assumption that each measurement or data vector is a linear combination of a small number of principal component vectors or singular vectors, is widely used to build prediction models. In contrast to the conventional subspace models, the subspace-based state-space system identification approach considered in this work identifies a dynamic model from a subspace realization that also constitutes the state sequence underlying the observed data. Consequently, a dynamic state-space model is identified in this work for the purposes of predictive control.*

Remark 4.4. *The system identification procedure requires that the manipulated inputs are persistently exciting signals, which corresponds to the fact that the projection matrix $\Pi^{\perp}_{U_i^T}$ can be computed and that the matrix inverse in Eq. (4.2.5) exists. Nevertheless, the criteria for ensuring that the inverse exists amounts to the input block Hankel matrix being full rank*

[71, 72, 77]. In this work, we consider this rank criteria to determine whether the inputs are persistently exciting, similar to the procedure in conventional system identification.

Remark 4.5. *Alternative approaches for handling multi-rate sampled data as missing values include interpolation techniques that impute values for the missing variables. The prediction capability of such missing data interpolation techniques is inherently predicated on the efficiency of the underlying model used to infer the unknown values. Moreover, the selection of a specific type of model to infer the values of the unknown data is not trivial, and is the whole point of the modeling exercise. Thus filling these unobserved data and then determining a subspace model is inconsistent with the notion of estimating an linear time-invariant subspace model. Furthermore, to simply down-sample the measurements to a common sampling frequency means that the frequent measurement samples available between infrequent sampling instances are discarded. Thus the relevant process information that could be used to identify a model and to implement frequent feedback control anachronisms is neglected. In contrast, the proposed approach uses all available information as best as possible.*

In this work, in order to calculate the intersection between two spaces that contain many missing variables, we employ the use of an incremental singular value decomposition [88, 89]. We will briefly review the key equations involved in the incremental SVD algorithm for completeness. Although the iSVD algorithm has been used to compute the principal components or singular values by identifying a subspace of low dimension given a data set consisting of missing values, the approach has not been utilized to identify a dynamic state-space model from the data. In the proposed approach, after the iSVD is used to compute the intersection between the subspaces of the past and future Hankel matrices, as shown in Eq. (4.3.11), the regular singular value decomposition is applied to the resulting intersection space to compute the state sequence.

To deal with the missing data in an arbitrary vector $v_t \in \mathbb{R}^{n_v}$ of a matrix $[v_1 \; v_2 \; \ldots \; v_t \ldots v_T]$ to be factorized using SVD in which only the components indicated by the set $\Omega_t \subset \{1, \ldots, n_v\}$ are measured or known, we observe the following subvector at iteration t:

$$(v_t)_{\Omega_t} = \left(\bar{U} w_t\right)_{\Omega_t} \tag{4.3.12}$$

where w_t is a known weight vector, $\bar{U}$ is an orthonormal matrix and the subscript Ω_t on a matrix or vector is used to indicate restriction to the rows indicated by Ω_t. Given initial SVD matrices U_t, Σ_t and V_t at some sampling instant t, we can calculate the SVD of a vector v_t with missing data by computing w_t and r_t as the least-squares weight and residual vector, respectively, defined with respect to only the set of observed indices Ω_t as follows

$$w_t = \arg\min_{w_t} \left\| (U_t w_t)_{\Omega_t} - (v_t)_{\Omega_t} \right\|_2^2$$

$$r_t = v_t - U_t w_t$$

Noting that

$$\begin{bmatrix} U_t \Sigma_t V_t & v_t \end{bmatrix} = \begin{bmatrix} U_t & \dfrac{r_t}{\|r_t\|} \end{bmatrix} \begin{bmatrix} \Sigma_t & w_t \\ 0 & \|r_t\| \end{bmatrix} \begin{bmatrix} V_t & 0 \\ 0 & 1 \end{bmatrix}^T \tag{4.3.13}$$

and computing the SVD of the update matrix:

$$\begin{bmatrix} \Sigma_t & w_t \\ 0 & \|r_t\| \end{bmatrix} = \hat{U} \hat{\Sigma} \hat{V}^T \tag{4.3.14}$$

and setting

$$U_{t+1} = \begin{bmatrix} U_t & \frac{r_t}{\|r_t\|} \end{bmatrix} \hat{U} \tag{4.3.15}$$

$$\Sigma_{t+1} = \hat{\Sigma} \tag{4.3.16}$$

$$V_{t+1} = \begin{bmatrix} V_t & 0 \\ 0 & 1 \end{bmatrix} \hat{V} \tag{4.3.17}$$

while retaining only the $\tilde{n}$ largest singular values yields an update of the initial SVD, taking into account the new vector of measurements ν_t, which had missing data within it. The procedure is then repeated in order to incorporate the next vector ν_{t+1} in the incremental SVD factorization. Therefore, the missing data incremental SVD algorithm can be applied to compute an estimate of the states $\tilde{X}_i$ and ultimately the model matrices.

Remark 4.6. *By definition, only the observable part of the system can be identified from the manipulated inputs and measured outputs, therefore the multi-rate system* $\left(A, \left[C^{\phi_1}, C^{\phi_2}\right]\right)$ *is always observable. The order of the identified system* $\tilde{n}$ *is selected based on how well the validation data is predicted, and the system order is always chosen so that the system* (A, B) *is controllable [71, 72, 77].*

Remark 4.7. *Note that the conventional subspace-based system identification procedure can not handle missing values, and the standard model is built using the correct corresponding values of the inputs. In contrast, the proposed multi-rate subspace-based system identification techniques utilizes the incremental singular value decomposition algorithm to identify a state sequence and thus the state-space model parameters, while avoiding the use of missing data imputation. Since, the incremental SVD algorithm computes the decomposition of matrix with arbitrarily missing values, the approach is not limited to just measurements sampled at different frequencies. The approach thus readily accommodates missing input values in the present application.*

4.4 Variable Duration Economic Model Predictive Control

In this section, we propose a novel two-tiered economic model predictive control algorithm capable of handling batches of varying durations. The proposed economic model predictive control formulation employs a tiered framework to achieve product that satisfies the end-point target while optimizing an economics-based cost function. To this end, the first tier of the EMPC computes the optimal achievable end-point that satisfies the desired product specifications at each sampling instance by solving the following mixed-integer quadratic programming problem

$$\min_{u\in\mathcal{U},\, n_t} \quad \mathcal{J}_1 = \left\|\hat{y}_e - y_{\text{des}}\right\|_{\Xi}^2 \tag{4.4.1}$$

$$\text{s.t.} \begin{cases} x_{k+1} = Ax_k + Bu_k \\ \hat{y}_k^{\phi_1} = C^{\phi_1} x_k + D^{\phi_1} u_k, \ \forall k \in \mathbb{K}^{\phi_1} \\ \hat{y}_k^{\phi_2} = C^{\phi_2} x_k + D^{\phi_2} u_k, \ \forall k \in \mathbb{K}^{\phi_2} \\ \hat{y}^{\phi_1} \in \mathcal{Y}^{\phi_1}, \quad \hat{y}^{\phi_2} \in \mathcal{Y}^{\phi_2} \\ \hat{y}_e = g\left(\hat{y}_{n_t}^{\phi_1}\right) \end{cases}$$

where $\hat{y}_e = g\left(\hat{y}_{n_t}^{\phi_1}\right)$ defines the batch end-point characteristics through the estimates of the output measurement variables at batch termination (n_t), $u \in \mathbb{R}^m$ denotes the vector of constrained input variables, taking values in a nonempty convex set $\mathcal{U} \subseteq \mathbb{R}^m$, Ξ is a positive definite matrix used to penalize the squared deviation of the predicted end-point variables with respect to the desired end-point values, $\mathcal{Y}^{\phi_1} \subseteq \mathbb{R}^{\phi_1}$ and $\mathcal{Y}^{\phi_2} \subseteq \mathbb{R}^{\phi_2}$ denote the constraints on the infrequent and frequent measurement variables, respectively, y_{des} denotes the desired end-point target specified by plant operators and n_t is the batch duration.

Subsequent to obtaining the optimal achievable end-point $\hat{y}_e^*$ that best satisfies the desired product specifications y_{des}, the next tier computes the economically optimal trajectory of manipulated input variables, albeit constricted with an additional constraint to satisfy the optimal achievable end-point product specifications. The second tier of the EMPC solves a mixed-integer quadratic programming problem to determine the optimal manipulated input trajectory by minimizing an economic objective function at every sampling time as follows

$$\min_{u\in\mathcal{U},\, n_t} \quad \mathcal{J}_2 = \delta \cdot \sum_{i=k}^{n_t-1} c^T u_i + c_{\Delta u}^T \Delta u_i^2 \tag{4.4.2}$$

$$\text{s.t.} \begin{cases} x_{k+1} = Ax_k + Bu_k \\ \hat{y}_k^{\phi_1} = C^{\phi_1} x_k + D^{\phi_1} u_k, \ \forall k \in \mathbb{K}^{\phi_1} \\ \hat{y}_k^{\phi_2} = C^{\phi_2} x_k + D^{\phi_2} u_k, \ \forall k \in \mathbb{K}^{\phi_2} \\ \hat{y}^{\phi_1} \in \mathcal{Y}^{\phi_1}, \quad \hat{y}^{\phi_2} \in \mathcal{Y}^{\phi_2} \\ h\left(\hat{y}_{n_t}^{\phi_1}, \hat{y}_e^*\right) \leq 0 \end{cases}$$

where $h\left(\hat{y}_{n_t}^{\phi_1}, \hat{y}_e^*\right) \leq 0$ denotes end-point constraints that are appropriately relaxed to an interval with $\hat{y}_e^*$ as a end-point restricting bound, δ is the sampling time or hold-time for the control action, $c \in \mathbb{R}^m$ and $c_{\Delta u} \in \mathbb{R}^m$ denote the operating costs associated with the manipulated variables and the rate of change of the manipulated input variables given by Δu.

Remark 4.8. *In this work, we penalize the rate of change of the input variables through the term $c_{\Delta u}^T \Delta u_i^2$ in the objective function. Another approach to minimize the difference between successive inputs involves penalizing the absolute value of the input change as $c_{\Delta u}^T |\Delta u_i|$, thus reformulating the optimization of the second tier into a linear programming problem. Regardless of the specific formulation used, the rate of change of the input variables may need to be penalized in the proposed economic MPC to mitigate the abrupt input moves that arise as a result of the shorter batch durations preferred from a cost perspective.*

Remark 4.9. *There have been several recent results focusing on EMPC including those that allow a non-quadratic cost function where the assumption of positive definiteness of the cost is not satisfied [59, 60]. In order to ensure that the closed-loop system resulting from the application of an economic MPC algorithm does in fact converge to the optimal equilibrium operating point, dissipativity conditions have been employed that are shown to be sufficient for optimal steady-state operation of a system as well as for convergence and stability analysis [58–62]. The key feature that differentiates continuous processes from batch and semi-batch processes, such as the EAF process, is that continuous processes have an equilibrium operating point whereas batch processes are typically not run long enough to reach a steady-state (and the steady-state is typically not the desired target point anyway). This precludes the direct implementation of these EMPC techniques on batch processes, and necessitates the development of batch specific control algorithms.*

Remark 4.10. *Considerable effort has been devoted in recent years to improve the computational tractability of model-based optimization problems through the derivation of convex formulations and by employing algorithms that exploit the underlying structure of the problem [47, 48]. Other attempts to avoid the challenges of on-line computing have involved moving the heavy computations off-line, where time and computational power are much more abundant, thus limiting the on-line operations to expedited decisions and simpler calculations. One such approach is multi-parametric programming, which generates off-line a register of explicit control laws to be employed on-line based on the estimated states of the system [90]. Furthermore, advanced-step MPC strategies are proposed that solve the detailed optimization problem in the background between sampling instances, assuming the computations can be completed within one sampling time, and apply sensitivity-based updates on-line when measurements become available [91, 92]. Another approach is the real-time nonlinear iteration scheme, which uses a continuation Newton-type framework and solves one quadratic programming problem at each iteration, thus allowing for multiple*

active set changes and ensuring that the nonlinear MPC algorithm performs at least as well as a linear MPC approach [93]. Another method is based on tracking the necessary conditions of optimality, where an optimality criteria-based parameterization of the input profiles is used to design a multivariable feedback scheme along with model adaptation to track the first-order optimality conditions, thereby driving the system towards optimality [81, 82]. More recently, the concept of reachability regions is used to implement model predictive control strategies where the controller, rather than driving the process to the desired end-point at all computation times, guides the process through a set of precomputed states that ensure the end-point is satisfied at batch termination [49, 50]. Note that the proposed approach poses minimal online computational issues due to the fact that the underlying model is linear.

4.5 Application to the Electric Arc Furnace

In this section, we first describe the electric arc furnace process, followed by simulation results that demonstrate the efficiency of the proposed approach to identify models from multi-rate sampled data and missing measurements using the test bed EAF process. Finally, the identified multi-rate subspace-based model is integrated into the proposed economic model predictive control framework, and the closed-loop simulation reuslts demonstrate the improvement in economic performance through the minimization of operating costs and optimization of batch durations.

4.5.1 Electric Arc Furnace Process

Integrated steel mills typically use the electric arc furnace process to produce steel predominantly from recycling post-consumer scrap, and occasionally using supplementary iron

sources such as direct reduced iron (DRI). The EAF process is a batch process, a batch is referred to as a heat, with a duration time of about one to two hours. A heat of an electric arc furnace begins with scrap metal being placed inside the furnace. The furnace will generally have some molten steel in place from the preceding heat in order to aid in the melting of the scrap metal. Once the furnace is charged with the scrap metal, a high intensity electric arc, which is typically the largest energy contributor in the melting operation, is discharged from electrodes into the furnace in order to melt the scrap metal. After a significant amount of scrap has been melted, oxygen gas and raw carbon are injected into the molten steel that react within the molten steel to create iron oxide and carbon monoxide. The injected oxygen and carbon also serve to foam slag on the surface of the molten steel through the diffusion of carbon monoxide, which aids in the removal of oxides and impurities from the molten steel. Furthermore, the foamed slag also serves as an insulator retaining heat, thus improving the efficiency of the steel production [41, 43]. Once the desired steel composition and temperature are obtained, the heat is tapped and the molten steel is transported to downstream operations for further processing.

The electric arc furnace operational challenges that we address in this study are the subspace-based identification of state-space models and the economically optimal control of the EAF process, subject to multi-rate and missing measurements. To this end, we utilize a first-principles mechanistic model as a test bed to implement and evaluate the efficiency of the proposed modeling and control approach. Specific details regarding the structure and configuration of the test bed mechanistic model can be found in previous studies [70], and are omitted here for brevity.

Recognizing the limited availability of process measurements in practice, in this work the measurements available to build the data-driven model and to implement the proposed control approach include infrequent and frequent measurement variables, where the infrequent

measurements related to the slag and molten steel are sampled twice as slowly as the frequent measurements corresponding to the off-gas composition that are available at each sampling instance. A list of the infrequent and frequent process measurement variables are given in Tables 3.2.1 and 3.2.2, respectively, and the manipulated inputs along with the associated costs are listed in Table 3.2.3. Furthermore, each historical heat has a duration of 70 min and a sampling time of $\delta = 1$ min for the frequent measurements. Additionally, the variability of the feed, measurement noise and conventional decentralized trajectory-tracking control schemes of the EAF process are kept consistent with previous studies [70]. In this work, the desired end-point attributes of the heat at batch termination are explicitly characterized through the melt temperature ($T_{t_f} \geq 1890$ K), mass fraction of carbon in the molten steel ($x_{C,t_f} \leq 0.005$ kg/kg) and the mass fraction of iron oxide in the slag ($x_{FeO,t_f} \leq 0.378$ kg/kg). Moreover, path constraints that limit the maximum achievable temperature of the molten steel ($T_t \leq 2000$ K, $t \in [0, t_f]$) and the relative pressure within EAFs ($P_t \leq 0$ Pa, $t \in [0, t_f]$) for safety considerations are considered as well.

4.5.2 Electric Arc Furnace Modeling Results

A historical database of past heats is generated to evaluate the efficacy of the multi-rate system identification procedure. To this end, a deterministic EAF process model is simulated to generate 50 normal operation batches of varying durations starting from diverse initial conditions. The heats are terminated between 62 min and 70 min, depending on whether the aforementioned end-point target criteria are satisfied. To represent practical measurement issues, 10% of the manipulated input variables have a missing input value, where the input value transmitted to the actuators was not recorded. In addition to the normal operation heats, five identification batches are used to augment the database, where a low-amplitude

pseudo-random binary sequence (PRBS) signal is added to the input values computed by the proportional-integral (PI) controllers.

In addition to the batches used for modeling purposes, a total of 50 additional heats are simulated for model validation purposes. For an objective evaluation of the multi-rate system identification procedure, we compare our proposed approach to a standard system identification method that predicts all available process variables at only the infrequent sampling instances. The number of states to incorporate in the standard infrequent-only model and proposed multi-rate model is determined through evaluating the root-mean-square error (RMSE) in predicting back the validation samples, which yielded 17 states for the proposed multi-rate modeling approach and 15 for the standard infrequent-only model. The model validation results for the measurement variables are given in Table 4.5.1 and the corresponding output predictions of the multi-rate model, standard infrequent-only model and actual variable profile trajectories from the test bed for a set of new initial conditions are shown in Figs. 4.5.1 and 4.5.2. For training batches, the subspace identification approach generates state trajectories for all batches, thus determining the initial subspace state for each batch. For a new batch, however, the underlying subspace state is unknown, requiring a state observer to first estimate the process state to in turn be able to predict the states and measured outputs forward in time and validate the model [94]. To this end, we utilize a multi-rate Kalman filter, which incorporates an on-line real-time adaptive learning algorithm to provide updated state estimates. In some sense, estimating the underlying state of the model can be thought of as a 'learning' of the new batch conditions. The shaded area until 20 min on the plots represents the initial phase of the heat where feedback from the measurements is used to correct the state estimates until convergence. For the proposed multi-rate models, a

multi-rate Kalman filter is implemented as

$$\hat{x}_k^- = A\hat{x}_{k-1} + Bu_k$$

$$P_k^- = AP_{k-1}A^T + Q$$

$$\left.\begin{aligned} L_k^{\phi_1} &= P_k^- C^{\phi_1 T}\left(C^{\phi_1} P_k^- C^{\phi_1 T} + R^{\phi_1}\right)^{-1} \\ \hat{x}_k &= \hat{x}_k^- + L_k^{\phi_1}\left(y_k^{\phi_1} - C^{\phi_1}\hat{x}_k^-\right) \\ P_k &= \left(I - L_k^{\phi_1} C^{\phi_1}\right) P_k^- \end{aligned}\right\} \forall k \in \mathbb{K}^{\phi_1}$$

or

$$\left.\begin{aligned} L_k^{\phi_2} &= P_k^- C^{\phi_2 T}\left(C^{\phi_2} P_k^- C^{\phi_2 T} + R^{\phi_2}\right)^{-1} \\ \hat{x}_k &= \hat{x}_k^- + L_k^{\phi_2}\left(y_k^{\phi_2} - C^{\phi_2}\hat{x}_k^-\right) \\ P_k &= \left(I - L_k^{\phi_2} C^{\phi_2}\right) P_k^- \end{aligned}\right\} \forall k \in \mathbb{K}^{\phi_2}$$

where L^{ϕ_1} and L^{ϕ_2} denote the Kalman gains for the infrequent and frequent sampling instances, respectively, and $\hat{x}^-$ and $\hat{x}$ denote the prior and posterior state estimates with error covariances P^- and P, respectively. Furthermore, the positive-definite matrices Q and R denote the covariances of the process disturbances and measurement noise, which can be tuned to improve the Kalman filter performance. For validation purposes, the convergence of the state estimates is evaluated using the error covariances to determine the point at which the Kalman filtering update of the states is stopped and subsequent predictions are made in an open-loop fashion where the predictions throughout the batch are not corrected and the model errors are allowed to accumulate over the entire batch duration. This is to test the ability of the model to predict reasonable future behavior for a candidate input profile, and thus establish its utility for feedback control purposes. Note that the state sequence for the model validation results, and in the development of predictive controllers, is not initialized arbitrarily. Rather, the state estimates obtained during the model development procedure

(Eq. (4.3.11)) for one of the training batches are used to initialize the state estimates (instead of initializing them at zero), which results in faster convergence.

It is readily observed that the standard system identification approach that neglects the frequent measurement variables does not predict the process variables well, resulting in higher RMSE values. Note that the only variable predicted well by the standard approach is the silicon dioxide in the slag, which is not a end-point target controlled variable. Accordingly, we do not consider the standard infrequent-only model to be sufficiently accurate to drive a predictive controller, and is hence not utilized further in this study.

4.5.3 Economic Model Predictive Control Results

The closed-loop simulation of 50 new initial conditions is performed using the proposed economic model predictive controller, and the performance of the proposed approach is compared against standard EAF operating policies involving PI control. The conventional PI control approach used as a comparison in this work involves closely tracking reference variable trajectories based on a historical batch that produced steel of the desired end-point. Details on the pairing of the controlled and manipulated variables, and the associated PI tuning parameters are available in Rashid et al. [70]. Furthermore, batches controlled using the conventional PI trajectory tracking approach were allowed to be terminated earlier than the duration of the reference batch if the end-point targets are satisfied in a shorter batch duration. All of the new initial conditions for evaluating the closed-loop performance of the proposed approach are obtained from the same distribution as the initial conditions in the training data. The batch termination time is allowed to vary in a predefined set $n_t = \{62 \text{ min}, \ldots, 70 \text{ min}\}$, and the two-tiers of the proposed EMPC are executed consecutively at each sampling instance through explicit enumeration. The first tier of the economic MPC determines the optimal

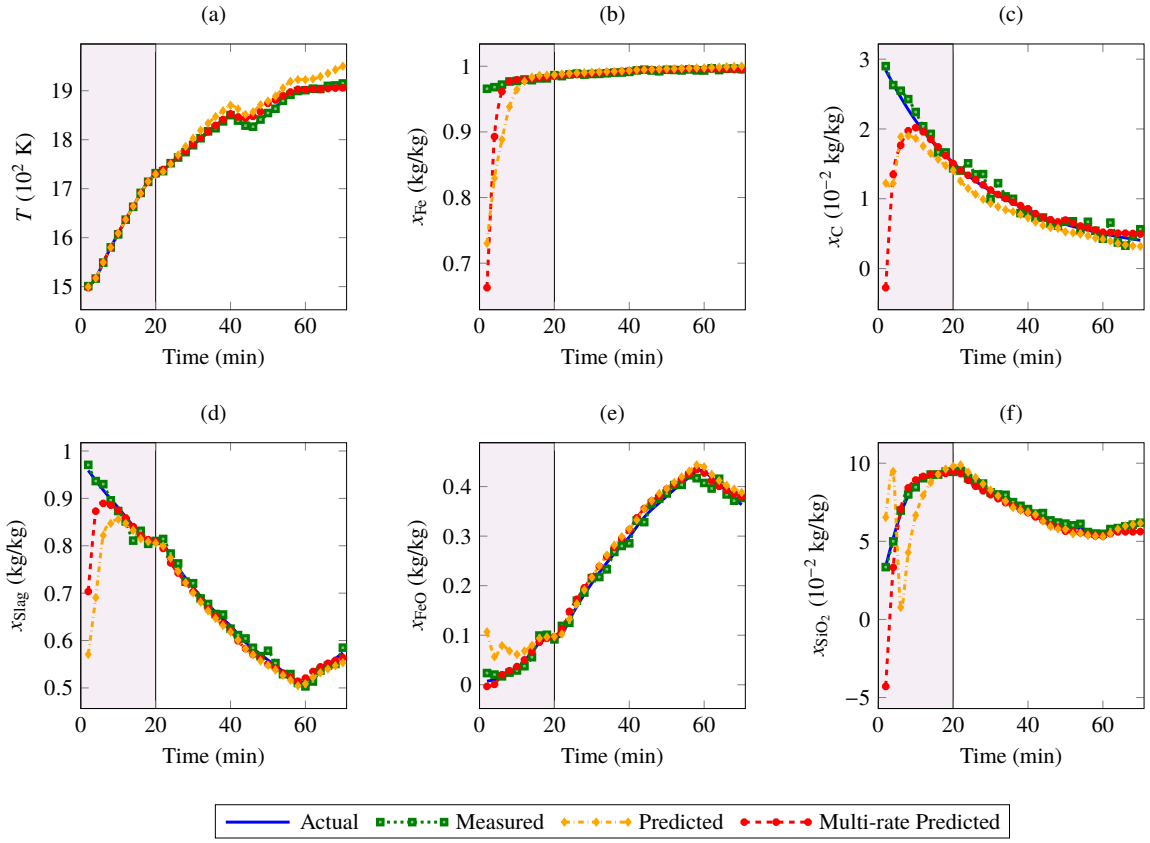

Figure 4.5.1: Model Validation Results for the Infrequent Measurement Variables of the EAF Process

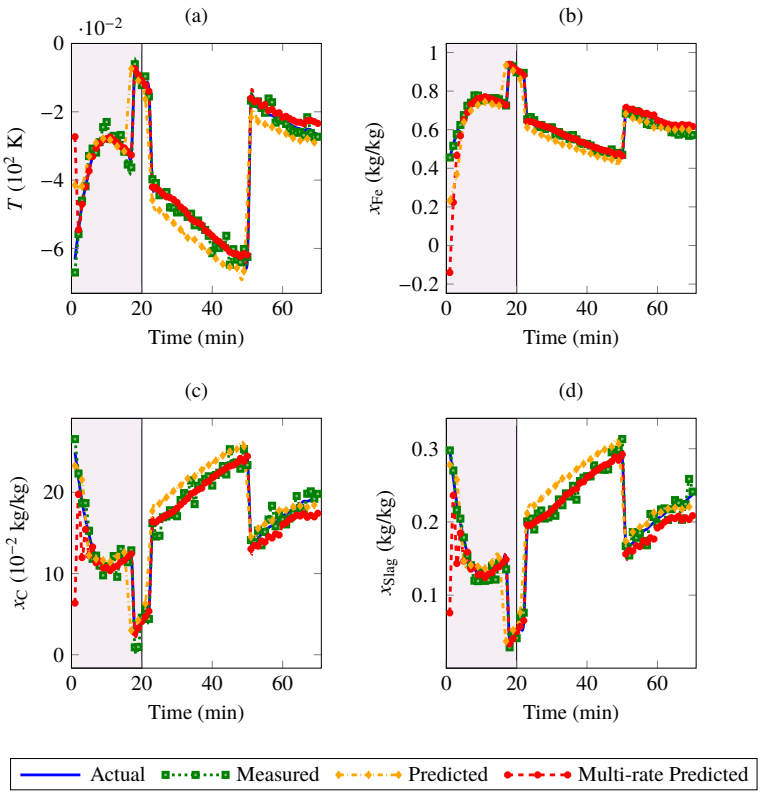

Figure 4.5.2: Model Validation Results for the Frequent Measurement Variables of the EAF Process

Table 4.5.1: Model Validation Results for the Infrequent and Frequent Measurement Variables of the EAF Process

Measurement Type	Variable	RMSE		Units
		Infrequent-only Model	Multi-rate Model	
Infrequent Measurements	T	22.4722	8.8419	K
	x_{Fe}	0.0025	0.0012	kg/kg
	x_{C}	0.0013	0.0004	kg/kg
	x_{Slag}	0.0111	0.0090	kg/kg
	x_{FeO}	0.0139	0.0124	kg/kg
	x_{SiO_2}	0.0026	0.0032	kg/kg
Frequent Measurements	P	0.3863	0.1333	Pa
	x_{CO}	0.0289	0.0208	kg/kg
	x_{CO_2}	0.0133	0.0094	kg/kg
	x_{N_2}	0.0158	0.0112	kg/kg

end-point for a given batch duration, and if a feasible solution exists, the second tier computes the economically optimal inputs. The most economical input variable trajectory with the lowest cost is implemented on the EAF process, and the tiered EMPC problem is solved at subsequent sampling instances with a shrinking horizon and with updated state estimates.

A representative set of closed-loop simulation results (batch no. 7) is presented in Figs. 4.5.3 and 4.5.4 for the infrequent and frequent process measurements, respectively. The closed-loop trajectories of the end-point target variables and the corresponding intervals of the end-point constraints are shown in Fig. 4.5.3 as well. Although both the proposed EMPC and the standard PI control approach are able to meet the desired product quality, the proposed economic MPC controller offered a significant cost advantage of approximately $\$5.5794\times10^3$ compared to $\$6.3632 \times 10^3$ for the standard approach, an average savings of \$783.80 per batch or approximately 12.32% improvement per batch. Furthermore, the average heat duration obtained through the proposed EMPC is 64.96 min, a 5.86% shorter batch duration compared to the conventional PI control approach.

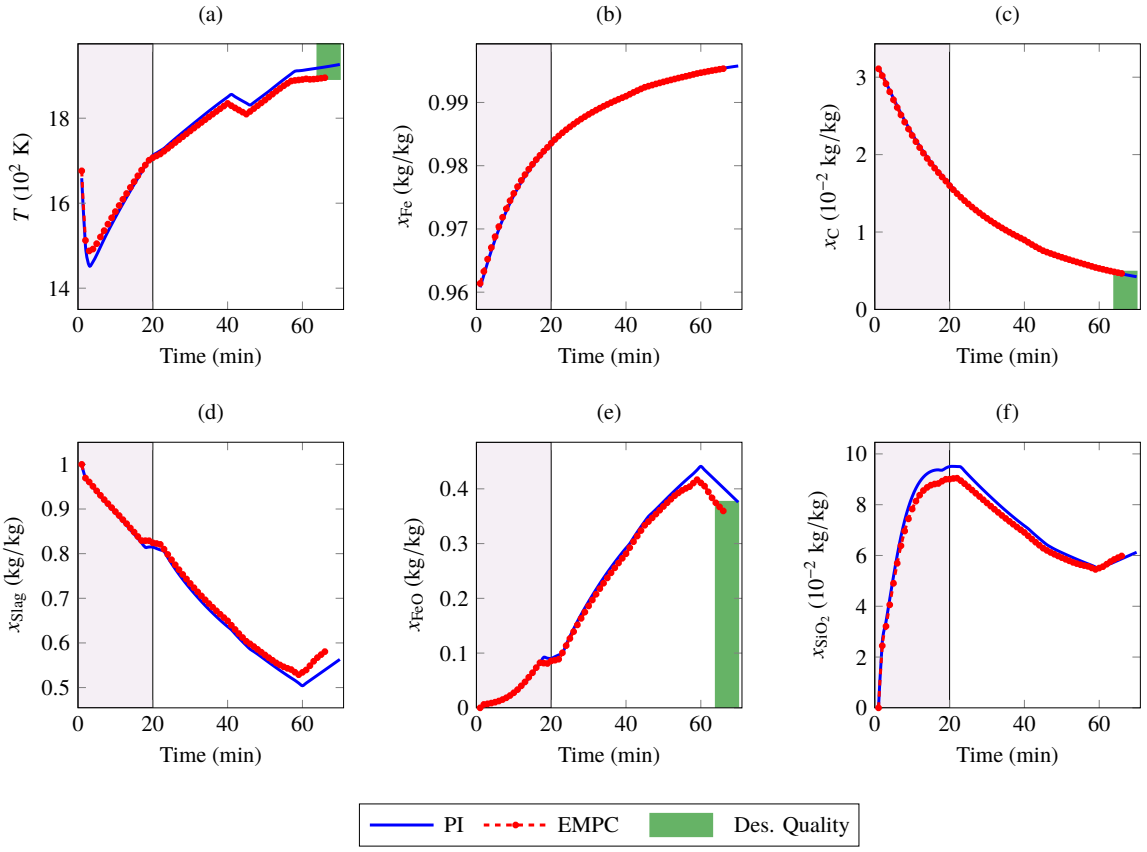

Figure 4.5.3: Comparison of the Trajectories for the Infrequent Measurement Variables Obtained from the Proposed Economic MPC and Conventional Method

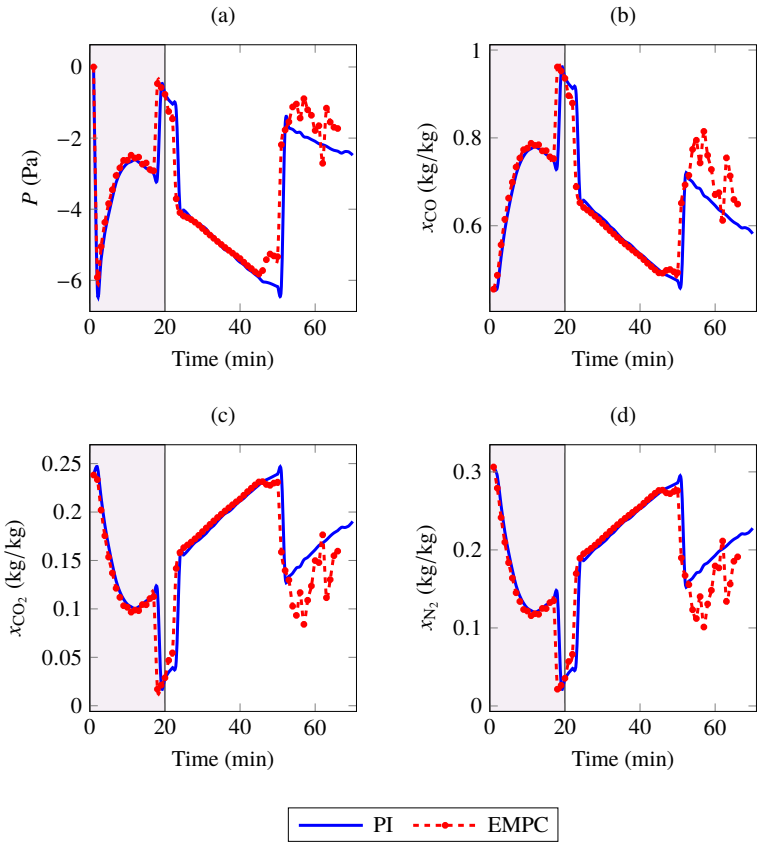

Figure 4.5.4: Comparison of the Trajectories for the Frequent Measurement Variables Obtained from the Proposed Economic MPC and Conventional Method

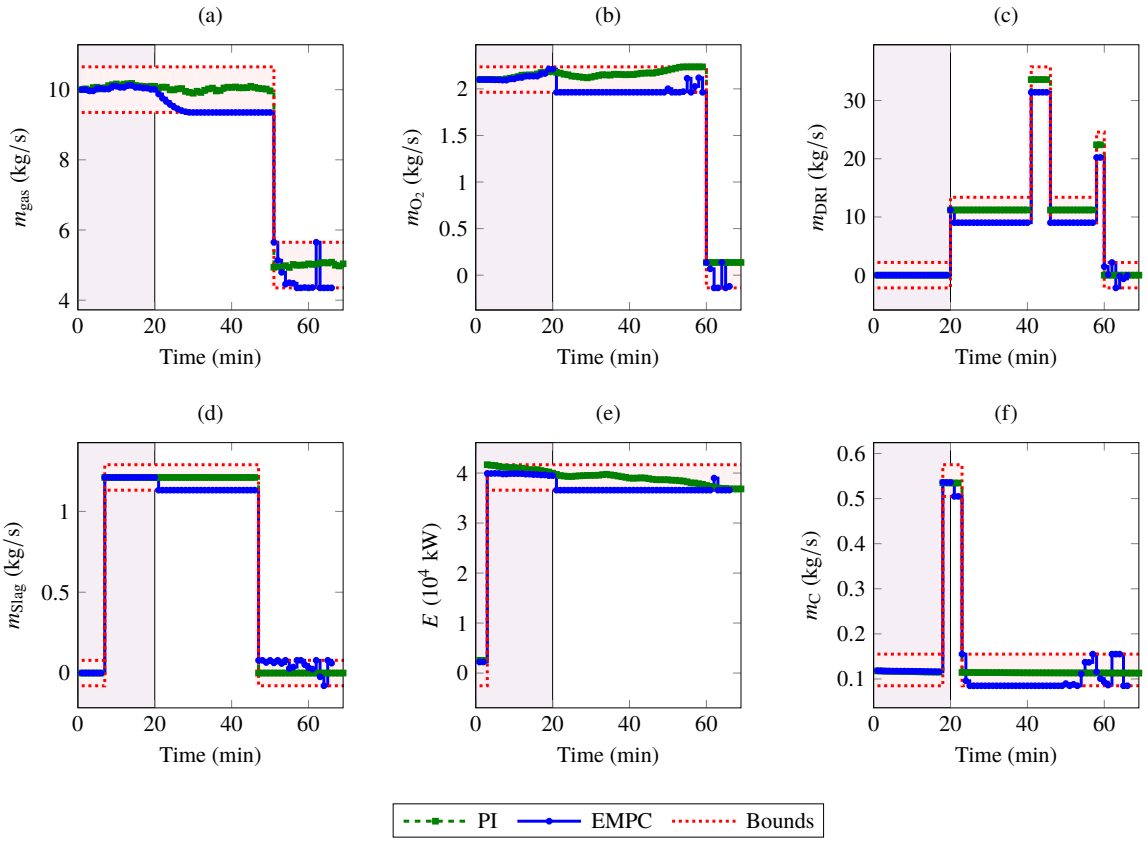

Figure 4.5.5: Closed-loop Profiles of the Manipulated Variables Obtained from the Proposed Economic MPC and Conventional Method for a Selected Batch of the EAF Process

The proposed economic MPC design was efficiently solvable with the average CPU time required to solve both the mixed-integer quadratic programming problems involved in the tiered approach with the longest prediction horizon as 4.42 s (maximum 4.97 s) using `MATLAB` on an Intel Core i7 machine with 8 GB RAM. Although the proposed EMPC formulation uses the subspace-based model and thus is computationally tractable, the efficiency of the optimization problem can be improved by parallelization [95] where the EMPC problems for varying batch termination times are solved in parallel using multiple CPU cores. The closed-loop input profiles are shown in Fig. 4.5.5 and it is readily observed that the EMPC approach recognizes that in certain instances, the end-point constraints are capable of being satisfied while maintaining the manipulated variables close to their lower bounds, due to which the operating costs of the EMPC approach are significantly lower. Overall, the simulation results demonstrated the advantages of implementing the proposed economic predictive controller over the standard operating policies.

4.6 CONCLUSION

In this work we develop a novel multi-rate subspace-based system identification and variable duration economic model predictive control framework for batch systems, and apply it to the electric arc furnace process. The system identification method uses the incremental singular value decomposition to identify a dynamic model from a finite number of noisy data samples disrupted with unmeasured process variables and asynchronous data. Furthermore, the proposed identification approach is capable of handling inconsistent batch lengths to optimize batches with variable durations. The identified dynamic model is integrated into a tiered EMPC formulation, where solutions to computationally tractable problems achieve the desired final product end-point specification by batch termination, while minimizing the operating costs. The proposed multi-rate modeling and EMPC framework are imple-

mented on the EAF process, and simulation case studies demonstrate the efficacy of the proposed approach subject to the limited availability of process measurements, missing data, measurement noise and constraints.

CHAPTER 5

CONCLUSIONS AND FUTURE WORK

In this chapter, the subsequent sections summarize the contributions of the research work, followed by suggestions for related future work.

5.1 Conclusions

In the initial phase of this research, in an effort to better detect and identify process faults, we propose a novel pattern matching based process monitoring approach. Traditional multivariate statistical processes monitoring (MSPM) techniques like principal component analysis (PCA) and partial least squares (PLS) are not well-suited in monitoring non-Gaussian processes because the derivation of T^2 and SPE indices requires the approximate multivariate Gaussian distribution of the process data. In this work, a novel pattern analysis driven dissimilarity approach is developed by integrating multidimensional mutual information (MMI) with independent component analysis (ICA) in order to quantitatively evaluate the statistical dependency between the independent component subspaces of the normal benchmark and monitored data sets. The new MMI based ICA dissimilarity index is derived from the higher-order statistics so that the non-Gaussian process features can be extracted efficiently. Moreover, the moving-window strategy is used to deal with process dynamics.

The multidimensional mutual information based ICA dissimilarity method is applied to the Tennessee Eastman Chemical process. The process monitoring results of the proposed method are demonstrated to be superior to those of the regular PCA, PCA dissimilarity, regular ICA and angle based ICA dissimilarity approaches.

In Chapter 3, we consider the problem of multi-rate modeling and economic model predictive control (EMPC) of electric arc furnaces (EAF), which are widely used in the steel industry to produce molten steel from scrap metal. The two main challenges that we address are the multi-rate nature of the measurement availability, and the requirement to achieve final product of a desired characteristic, while minimizing the operation cost. To this end, multi-rate models are identified that include predictions for both the infrequently and frequently measured process variables. The models comprise local linear models and an appropriate weighting scheme to capture the nonlinear nature of the EAF. The resulting model is integrated into a two-tiered predictive controller that enables the target end-point to be achieved while minimizing the associated cost. The EMPC is implemented on the EAF process and the closed-loop simulation results subject to the limited availability of process measurements and noise illustrate the improvement in economic performance over existing trajectory-tracking approaches.

In Chapter 4, we consider the problem of variable duration economic model predictive control (EMPC) of batch processes subject to multi-rate and missing data. To this end, we first generalize a recently developed subspace-based model identification approach for batch processes to handle multi-rate and missing data by utilizing the incremental singular value decomposition technique. Exploiting the fact that the proposed identification approach is capable of handling inconsistent batch lengths, the resulting dynamic model is integrated into a tiered EMPC formulation that optimizes process economics (including batch duration). Simulation case studies involving application to the energy intensive electric arc furnace

process demonstrate the efficacy of the proposed approach compared to a traditional trajectory tracking approach subject to limited availability of process measurements, missing data, measurement noise and constraints.

5.2 FUTURE WORK

The contributions and results of this thesis suggest the following topics for future work:

1. on-line adaption of linear time-invariant models resulting from subspace-based system identification approaches;

2. fault detection and isolation and fault-tolerant control of batch processes.

Below, a summary of the research potential, important developments and main contributions in these future research areas is provided.

Most model predictive control systems discussed in literature are derived from models that are developed under the assumption of flawless communications among the sensors, controllers and actuators, along with continuous or synchronous measurement sampling. However, many industrial processes are operated with little instrumentation and thus the reliable and frequent process measurements that are necessary to implement feedback control are simply not available. The main contribution of this work will be the design of an on-line adaptive model updating scheme and feedback control framework for processes with insufficient output measurement availability due to instrumentation challenges. The addition of an adaptive element to model-based control designs, where the model parameters are updated on-line at each sampling instant, is a popular approach for handling system uncertainty and improving closed-loop performance. The adaptive update of a first-principles deterministic model involves the estimation of a subset of the uncertain, possibly time-varying, model parameters.

In contrast, the entire set of model parameters is typically updated in the adaptation of empirical data-driven models that are commonly obtained through subspace-based system identification approaches. Regardless of the nature of the model, the key to successful on-line adaptive models is a well-designed real-time, recursive parameter estimation algorithm. Although some of the subspace-based system identification algorithms have been modified for on-line adaption, the approaches are limited to situations where the complete set of output measurements are available frequently. Accordingly, the main contributions in this phase of research will involve the adaption of linear time-invariant state-space models under non-ideal sporadic sampling situations.

Chemical processes routinely suffer from both severe faults and numerous minor process disturbances that have significant accumulated effects on production outages and excess resource use over time. Furthermore, the strong interactions between integrated process components (i.e., sensors, actuators, controllers, and units) profoundly influence the inherent stability and robustness properties of closed-loop systems and pose serious reliability, continuity, controllability, and stability issues. The problems of fault detection and isolation (FDI), fault-tolerant control (FTC), and fault-accommodating control design have been an active research topic within the process control community over the last decade. In the FDI framework, abnormal operating conditions are detected by setting a (fixed or variable) threshold on residual signals, where the diagnostic residual signals are generated through the use of an observer-based approach. As a complement to FDI, the traditional reactive fault-tolerant control method reconfigures the control system in an effort to minimize the impact of a faulty sensor, actuator, or process component. A new and less extensively studied extension to fault-accommodating control schemes deals with proactive fault-tolerant control approaches, where appropriate actions are taken before an incipient fault occurs to predict

and minimize the negative effects of impending fault scenarios, which can help to avoid process shutdowns, product deterioration, or more serious catastrophic losses.

Despite the potential benefits of fault detection and isolation and fault-handling control of continuous chemical processes, limited studies have extended these techniques to batch processes. Batch processes are typically characterized by strong process nonlinearity, transient operating dynamics, lack of equilibrium operating conditions, batch-to-batch variations, multiple operating phases, and system uncertainty, which pose significant challenges for the on-line state estimation and residual generation methodologies. In this research work, the main contributions will involve the FDI of batch processes through the use of time-varying residuals that also account for system uncertainty. Other potential research directions in this field include the development of a proactive fault-tolerant control approach for batch processes to mitigate the consequences of potential impending faults, and the extension of the FDI and FTC methods to processes with the limited availability of output measurements.

LIST OF REFERENCES

[1] J. Yu and S.J. Qin. Multiway Gaussian mixture model based multiphase batch process monitoring. *Ind. Eng. Chem. Res.*, 48:8585–8594, 2009.

[2] J.F. MacGregor and T. Kourti. Statistical process control of multivariate processes. *Control Eng. Practice*, 3:403–414, 1995.

[3] K.A. Kosanovich, K.S. Dahl, and M.J. Piovoso. Improved process understanding using multiway principal component analysis. *Ind. Eng. Chem. Res.*, 35:138–146, 1996.

[4] M. Kano, S. Hasebe, I. Hashimoto, and H. Ohno. Statistical process monitoring based on dissimilarity of process data. *AIChE J.*, 48:1231–1240, 2002.

[5] J. Flores-Cerrillo and J.F. MacGregor. Multivariate monitoring of batch processes using batch-to-batch information. *AIChE J.*, 50(6):1219–1228, 2004.

[6] X. Liu, U. Kruger, T. Littler, L. Xie, and S. Wang. Moving window kernel PCA for adaptive monitoring of nonlinear processes. *Chemometrics Intell. Lab. Syst.*, 96: 132–143, 2009.

[7] B.M. Wise and N.B. Gallagher. The process chemometrics approach to process monitoring and fault detection. *J. Proc. Cont.*, 6:329–348, 1996.

[8] B.R. Bakshi. Multiscale PCA with application to multivariate statistical process monitoring. *AIChE J.*, 44:1596–1610, 1998.

[9] C.-C. Ku and K.Y. Lee. Diagonal recurrent neural networks for dynamic systems control. *IEEE Trans. Neural Net.*, 6:144–156, January 1995.

[10] B. Lennox, G.A. Montague, H.G. Hiden, G. Kornfeld, and P.R. Goulding. Process monitoring of an industrial fed-batch fermentation. *Biotechnology and Bioengineering*, 74(2):125–135, 2001.

[11] S.J. Qin. Statistical process monitoring: Basics and beyond. *J. Chemomotrics*, 17: 480–502, 2003.

[12] E.B. Martin and A.J. Morris. Non-parametric confidence bounds for process performance monitoring charts. *J. Proc. Cont.*, 6:349–358, 1996.

[13] W. Ku, R.H. Storer, and C. Georgakis. Disturbance detection and isolation by dynamic principal component analysis. *Chemometrics Intell. Lab. Syst.*, 30:179–196, Nov 1995.

[14] L.H. Chiang, E.L. Russell, and R.D. Braatz. Fault diagnosis in chemical processes using Fisher discriminant analysis, discriminant partial least squares, and principal component analysis. *Chemometrics Intell. Lab. Syst.*, 50:243–252, 2000.

[15] L.H. Chiang, E.L. Russell, and R.D. Braatz. *Fault Detection and Diagnosis in Industrial Systems*. Advanced Textbooks in Control and Signal Processing. Springer-Verlag, London, Great Britain, 2001.

[16] L.H. Chiang and R.J. Pell. Genetic algorithms combined with discriminant analysis for key variable identification. *J. Proc. Cont.*, 14:143–155, 2004.

[17] J. Yu. Localized Fisher discriminant analysis based complex chemical process monitoring. *AIChE J.*, 57:1817–1828, 2011.

[18] J. Yu. Multiway discrete hidden Markov model-based approach for dynamic batch process monitoring and fault classification. *AIChE J.*, 2011. DOI: 10.1002/aic.12794.

[19] L.H. Chiang, M.E. Kotanchek, and A.K. Kordon. Fault diagnosis based on Fisher discriminant analysis and support vector machines. *Computer Chem. Eng.*, 28: 1389–1401, 2004.

[20] J. Yu. A Bayesian inference based two-stage support vector regression framework for soft sensor development in batch bioprocesses. *Computer Chem. Eng.*, 41:134–144, 2012.

[21] K.S. McClure, R.B. Gopaluni, T. Chmelyk, D. Marshman, and S.L. Shah. Nonlinear process monitoring using supervised locally linear embedding projection. *Ind. Eng. Chem. Res.*, 53:5205–5216, 2014.

[22] J. Yu and S.J. Qin. Multimode process monitoring with Bayesian inference-based finite Gaussian mixture models. *AIChE J.*, 54:1811–1829, 2008.

[23] J. Yu and S.J. Qin. Multiway Gaussian mixture model based multiphase batch process monitoring. *Ind. Eng. Chem. Res.*, 48:8585–8594, 2009.

[24] J. Yu. A nonlinear kernel Gaussian mixture model based inferential monitoring approach for fault detection and diagnosis of chemical processes. *Chem. Eng. Sci.*, 68: 506–519, 2012.

[25] H. Albazzaz and X.Z. Wang. Statistical process control charts for batch operations based on independent component analysis. *Ind. Eng. Chem. Res.*, 43:6731–6741, 2004.

[26] Y. Zhang. Enhanced statistical analysis of nonlinear processes using KPCA, KICA and SVM. *Chem. Eng. Sci.*, 64:801–811, 2009.

[27] P.P. Odiowei and Y. Cao. State-space independent component analysis for nonlinear dynamic process monitoring. *Chemometrics Intell. Lab. Syst.*, 103:59–65, 2010.

[28] J.-M. Lee, C.K. Yoo, and I.-B. Lee. Statistical process monitoring with independent component analysis. *J. Proc. Cont.*, 14:467–485, 2004.

[29] A. Singhal and D.E. Seborg. Pattern matching in historical batch data using PCA. *IEEE Cont. Sys. Mag.*, 22:53–63, Oct 2002.

[30] A. Singhal and D.E. Seborg. Evaluation of a pattern matching method for the Tennessee Eastman challenge process. *J. Proc. Cont.*, 16:601–613, Jul 2006.

[31] Z. Ge and Z. Song. Process monitoring based on independent component analysis-principal component analysis (ICA-PCA) and similarity factors. *Ind. Eng. Chem. Res.*, 46:2054–2063, 2007.

[32] A. Hyvärinen. Fast and robust fixed-point algorithms for independent component analysis. *IEEE Trans. Neural Net.*, 10:626–634, 1999.

[33] A. Hyvärinen and E. Oja. Independent component analysis: algorithms and applications. *IEEE Trans. Neural Net.*, 13:411–430, 2000.

[34] A. Kraskov, H. Stögbauer, and P. Grassberger. Estimating mutual information. *Phys. Rev. E.*, 69:066138, Jun 2004.

[35] A. Kraskov, H. Stögbauer, R.G. Andrzejak, and P. Grassberger. Hierarchical clustering using mutual information. *EPL*, 70:278–284, 2005.

[36] M. Vejmelka and M. Paluš. Inferring the directionality of coupling with conditional mutual information. *Phys. Rev. E.*, 77:026214, 2008.

[37] C.M. Bishop. *Neural Networks for Pattern Recognition*. Oxford University Press, Oxford, UK, 1995.

[38] J.J. Downs and E.F. Vogel. A plant-wide industrial process control problem. *Computer Chem. Eng.*, 17:245–255, Mar 1989.

[39] N.L. Ricker. Decentralized control of the Tennessee Eastman challenge process. *J. Proc. Cont.*, 6:205–221, 1996.

[40] A. Gosiewski and A. Wierzbicki. Dynamic optimization of a steel-making process in electric arc furnace. *Automatica*, 6:767–778, 1970.

[41] J.G. Bekker, I.K. Craig, and P.C. Pistorius. Modelling and simulation of an electric arc furnace process. *ISIJ Int.*, 39:23–32, 1999.

[42] D.J. Oosthuizen, I.K. Craig, and P.C. Pistorius. Economic evaluation and design of an electric arc furnace controller based on economic objectives. *Control Eng. Practice*, 12:253–265, 2004.

[43] R.D.M. MacRosty and C.L.E. Swartz. Dynamic modeling of an industrial electric arc furnace. *Ind. Eng. Chem. Res.*, 44:8067–8083, 2005.

[44] R.D.M. MacRosty and C.L.E. Swartz. Dynamic optimization of electric arc furnace operation. *AIChE J.*, 53:640–653, 2007.

[45] D. Shi, N.H. El-Farra, M. Li, P. Mhaskar, and P.D. Christofides. Predictive control of particle size distribution in particulate processes. 61:268–281, 2006.

[46] P.D. Christofides, N.H. El-Farra, M. Li, and P. Mhaskar. Model-based control of particulate processes. *Chem. Eng. Sci.*, 63:1156–1172, 2008.

[47] B. Chachuat, A. Marchetti, and D. Bonvin. Process optimization via constraints adaptation. *J. Proc. Cont.*, 18:244–257, 2008.

[48] B. Chachuat, B. Srinivasan, and D. Bonvin. Adaptation strategies for real-time optimization. *Computer Chem. Eng.*, 33:1557–1567, 2009.

[49] S. Aumi and P. Mhaskar. Safe-steering of batch process systems. *AIChE J.*, 55: 2861–2872, 2009.

[50] S. Aumi and P. Mhaskar. Robust model predictive control and fault handling of batch processes. *AIChE J.*, 57:1796–1808, 2011.

[51] P. Rivotti and E.N. Pistikopoulos. Constrained dynamic programming of mixed-integer linear problems by multi-parametric programming. *Computer Chem. Eng.*, 70: 172–179, 2014.

[52] P. Rivotti and E.N. Pistikopoulos. A dynamic programming based approach for explicit model predictive control of hybrid systems. *Computer Chem. Eng.*, 72:126–144, 2015.

[53] X. Jin and B. Huang. Robust identification of piecewise/switching autoregressive exogenous process. *AIChE J.*, 56:1829–1844, 2010.

[54] T. Takagi and M. Sugeno. Fuzzy identification of systems and its applications to modeling and control. *IEEE Trans. Syst. Man Cybern.*, 15:116–132, 1985.

[55] N.M. Fletcher, A.J. Morris, G. Montague, and E.B. Martin. Local dynamic partial least squares approaches for the modelling of batch processes. *Can. J. of Chem. Eng.*, 86:960–970, 2008.

[56] S. Aumi and P. Mhaskar. Integrating data-based modeling and nonlinear control tools for batch process control. *AIChE J.*, 58:2105–2119, 2012.

[57] S. Aumi, B. Corbett, T. Clarke-Pringle, and P. Mhaskar. Data-driven model predictive quality control of batch processes. *AIChE J.*, 59:2852–2861, 2013.

[58] M. Diehl, R. Amrit, and J.B. Rawlings. A Lyapunov function for economic optimizing model predictive control. *IEEE Trans. Auto. Cont.*, 56:703–707, 2011.

[59] M. Heidarinejad, J. Liu, and P.D. Christofides. Economic model predictive control of nonlinear process systems using Lyapunov techniques. *AIChE J.*, 58:855–870, 2012.

[60] R. Amrit, J.B. Rawlings, and L.T. Biegler. Optimizing process economics online using model predictive control. *Computer Chem. Eng.*, 58:334–343, 2013.

[61] M. Ellis, H. Durand, and P.D. Christofides. A tutorial review of economic model predictive control methods. *J. Proc. Cont.*, 24:1156–1178, 2014.

[62] M. Ellis and P.D. Christofides. On finite-time and infinite-time cost improvement of economic model predictive control for nonlinear systems. *Automatica*, 50:2561–2569, 2014.

[63] J.G. Bekker. Modelling and control of an electric arc furnace off-gas process. Master's thesis, University of Pretoria, South Africa, 1999.

[64] P. Clerici, F. Dell'Acqua, J. Maiolo, and S. Vittorio. Tenova's intelligent arc furnace 'iEAF' – Concept and technical overview. *Steel Times Int.*, May/June 2008.

[65] C. Wang, M. Larsson, C. Ryman, C.-E. Grip, J.-O. Wikström, A. Johnsson, and J. Engdahl. A model on CO_2 emission reduction in integrated steelmaking by optimization methods. *Int. J. Energy Res.*, 32:1092–1106, 2008.

[66] C.L.E. Swartz. An algorithm for hierarchical supervisory control. *Computer Chem. Eng.*, 19:1173–1180, 1995.

[67] Z. Chong and C.L.E. Swartz. Optimal operation of process plants under partial shutdown conditions. *AIChE J.*, 59:4151–4168, 2013.

[68] J. Flores-Cerrillo and J.F. MacGregor. Latent variable MPC for trajectory tracking in batch processes. *J. Proc. Cont.*, 15:651–663, 2005.

[69] M. Golshan, J.F. MacGregor, M.-J. Bruwer, and P. Mhaskar. Latent variable model predictive control (LV-MPC) for trajectory tracking in batch processes. *J. Proc. Cont.*, 20:538–550, 2010.

[70] M.M. Rashid, P. Mhaskar, and C.L.E. Swartz. Multi-rate modeling and economic model predictive control of the electric arc furnace. *J. Proc. Cont.*, 40:50–61, 2016.

[71] M. Moonen, B. De Moor, L. Vandenberghe, and J. Vandewalle. On- and off-line identification of linear state-space models. *Int. J. Control*, 49:219–232, 1989.

[72] M. Jansson and B. Wahlberg. On consistency of subspace methods for system identification. *Automatica*, 34:1507–1519, 1998.

[73] R. Shi and J.F. MacGregor. Modeling of dynamic systems using latent variable and subspace methods. *J. Chemom.*, 14:423–439, 2000.

[74] S.J. Qin. An overview of subspace identification. *Computer Chem. Eng.*, 30: 1502–1513, 2006.

[75] B. Corbett and P. Mhaskar. Subspace identification for data-driven modeling and quality control of batch processes. *AIChE J.*, 62:1581–1601, 2016.

[76] B. De Moor P. Van Overschee. *Subspace Identification for Linear Systems: Theory, Implementation, Applications*. Kluwer Academic Publishers, Norwell, MA, USA, 1996.

[77] L. Ljung. *System Identification: Theory for the User*. Prentice-Hall, Inc., Englewood Cliffs, New Jersey, 1999.

[78] Z. Liu, A. Hansson, and L. Vandenberghe. Nuclear norm system identification with missing inputs and outputs. *Sys. Cont. Let.*, 62:605–612, 2013.

[79] Z. Liu and L. Vandenberghe. Interior-point method for nuclear norm approximation with application to system identification. *SIAM J. Mat. Anal. Appl.*, 31:1235–1256, 2009.

[80] S. Gibson and B. Ninness. Robust maximum-likelihood estimation of multivariable dynamic systems. *Automatica*, 41:1667–1682, 2005.

[81] B. Srinivasan and D. Bonvin. Real-time optimization of batch processes by tracking the necessary conditions of optimality. *Ind. Eng. Chem. Res.*, 46:492–504, 2007.

[82] D. Bonvin and B. Srinivasan. On the role of the necessary conditions of optimality in structuring dynamic real-time optimization schemes. *Computer Chem. Eng.*, 51: 172–180, 2013.

[83] B. Srinivasan, S. Palanki, and D. Bonvin. Dynamic optimization of batch processes: I. Characterization of the nominal solution. *Computer Chem. Eng.*, 27:1–26, 2003.

[84] B. Srinivasan, D. Bonvin, E. Visser, and S. Palanki. Dynamic optimization of batch processes: II. Role of measurements in handling uncertainty. *Computer Chem. Eng.*, 27:27–44, 2003.

[85] P. Van Overschee and B. De Moor. A unifying theorem for three subspace system identification algorithms. *Automatica*, 31:1853–1864, 1995.

[86] H. Raghavan, A.K. Tangirala, R.B. Gopaluni, and S.L. Shah. Identification of chemical processes with irregular output sampling. *Control Eng. Practice*, 14:467–480, 2006.

[87] R.B. Gopaluni. Nonlinear system identification under missing observations: The case of unknown model structure. *J. Proc. Cont.*, 20:314–324, 2010.

[88] L. Balzano and S. J. Wright. On GROUSE and incremental SVD. In *Computational Advances in Multi-Sensor Adaptive Processing (CAMSAP), 2013 IEEE 5th International Workshop on*, pages 1–4, St. Martin, 2013.

[89] L. Balzano and S.J. Wright. Local convergence of an algorithm for subspace identification from partial data. *Found Comput Math*, 15:1279–1314, 2015.

[90] A. Bemporad, M. Morari, V. Dua, and E.N. Pistikopoulos. The explicit linear quadratic regulator for constrained systems. *Automatica*, 38:3–20, 2002.

[91] X. Yang and L.T. Biegler. Advanced-multi-step nonlinear model predictive control. *J. Proc. Cont.*, 23:1116–1128, 2013.

[92] J. Jäschke, X. Yang, and L.T. Biegler. Fast economic model predictive control based on NLP-sensitivities. *J. Proc. Cont.*, 24:1260–1272, 2014.

[93] M. Diehl, H.G. Bock, and J.P. Schlöder. A real-time iteration scheme for nonlinear optimization in optimal feedback control. *SIAM J. Cont. Opt.*, 43:1714–1736, 2005.

[94] D.J. Kozub and J.F. MacGregor. State estimation for semi-batch polymerization reactors. *Chem. Eng. Sci.*, 47:1047–1062, 1992.

[95] I.D. Washington and C.L.E. Swartz. Design under uncertainty using parallel multiperiod dynamic optimization. *AIChE J.*, 60:3151–3168, 2014.